TECHNICAL REPORT STANDARD TITLE PAGE

1. Report No.	2. Government Accession No.	3. Recipient's Catalog No.

4. Title and Subtitle	5. Report Date
"The Characterization of Road Roughness on Bridge Decks and the Adjoining Pavement"	April 1975
	6. Performing Organization Code
7. Author(s)	8. Performing Organization Report No.
David B. Law, Hugh J. Williamson, and W. Ronald Hudson	Research Report 156-4
9. Performing Organization Name and Address	10. Work Unit No.
Center for Highway Research The University of Texas at Austin Austin, Texas 78712	11. Contract or Grant No. Research Study 3-8-71-156
	13. Type of Report and Period Covered
12. Sponsoring Agency Name and Address	Interim
Texas Highway Department Planning & Research Division P. O. Box 5051 Austin, Texas 78763	14. Sponsoring Agency Code

15. Supplementary Notes

Work done in cooperation with the Federal Highway Administration, Department of Transportation.
Research Study Title: "Surface Dynamics Road Profilometer Applications"

16. Abstract

An investigation into the characterization of surface profile and roughness on bridges and the adjoining pavement has been made and the results are reported herein. This investigation included the decomposition of measured roughness on a wavelength basis, thereby making possible numerous comparisons and analyses of the components of roughness. In this report of the pilot study, several methods of characterizing and contrasting roughness types between bridge deck and the adjoining pavement are presented, along with limited results obtained from the analyses of three bridge projects.

17. Key Words	18. Distribution Statement
digital filtering, General Motors Profilometer, road profile, road roughness, bridge deck roughness	

19. Security Classif. (of this report)	20. Security Classif. (of this page)	21. No. of Pages	22. Price
Unclassified	Unclassified	165	

Form DOT F 1700.7 (8-69)

THE CHARACTERIZATION OF ROAD ROUGHNESS ON BRIDGE DECKS AND THE ADJOINING PAVEMENT

by

David B. Law
Hugh J. Williamson
W. Ronald Hudson

Research Report Number 156-4

Surface Dynamics Road Profilometer Applications
Research Project 3-8-71-156

conducted for

The Texas Highway Department

in cooperation with the
U. S. Department of Transportation
Federal Highway Administration

by the

CENTER FOR HIGHWAY RESEARCH
THE UNIVERSITY OF TEXAS AT AUSTIN

April 1975

PREFACE

This is the fourth in a series of reports presenting results from Research Project 3-8-71-156, "Surface Dynamics Road Profilometer Applications." The project was initiated to carry out the implementation and operation of the Surface Dynamics Road Profilometer in field and research applications for the Texas Highway Department.

Although continual efforts will be made to improve the measurement accuracy and efficiency, the SD Profilometer is already an effective measurement system, as evidenced by the numerous successful research results obtained in the last few years.

This report discusses the use of road profile information obtained with the SD Profilometer to analyze road roughness from the standpoint of comparing and characterizing surface roughness present on bridge decks and the adjoining pavement.

The authors appreciate the helpful suggestions made by Texas Highway Department Contact Representative James L. Brown. Special appreciation goes to Mr. H. H. Dalrymple whose continual development of this equipment has made its use here possible. Mr. Noel Wolf is also thanked, for his engineering consultation and SDP measurements.

David B. Law
Hugh J. Williamson
W. Ronald Hudson

April 1975

LIST OF REPORTS

Report No. 156-1, "Correlation Study of the Mays Road Meter with the Surface Dynamics Profilometer," by Roger S. Walker and W. Ronald Hudson, discusses a study of the correlation between measurements made with the Mays Road Meter and the Surface Dynamics Profilometer and, based on this study, provides a set of calibration, operation, and control procedures for operation of the Mays Road Meter using serviceability index values from the profilometer as a measurement standard.

Report No. 156-2, "The Use of Spectral Estimates for Pavement Characterization," by Roger S. Walker and W. Ronald Hudson, discusses the general uses of road profile spectral estimates for pavement characterization. A model for predicting serviceability index based on road profile amplitude estimates is also described.

Report No. 156-3, "Analysis of Characteristic Roughness Patterns in Pavement and the Relationship Between Roughness and Pavement Distress," by Hugh J. Williamson and W. Ronald Hudson, discusses the characterization and comparison of the roughness on pavements of differing types and ages. The application of digital filtering is treated, and pilot study results are presented.

Report No. 156-4, "The Characterization of Road Roughness on Bridge Decks and the Adjoining Pavement," by David B. Law, Hugh J. Williamson and W. Ronald Hudson, discusses the characterization and comparison of the roughness on bridge decks and the adjoining pavement. Several methods of analysis are presented for analyzing various components of roughness.

ABSTRACT

An investigation into the characterization of surface profile and roughness on bridges and the adjoining pavement has been made and the results are reported herein. This investigation included the decomposition of measured roughness on a wavelength basis, thereby making posssible numerous comparisons and analyses of the components of roughness. In this report of the pilot study, several methods of characterizing and contrasting roughness types between bridge deck and the adjoining pavement are presented, along with limited results obtained from the analyses of three bridge projects.

KEY WORDS: digital filtering, General Motors Profilometer, road profile, road roughness, bridge deck roughness

SUMMARY

The types of road roughness present on bridge decks differ appreciably from the roughness existing on the adjoining pavement. Through various methods of analysis, these different types can be characterized and compared. In the pilot study discussed herein, the roughness of three bridges and the adjoining pavement was examined in some detail.

Through the process of digital filtering, whereby a new profile is computed from the original road profile in order to isolate the type of roughness which is of specific interest, e.g., that with wavelengths from 0 to 15 feet, it is seen from observation of both the filtered and original road profile plots that

(1) short wavelength roughness (0 to 15 feet) is generally much more prevalent on the bridge deck than on the adjoining pavement, with the roughness increasing significantly at approximately 50 feet in advance of the bridge;

(2) long wavelength roughness (60 feet or more) tends to increase slightly near the beginning of the bridge, and then tends to disappear on the bridge deck itself;

(3) waves corresponding to the span length are noticeable on the bridge deck and possess amplitudes on the order of .1 inch;

(4) the bumps at the end of the bridge consist of extremely short wavelength roughness, with amplitudes of approximately .25 inch; and

(5) similar short wavelength roughness exists at the expansion joints, although the amplitudes generally tend to be smaller.

Mean amplitude-wavelength charts can be used to compare the mean of the roughness amplitudes observed on the bridge deck to the mean amplitudes observed on the adjoining pavement, as a function of the wavelength of the road surface irregularities. For each of the three projects studied, it is seen that

(1) significant differences in roughness amplitudes generally occur between adjoining pavement and bridge deck for both long and short wavelength roughness, and

(2) lane-to-lane variations within each pavement type (bridge deck or adjoining pavement) tend to be less than the differences between pavement types themselves.

Certain statistical techniques, particularly nested analysis of variance, are valuable in making quantitative comparisons of roughness present on bridge decks and on the adjoining pavement. Through these various techniques, the following features were observed:

(1) The repeat measurement variation of the profilometer is small enough so that differences between wheelpaths in the same lane can be recognized in spite of random errors.

(2) Differences from lane-to-lane are not significantly greater than the differences from wheelpath-to-wheelpath within the individual lanes from either pavement type.

(3) The largest percentage of variance among roughness amplitudes is explained by differences in pavement type whereas the smallest percentage of variation is generally explained by differences between the lanes. Other sources of roughness variance considered include wheelpath-to-wheelpath differences and differences between replicate measurements.

In addition to measures of overall roughness, methods are available for studying measures of the worst roughness in a given section. By means of numerical comparisons of the roughness amplitude distribution measures, the type of road roughness both on the bridge deck and the adjoining pavement can be characterized. Analyzing the results of this study shows that

(1) the type of roughness present depends on the span length -- the greater this length, the less objectionable the roughness;

(2) for short wavelength roughness, the amplitudes on the bridge deck are generally both more severe and more diverse than those found on the adjoining pavement, while, for the long wavelength roughness, the amplitudes on the bridge deck tend to be fairly uniform and less severe than those on the adjoining pavement;

(3) for short wavelengths, the transverse roughness (rolling effect) is worse than the longitudinal roughness, and

(4) this transverse roughness tends generally to decrease with increasing wavelength on the bridge deck, and it is fairly uniform at longer wavelengths and diverse at shorter wavelengths.

IMPLEMENTATION STATEMENT

The objective of this report is to present findings obtained in a pilot study done under Project 156. That study involved the comparison of various types of roughness found on bridge decks and the pavement immediately adjoining these bridges. Methods of analysis are demonstrated, and, within the scope of a pilot study, results are presented.

The basic objective of this study was to gain insights into the types of roughness present on and near bridges, so that further steps can be taken towards improving maintenance processes by which roughness in this area can be alleviated. A full-scale study could prove the capability to accomplish this.

The following steps, which would also be necessary for conducting such a full-scale study, were carried out in the investigation reported herein. Mathematical tools for analyzing road profile data have been developed. The digital filtering and statistical methods demonstrated in this report can be used to describe the condition of a road surface on the basis of (a) the lengths of the roughness waves, (b) the overall average amplitude of a section, and (c) the presence of a few severe bumps.

TABLE OF CONTENTS

CHAPTER 1. INTRODUCTION

The purpose of this report is to present several methods of characterizing and comparing road roughness patterns on bridge decks and the adjoining pavements. This report of the work which was intended as a pilot study also includes limited results obtained from the analyses of three bridge projects studied in detail. The study was concerned with three major areas of interest: the adjoining pavement, the bump at the transition from adjoining pavement to bridge deck, and the bridge deck itself.

BACKGROUND

Road roughness is a problem which has faced pavement engineers ever since the first road was constructed. While considerable effort has been directed towards improving the quality of the riding surface, roughness still remains a severe problem for today's engineers. Because the concepts of performance and serviceability are based heavily on surface roughness, a better insight into the problems and causes of road roughness is needed.

It is generally agreed that the purpose of a road is to provide a comfortable, safe, and convenient method of travel for drivers and their passengers and for the transporting of commodities. How well a pavement satisfies this purpose at a specific time is called its serviceability. Performance is a measure of a pavement's serviceability-age history. In order to determine a pavement's serviceability, subjective measures of that pavement's present riding quality, called the Present Serviceability Rating (PSR), are obtained. A panel of typical road users rate the riding quality of the road on the scale of zero to five, with zero indicating an impassible road surface and five a perfect ride. The average of each of these users' ratings is the PSR. For more information see Ref 1.

Several factors are known to have an influence on the serviceability rating given a road section by an individual. These factors include cracking, patching, rut depth, surface deterioration, and profile roughness. From studies described in Ref 2, 89 percent of the variation in PSR was explained by variations in the road profile roughness, thereby indicating that roughness of the road profile is highly correlated with pavement serviceability.

Thus, it can be seen that if a pavement is to maintain a high level of performance, it is essential that objectionable road surface roughness be eliminated, or at least significantly reduced. Therefore, investigation of this roughness is necessary if improvements in the pavement design system are to be accomplished. While objectionable road roughness can occur anywhere, there are several areas where this roughness is especially noticeable. Included in this category are railroad crossings, swelling clay sections, and bridge decks with their adjoining pavements. Each of these is common enough and the roughness severe enough to merit special individual studies.

Several methods of analysis, both qualitative and quantitative, exist that are capable of roughness characterization. By use of such mathematical techniques as power spectra and digital filtering, the road roughness can be decomposed on a wavelength basis, thereby making possible numerous comparisons and analyses involving the components of roughness. Comparisons of roughness patterns among various pavement types can be made with the use of these techniques.

PROJECT DESCRIPTIONS

The detailed investigation of objectionable road roughness is necessary if significant improvements in pavement performance are to be accomplished. In the case of roughness on and adjacent to bridge decks, numerous bridges of various types must be observed and analyzed. Such an undertaking is beyond the scope of the work reported here, which was intended solely as a pilot study. However, three projects that include bridge decks were closely studied in an attempt to compare and characterize the surface roughness of the bridge decks and the adjoining pavements. The three projects studied in detail include the MoPac project, the Big Sandy project, and the Plum Creek project. The physical details of each project are presented in this section, along with a description of which types of filtered profile plots were used. A description of the method of obtaining filtered output from a road surface profile is given in some detail in Chapter 2. Table 1.1, at the end of this chapter, summarizes the details of each of the three projects.

MoPac Bridge Project

The MoPac Bridge project is located in southwest Austin. The data for the recently constructed project was collected at the end of 1973, just before the road was to be opened for public use. Only the southbound lanes were accessible at the time of measurement with the profilometer. The area of interest included two bridges with a 900-foot flexible pavement section in between. While the first bridge was not studied in detail nor included in the chapter on visual observation of the profile plots, it did have a significant effect upon the roughness observed on the flexible pavement since 100-foot waves were constructed here. This effect, caused by the stationing of the project, is discussed in Chapter 3. Although the second bridge was about 1400 feet long, only about 1000 feet were available for measuring by the profilometer because of construction barriers and the need for a safe stopping distance. This bridge consisted of a Portland cement concrete decking with 97-foot span lengths. Two replicate runs with the profilometer were made in each lane.

For the MoPac project, only plots of the right profile and the right-left difference profile for a measure of transverse roughness for the 0 to 15-foot passband are included in Appendix A, although plots of the left profile were also obtained. Wavelengths greater than this were not plotted due to the long span lengths of the bridge and to the fact that, during the measurement with the profilometer, very short wavelengths, on the order of 5 feet or less, were felt by the profilometer operators whereas no sensation of longer wavelengths was felt. Visual observation of the unfiltered profile plots confirmed the suspicion that no significant long wavelength roughness existed on the MoPac Bridge at time of measurement with the profilometer. Only one lane was plotted, as significant variations from lane to lane should have been nonexistent since this roadway section was not yet open to traffic. Analysis of variance studies showed that at the 90 percent confidence level, lane to lane differences were insignificant at all wavelengths of interest. Variations from wheelpath to wheelpath were small enough that it was not necessary to include the plots of the left profile in this report.

Big Sandy Bridge Project

The Big Sandy Bridge is located in Llano County, on Highway 71. Approximately 20 miles east of Llano, the bridge carries an annual average daily traffic of about 1000 vehicles. The bridge consists of ten 48-foot spans and provides two lanes, one in each direction. Two replicate runs with the profilometer were made in each lane.

For the Big Sandy Bridge, three passbands were studied. The 0 to 15-foot passband was of particular interest because of the short wavelengths. Roughness corresponding to 30-foot to 60-foot wavelengths was included because this passband was centered at approximately the span length of the bridge, 48 feet. The other passband studied ranged from 80 feet to 110 feet and was centered at twice the span length of the bridge. These latter two passbands were included to study the effect that span length might have upon bridge deck roughness.

Plots of both lanes on the bridge are included in Appendix A, since differences between lanes were expected to be significant because of the effects of time and traffic. For each lane, both the right profile and the right-left difference profile are included. The left profile was plotted but not included in Appendix A, however, as it was felt that enough information could be obtained from the other plots.

Plum Creek Bridge Project

Plum Creek Bridge is located on Highway 183 in Caldwell County, south of Luling, about one mile north of Interstate 10. This section of roadway has an annual daily traffic of approximately 3500 vehicles. This project consists of two separate roadways and bridges, one for each direction. Each bridge has two lanes. The bridge decks are comprised of concrete slabs overlaid with hot mix asphalt, while the adjoining pavement on both sides consists of asphaltic concrete. The northbound bridge consists of five 39-foot spans followed by 37 spans whose length is either 30 feet or 30.5 feet, a total length of 1310 feet. The bridge is much newer than the southbound bridge, which has a total length of approximately 1200 feet. The southbound bridge consists of thirty-six 28.5-foot spans followed by a 121-foot metal trestle and two more 28.5 foot spans. In addition, approach ramps of about 15 feet are present on both sides of this bridge. In addition, this bridge contains a benchmark dated 1935.

For the southbound bridge, only the right profile plot of the outside lane is included. Due to the length of the bridge, two sets of plots were made so that the entire length of the bridge as well as sufficient sections of adjoining pavement on either side could be studied. This was done partially because of the steel trestle which was part of the bridge and because the effect that this bridge within a bridge was of interest; and partially because a comparison of the bumps at both ends of the bridge was desired. Thus, a plot of the entire bridge deck profile is available for the 0 to 15-foot passband. Rather than use the same upper passband for both sets of plots, it was felt that enough information for a given passband could be obtained from half of the bridge deck, and that a different passband could be used for each set of plots. Therefore, a 60 to 100-foot passband was used for the first half of the bridge, while a 15 to 60-foot passband was used for the second half of the bridge.

For the northbound bridge over Plum Creek, the right profile plots for both lanes are included. For the inner lane, a 0 to 15-foot passband was used to observe the short wavelengths, while a 60 to 100-foot passband was used to observe the longer wavelengths. Four passbands for the outer lane were studied. In addition to the 0 to 15-foot passband and the 60 to 100-foot passband, a 20 to 40-foot passband was used to observe waves having a length coinciding with the span length of about 30 feet. A 50 to 70-foot passband was also used, to study waves twice as long as the span length. Due to the length of the bridge, it was impossible to plot the entire bridge deck with just one set of plots. Therefore, only about the first 800 feet of the bridge deck was plotted, along with about 130 feet of adjoining pavement.

OVERVIEW

Chapter 2 contains a description of the methods used to analyze the various components of roughness. This section includes descriptions of the profilometer, amplitude vs. wavelength analysis, and statistical analysis of roughness data. If the reader is interested only in the results, Chapter 2 can be skipped without a lack of continuity. Chapter 3 contains a summary of the overall comparison of the roughness on the bridge deck versus the roughness on the adjoining pavement by direct visual observations of road surface profile plots. Also included in Chapter 3 is the study of the bump at the end of the bridge and the effect of waves on the bridge deck that are coincident with the span length of the bridge. Chapter 4 includes the comparison of roughness on bridge decks and the adjoining pavement through the use of various mathematical techniques such as power spectral analysis, digital filtering, and analysis of variance. The purpose is to supplement the visual observation of Chapter 4 with quantitative analyses. In addition to examination of roughness patterns on bridges and the nearby pavements, the replication errors of the roughness amplitudes computed from road surface profiles measured by the THD General Motors Surface Dynamics Profilometer are studied in some detail and shown to be small enough for almost any practical purpose. Chapter 5 contains the report summary and conclusions. Included in Appendix A is a detailed description of the filtered profile plots as well as the plots themselves. Chapter 3 summarizes these observations. Appendix B contains the results of the roughness amplitude distribution study discussed in Chapter 4.

TABLE 1.1. PROJECT INFORMATION

Project	Span Length	No. of Lanes	Surface Type	AADT	Bridge Length	Type of Profilometer Runs Used	Location
Mopac Bridge Project	97'	3 per direction	Portland cement bridge deck asphaltic concrete adjoining pavement	None	~1400'	2 runs for each of 2 lanes	Southwest Austin Mopac Freeway
Big Sandy	48'	1 per direction	Same as above	~1000	480'	2 runs for each lane	Highway 71 Llano Co.
Plum Creek	28.5'-39' varies	2 per direction	Hot mix overlay on concrete slabs adjoining pavement is asphaltic concrete	~3500	~1300' northbound ~1200' southbound	1 run for each lane	Highway 183 Caldwell Co.

CHAPTER 2. DISCUSSION OF METHODS

GENERAL MOTORS PROFILOMETER

The road profile data which were necessary for this study were collected with the Texas Highway Department General Motors Surface Dynamics Profilometer operated by the Center for Highway Research.

A road profile is obtained by the profilometer by means of two small road wheels which are mounted on trailing arms underneath the vehicle, one in each wheelpath. These road wheels are held in contact with the pavement surface by a 300 lb. spring force. The relative motion of each road wheel and the vehicle body is then measured by a potentiometer. Accelerometers attached to the vehicle body measure the vertical acceleration of the vehicle relative to an earth-fixed coordinate system. This information is then input into an analog computer where it is double-integrated and then combined with the information gathered from the two potentiometers to obtain the true road profile. Thus, the profilometer provides, for each pavement section, separate analog profile records for both the right and left wheelpaths.

This description of the process of obtaining a true road profile has been simplified. If a greater understanding of the mechanics of the profilometer is sought, many sources are readily available, including Refs 3 and 4.

ANALYSIS OF ROUGHNESS PATTERNS VIA AMPLITUDE VS. WAVELENGTH DATA

The road profile information measured by the profilometer and presented in the section on qualitative analysis is valuable for obtaining a visual impression of roughness patterns and studying certain special effects. Calculation of roughness measures, however, facilitates further analysis.

In particular, we are interested in the degree of roughness at various wavelengths. An approach for decomposing the roughness on the basis of wavelength by using power spectra is discussed in Ref 2. Basically, the fast Fourier transform is used to compute the power spectrum, and the power values are converted to r.m.s. amplitude estimates. This is done by computing the r.m.s. amplitude of the sinusoid at the center of each frequency band which has the power spectral value actually computed.

The mathematics of the power spectral calculations are covered in Appendix 1 of Ref 2. The important point here is that r.m.s. amplitude estimates are obtainable for comparing road profiles on the basis of roughness of various wavelengths.

STATISTICAL COMPARISONS AMONG ROUGHNESS AMPLITUDES

We now consider statistical comparisions among road profiles. We will explore the following questions:

(1) Is the repeat measurement variation small enough so that differences between wheelpaths in the same lane can be recognized in spite of random errors?

(2) Are the differences from lane to lane significantly greater than the differences from wheelpath to wheelpath within the individual lanes?

(3) Are the differences from bridge deck to nearby pavement significantly greater than the differences from lane to lane within either bridge deck or pavement?

These three questions will be considered separately for each of a set of wavelengths. Questions 1 and 3 are of primary interest.

Question 1 is of interest because of its importance relative to the measurement accuracy of the profilometer; if the system is capable of measuring wheelpath differences within the same lane, then surely the accuracy is good enough for any reasonable practical purpose. This implies that the run-to-run, or replicate run, measurement errors are so small that differences between lanes are distinguishable.

Question 3 is important in identifying and comparing characteristic roughness patterns on bridges and approaching pavements.

The three questions can be addressed by using a nested analysis of variance approach (Ref 5). The "nesting" arrangement for this study is shown in Fig 2.1.

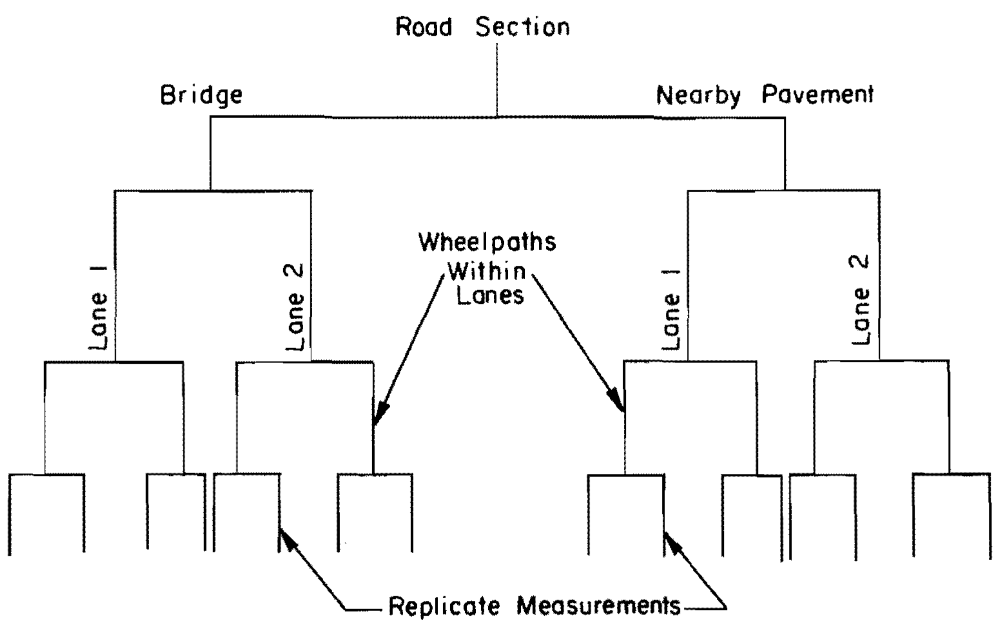

Fig 2.1. Nested Analysis of Variance

Thus, we consider the following mathematical model.

$$Y_{ijkl} = \mu + S_i + L_{ij} + W_{ijk} + e_{ijkl},$$

where

Y_{ijkl} = the measured amplitude (for a given wavelength) on the nearby pavement if $i = 1$ and on the bridge if $i = 2$, in lane j, wheelpath k, replicate measurement l;

μ = the overall average amplitude for this wavelength;

S_i = the effect of the i^{th} structure (bridge, nearby pavement);

L_{ij} = the effect of the j^{th} lane on the i^{th} structure;

W_{ijk} = the effect of the k^{th} wheelpath of the j^{th} lane in structure i; and

e_{ijkl} = a measurement error term.

Thus, considering the terms S, L, W, and e to be random variables,* the three questions above can be restated mathematically as follows:

(1) Is $\sigma_\omega^2 = 0$?

(2) Is $\sigma_L^2 = 0$?

(3) Is $\sigma_S^2 = 0$?

It is precisely these questions that analysis of variance addresses. The nested analysis of variance approach is summarized in Table 2.1.

The mean squares (MS) are the sums of squares divided by the corresponding numbers of degrees of freedom. The expected mean squares are simply the expected values of the mean squares.

Thus, to test the hypothesis $\sigma_S^2 = 0$, we use the test statistic

*If the bridge-nearby pavement effect were considered "fixed" (in analysis of variance terms), we would simply replace σ_S^2 by $(S_1^2 + S_2^2)/(2-1) = S_1^2 + S_2^2$. The analysis would be otherwise unaffected.

TABLE 2.1. ANALYSIS OF VARIANCE SUMMARY

Source	Degrees of Freedom	Sum of Squares (SS)	Expected Mean Square (EMS)
Structure	n_S-1	$\sum_{i=1}^{n_S} (\overline{Y}_{i...} - \overline{Y}_{....})^2$	$\sigma_e^2+n_e\sigma_w^2+n_w n_e\sigma_L^2+n_e n_w n_L\sigma_S^2$
Lane	$(n_L-1)n_S$	$\sum_{i=1}^{n_S} \sum_{j=1}^{n_L} (\overline{Y}_{ij..}-\overline{Y}_{i...})^2$	$\sigma_e^2+n_e\sigma_w^2+n_w n_e\sigma_L^2$
Wheelpaths	$(n_w-1)n_L n_S$	$\sum_{i=1}^{n_S} \sum_{j=1}^{n_L} \sum_{k=1}^{n_w}(\overline{Y}_{ijk.}-\overline{Y}_{ij..})^2$	$\sigma_e^2+n_e\sigma_w^2$
Error	$(n_e-1)n_w n_L n_S$	$\sum_{i=1}^{n_S} \sum_{j=1}^{n_L} \sum_{k=1}^{n_w} \sum_{l=1}^{n_e}(\overline{Y}_{ijkl}-\overline{Y}_{ijk.})^2$	σ_e^2

n_S, n_L, n_w, and n_e are the numbers of "levels" of the various factors; e.g., n_L is the number of lanes included in either the bridge or the nearby pavement. The dot and bar notation indicate averages; for example,

$$\overline{Y}_{ij..} = \frac{1}{n_w n_e} \sum_{k=1}^{n_w} \sum_{l=1}^{n_e} Y_{ijkl} \quad .$$

$$\frac{MS(\text{Structures})}{MS(\text{Lanes})} .$$

From the EMS column, we see that numerator and denominator have the same expected value if $\sigma_s^2 = 0$, but the expected value of the numerator is larger by $n_e n_w n_L \sigma_S^2$ if $\sigma_S^2 \neq 0$. The other two hypothesis tests are motivated similarly.

COMPONENTS OF VARIANCE

We now consider the variance contributions of the various factors, S (structure), L (lane), w (wheelpath), and e (error). The purpose of this statistical test is to determine, for a given road section including adjoining pavement and a bridge, (1) the percentage of the variation among roughness amplitudes attributable to measurement error, for each of a set of wavelengths, and (2) the amount of variation attributable to differences between the bridge and the nearby pavement?

Using MS to denote mean square as before, and referring to Table 2.1, we see

$$E(MS(\text{Structure})) - E(MS(\text{Lane})) = (\sigma_e^2 + n_e\sigma_w^2 + n_w n_e \sigma_L^2 + n_e n_w n_L \sigma_S^2) - (\sigma_e^2 + n_e \sigma_w^2 + n_w n_e \sigma_L^2) = n_e n_w n_L \sigma_S^2 .$$

Thus, $\dfrac{MS(\text{Structure}) - MS(\text{Lane})}{n_e n_w n_L}$

is an estimate of σ_S^2 .

Estimates of σ_L^2, σ_w^2, and σ_e^2 are obtained similarly.

Thus it is estimated that

$$\sigma_L^2 = \frac{MS(\text{Lane}) - MS(\text{Wheelpath})}{n_e n_w}$$

$$\sigma_w^2 = \frac{MS(\text{Wheelpath}) - MS(\text{Replication})}{n_e}$$

$$\sigma_e^2 = MS(\text{Replication})$$

The components of variance for a given wavelength are then determined by the percentage of variation contributed by each specific factor compared to the overall variance.

ROUGHNESS AMPLITUDE DISTRIBUTION MEASURES

While the methods presented above involve only an overall measure of roughness, it is desirable to take into account the variability of roughness within a given section of roadway. There may be areas of extreme roughness which adversely affect the pavement's riding quality to a measurable extent but are averaged out over a section of roadway so that their impact is basically unnoticeable. That is, the averaging of these extreme amplitudes with all the remaining roughness of the same wavelength over the length of pavement section of interest tends to minimize the effect of these areas.

In order to analyze these localized areas of severe roughness, it is first necessary to mathematically compute artificial profiles from the actual road profile. These artificial profiles contain only specified roughness, such as the 0 to 15-foot wavelengths. Measures of local roughness can then be computed at discrete steps throughout the section. Local measures are obtained from the profile data over a length equal to the upper bound of the passband, with a step size of approximately 2 inches.

From these local roughness measures, it is possible to compute the distribution for each passband of interest. Various measures can then be defined in terms of percentiles. For this study, the 50th percentile, commonly called the median, and the 75th, 90th, 95th, and 99th percentile amplitudes were calculated. The qth percentile is defined as the measure which exceeds or equals exactly q percent of all measures. Thus, the 90th percentile, for example, is the amplitude which is greater than or equal to exactly 90 percent of all the local roughness amplitudes.

This process can be carried out for both longitudinal roughness and transverse roughness, obtained from the right-left difference profile. Through such measures of local roughness, a better characterization of road roughness can be developed.

CHAPTER 3. GENERAL DISCUSSION OF THE QUALITATIVE ANALYSIS OF ROAD ROUGHNESS DATA

This chapter contains a discussion of the findings obtained from visual observation of the road profile plots of the three projects studied in detail, the MoPac project, the Big Sandy project, and the Plum Creek project. Several profile plots are also included to illustrate and clarify the discussion. To aid the reader in better understanding these profile plots, vertical lines have been placed along the position scale of these plots to indicate features of the bridge deck that are of interest. A long mark is used to indicate either the beginning or end of the bridge deck, while a short mark is used to indicate the location of expansion joints. A more detailed discussion of these plots is contained in Appendix A, along with the complete set of profile plots.

Road surface profiles of both the right and left wheelpaths can be accurately measured by the General Motors profilometer, currently owned by the Texas Highway Department and operated by the Center for Highway Research. These road profiles are in the form of road surface elevations observed at equally spaced distances and are an essential tool for the development of a better understanding of the changes in roughness caused by the presence of any physical structure, in this case bridge decks. From the plots of both the filtered and unfiltered profiles, a great amount of information can be obtained merely by visual observation.

Here, digital filtering is referred to as a method for computing a new profile from the original road profile in order to isolate a certain type of roughness which is of specific interest, e.g., that with wavelengths from 0 to 15 feet. Thus, the components of the road roughness can be observed and analyzed separately, thereby enabling a more thorough investigation into roughness characterization.

The reader should be aware of one slight problem in using road profile plots directly. The operation of the electronic measuring system aboard the profilometer requires certain processing (analog filtering) of the road profile data which introduces a frequency dependent "phase shift." This "phase shift" is simply a positive spatial translation of the waves. While the short waves are virtually unaffected, roughness with wavelengths longer than 32 feet is shifted somewhat to the right on the profile plots; the longer the wavelength, the greater this phase shift. Thus, some of the long wavelength roughness on the adjoining pavement appears to extend onto the bridge by a fraction of a wavelength. While further work is needed to formulate and implement an acceptable cure for the phase shift problem, much meaningful information can be obtained from the present data as long as this problem is recognized. The reader who is interested in studying the characteristics of the frequency response to phase shift should see pages 8-10 of Ref 3.

SHORT WAVELENGTH ROUGHNESS

It is observed from Figs 3.1 through 3.4 that the profile is much smoother on the adjoining pavement than it is on the bridge deck for all three projects studied. This is due to the increased amplitudes of the short waves that occur after they pass onto the bridge deck. On the adjoining pavement, the profile consists of short waves having small amplitudes. Beginning about 50 feet before the bridge deck, or more in the case of the MoPac project, the wavelengths and amplitudes of these short waves begin to increase. Once onto the bridge deck, the waves then tend to become very short and have much larger amplitudes than those present on the adjoining pavement.

In relation to the overall longitudinal roughness, spikes, defined here as extremely short wavelength roughness having large amplitudes, are generally very noticeable on the bridge deck where expansion joints occur, particularly on the older bridges. The amplitude of these spikes often exceeds .25 inch, as seen in Fig 3.3.

The plots presented in Appendix A of the right-left difference profile, a measure of the transverse roughness, indicate that this transverse roughness is also more severe on the bridge deck than on the adjoining pavement. On the bridge deck, it is very difficult to detect the location of the expansion joints due to the magnitude of the surrounding transverse roughness. While the spikes marking expansion joints generally have large amplitudes, the amplitudes of the normal roughness varies from about .20 inch for the Big Sandy project to about

Filter Passband: 0.0 to 15.0 ft. Wavelengths - Outer Lane - Right Profile Frame 1

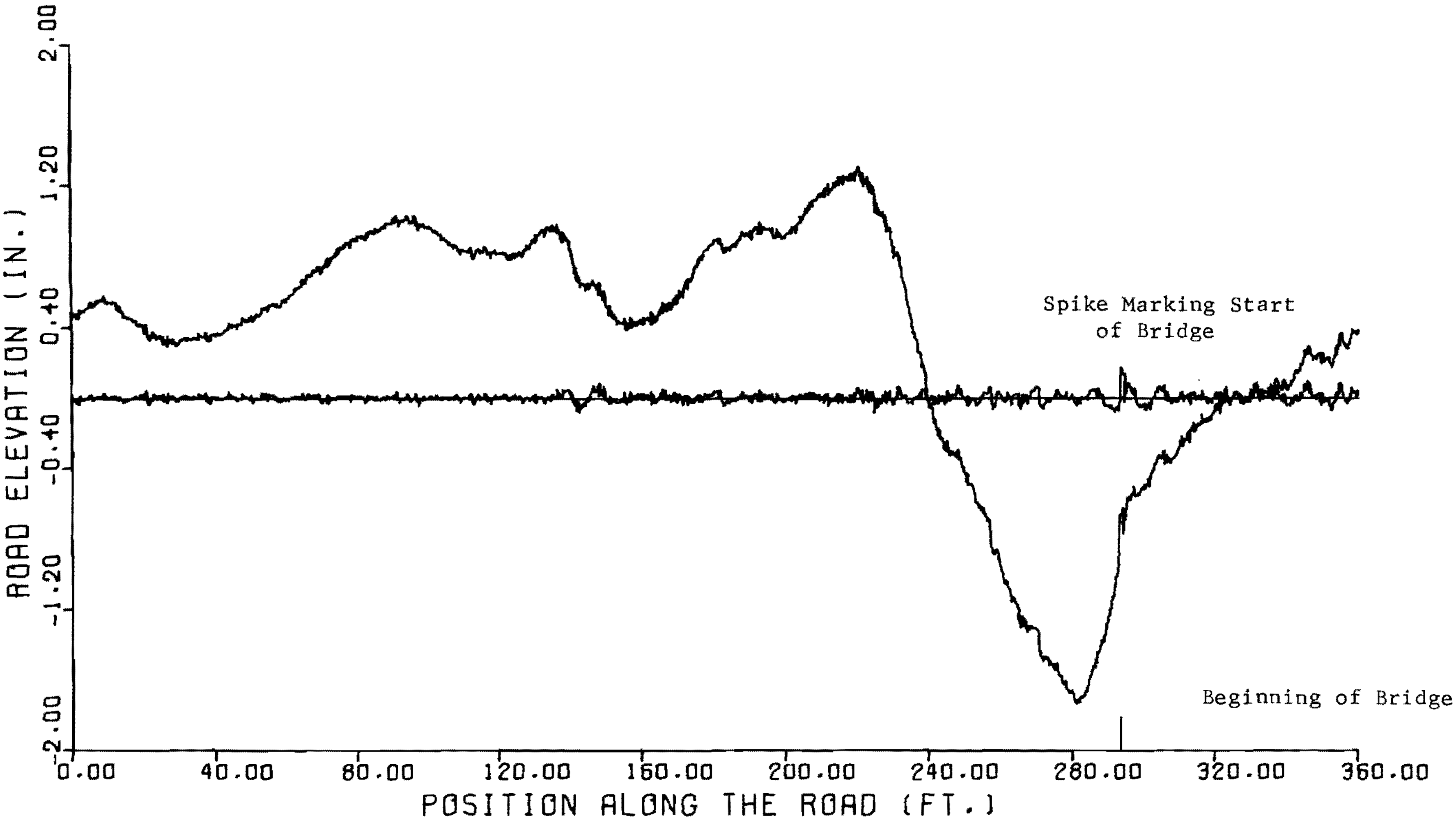

Fig 3.1. MoPac Bridge

Filter Passband: 0.0 to 15.0 ft. Wavelengths - Outer Lane - Right Profile Frame 2

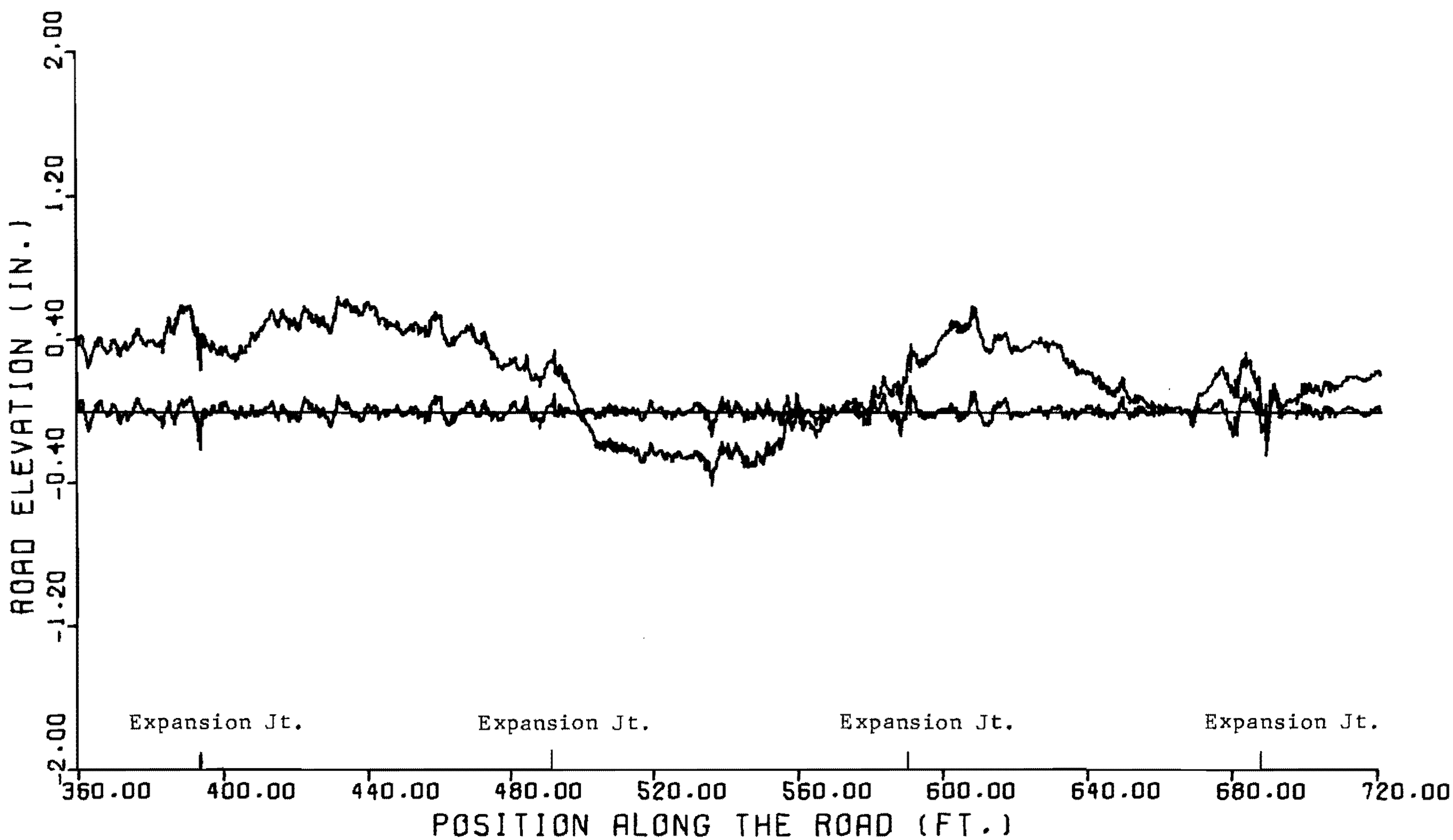

Fig. 3.2. MoPac Bridge

Filter Passband: 0.0 to 15.0 ft. Wavelengths - Westbound Lane - Right Profile Frame 2

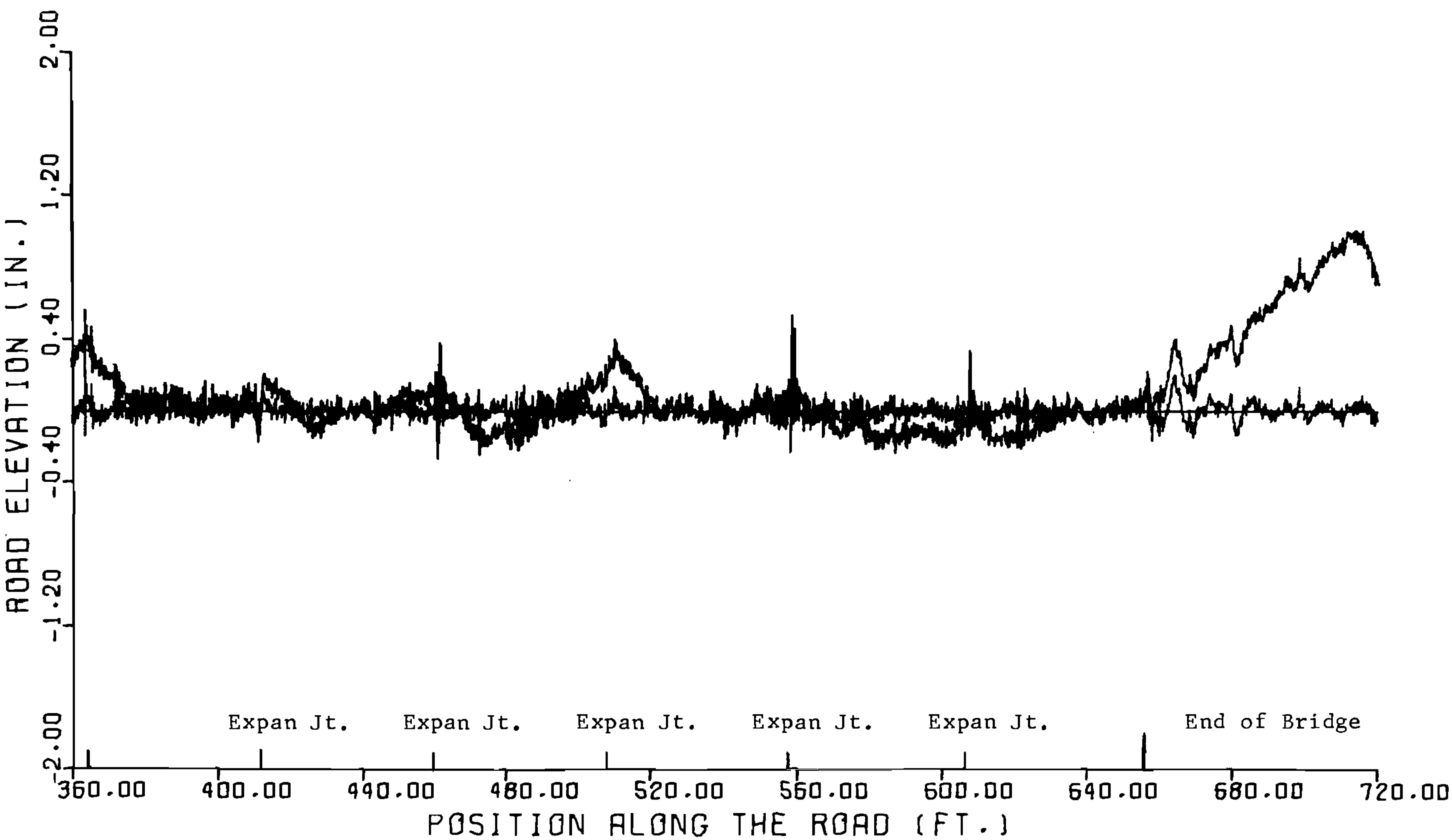

Fig. 3.3. Big Sandy Bridge

Filter Passband: 0.0 to 15.0 ft. Wavelengths - Northbound Lane - Right Profile Frame 1

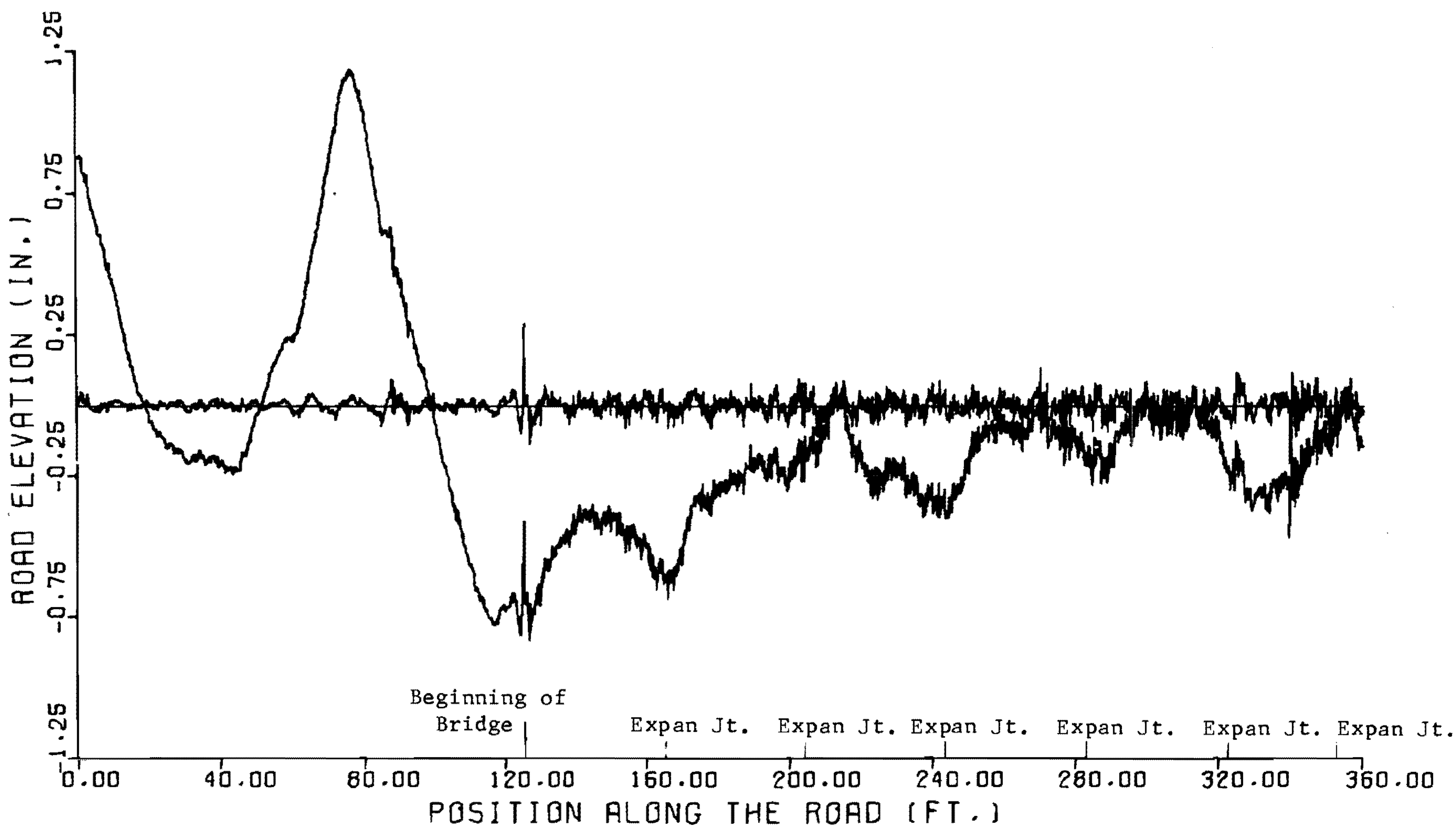

Fig. 3.4. Plum Creek Bridge

.10 inch for the MoPac project. This roughness becomes significant when it is realized that the wavelength is extremely short.

This large amplitude transverse roughness is also capable of being detected by a driver, as it tends to cause him to sway slightly from side to side. Although this effect is not severe, it is considered undesirable.

ROUGHNESS WITH WAVELENGTH CORRESPONDING TO THE SPAN LENGTH

From observation of Figs 3.5 and 3.6, which plot roughness corresponding to the span lengths of the Big Sandy and Plum Creek projects, it is readily apparent that the length of the spans of a bridge greatly influences the type of roughness found on the bridge deck. Roughness with wavelengths corresponding to the span lengths exists with generally sizable amplitudes. The peaks of these waves occur at expansion joints, which serve to locate the bridge columns. The beams span from two such columns. Vertical deflection is restrained at these locations, whereas, along the length of the span, vertical deflection is possible and should increase with both age and span length.

Several studies have been conducted which indicate that PSR is more dependent on short wavelength roughness than on roughness with long wavelength. For example, Reference 6 indicates that wavelengths on the order of 10 feet have the most effect on PSR. Thus it seems desirable to use longer spans in order to minimize the detrimental effect that the span length has on roughness. Another feasible possibility includes using a variable span length, thereby eliminating the steady rhythm caused by constant oscillation.

The amplitude of these waves is generally greatest near the center of the bridge deck, whereas, near the ends, the amplitudes are at a minimum. For the two older projects (Big Sandy and Plum Creek), short span lengths of 48 feet and about 30 feet were used, and the plots of the surface profile revealed amplitudes on the order of .1 inch for each project.

From a study of the transverse roughness plots presented in Appendix A, it is observed that the bridge deck tends to lack significant roughness corresponding to the span lengths of the bridge, although roughness can be found on the adjoining pavement with similar wavelength. Thus, it appears that transverse roughness is unaffected by the span length.

Filter Passband: 30.0 to 60.0 ft. Wavelengths - Westbound Lane - Right Profile Frame 2

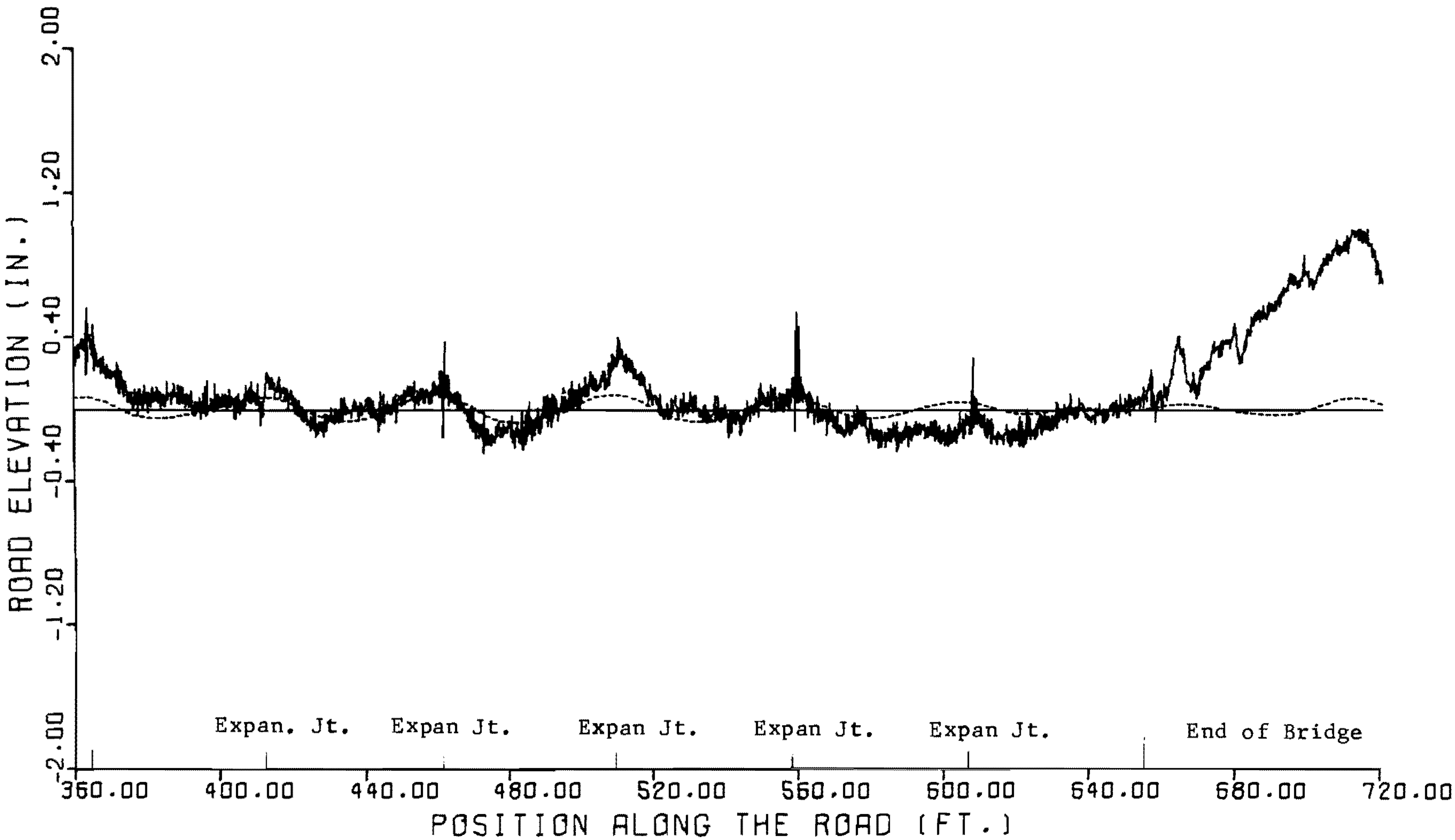

Fig. 3.5. Big Sandy Bridge

Filter Passband: 20.0 to 40.0 ft. Wavelengths - Northbound Lane - Right Profile Frame 2

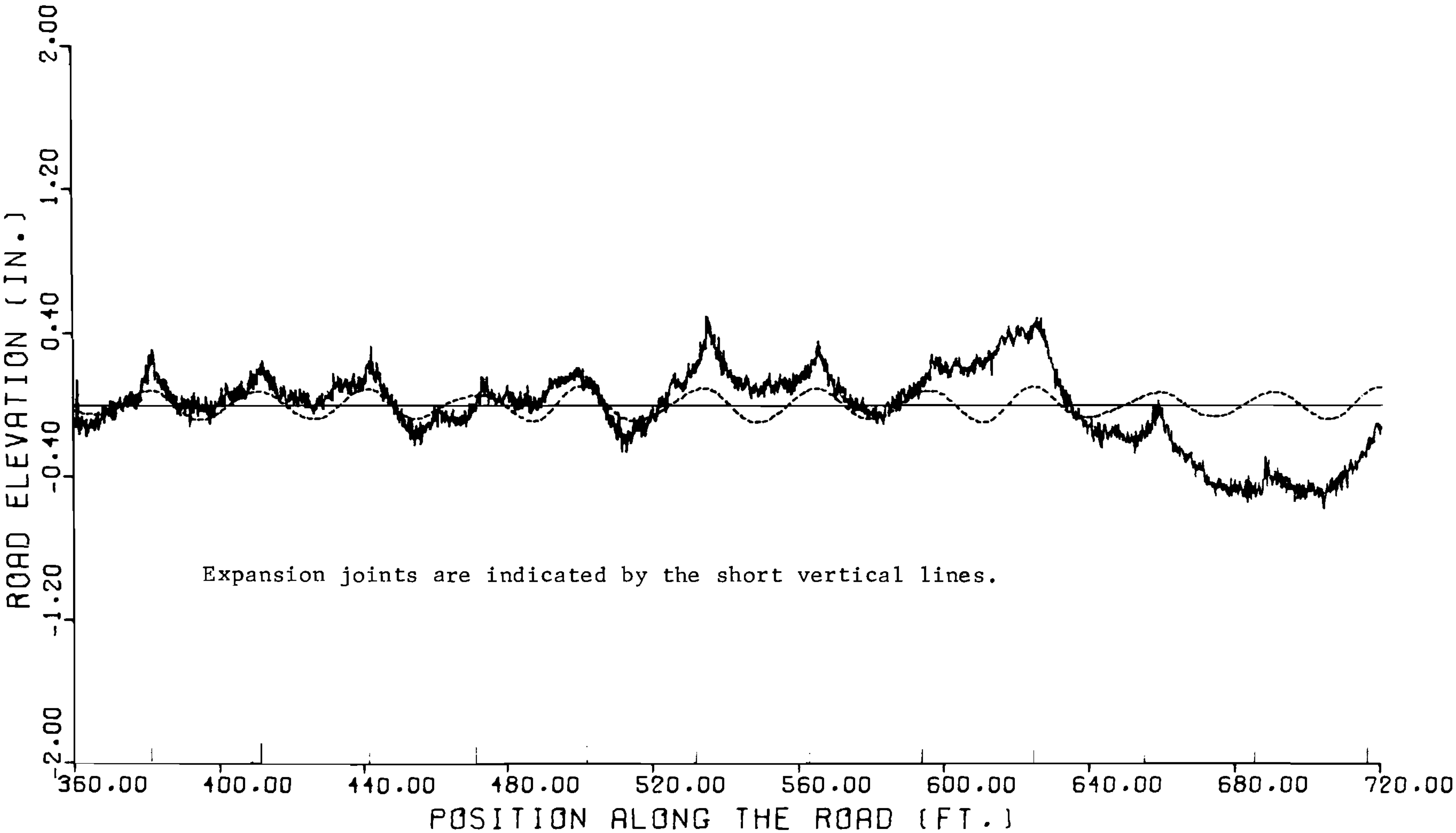

Fig. 3.6. Plum Creek Bridge

LONG WAVELENGTH ROUGHNESS

From Figs 3.7 and 3.8, it is observed that roughness with a wavelength longer than about 60 feet is virtually absent on bridge decks, whereas, immediately before and after the bridge, roughness having considerable amplitude does exist. It is also noticed that on the adjoining pavement, this roughness tends to increase as the bridge is approached.

One very interesting feature observed in Fig 3.9 is the effect that "stationing" of the MoPac project has on surface roughness. A station is a distance of 100 feet, which is used by surveyors to space grade stakes. Generally, at every 50-foot interval, or half station, the desired elevation of the roadway is marked in relation to the existing grade by means of cut or fill stakes. This allows the operators of the grading equipment to more accurately set the grade.

From Fig 3.9, it can be seen that 100-foot waves are generated, starting about 300 feet from the beginning of the bridge deck. While the elevation of these stakes appears to be the same, 100-foot waves exist, probably due to the fact that the operators of the grading equipment had too few grade stakes to "aim" for. The nearer they approached the bridge, the fewer the grade stakes available to use, which perhaps explains why the amplitude became greater. This problem could be minimized by decreasing the distance between grade stakes when approaching a bridge, or any other structure. In practice these grade stakes may be actually placed every 25 feet, although the profile plots seem to strongly indicate a 50 foot spacing.

Filter Passband: 80.0 to 110.0 ft. Wavelengths - Westbound Lane - Right Profile Frame 1

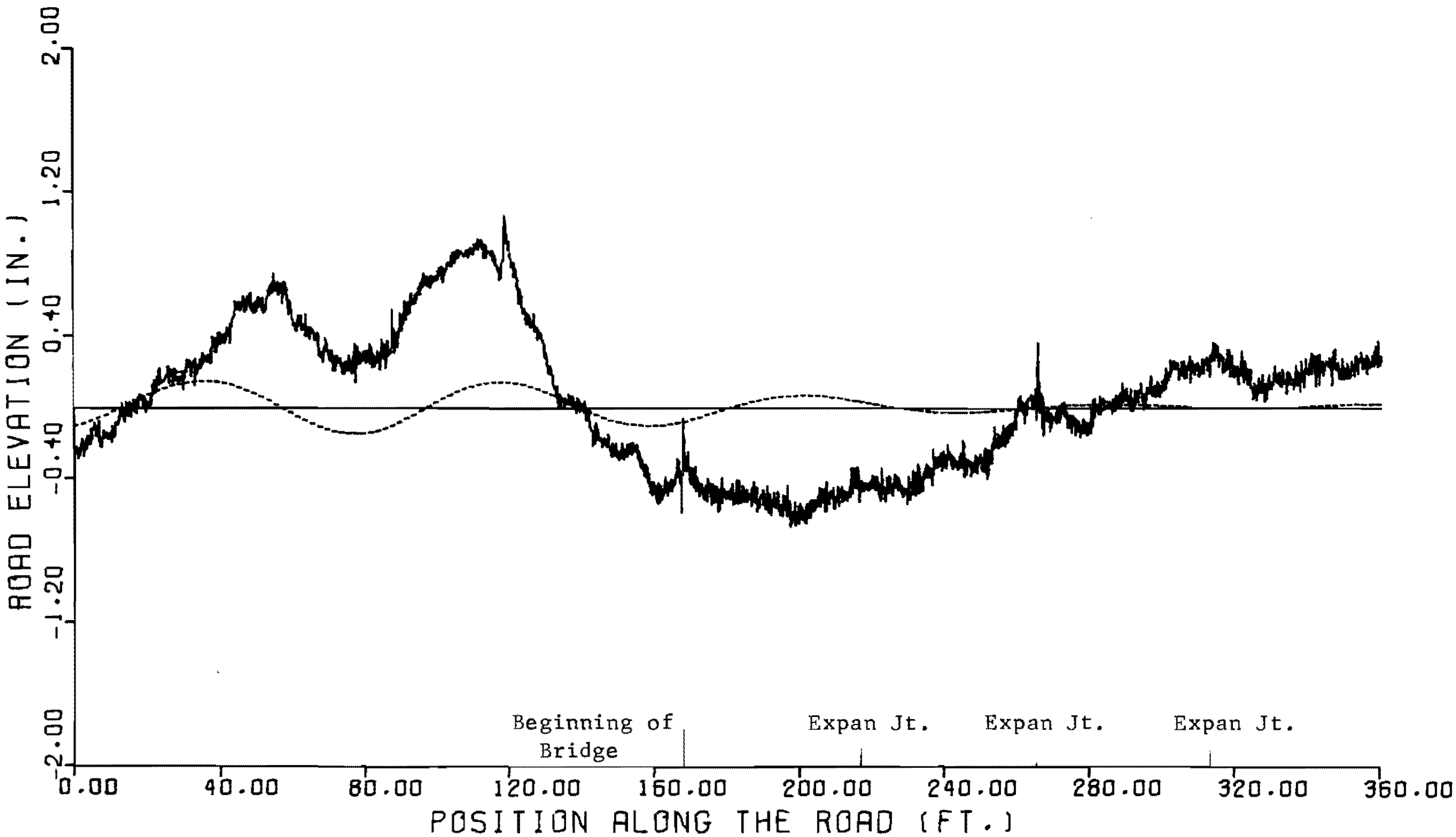

Fig. 3.7. Big Sandy Bridge

Filter Passband: 60.0 to 100.0 ft. Wavelengths - Northbound Lane - Right Profile Frame 1

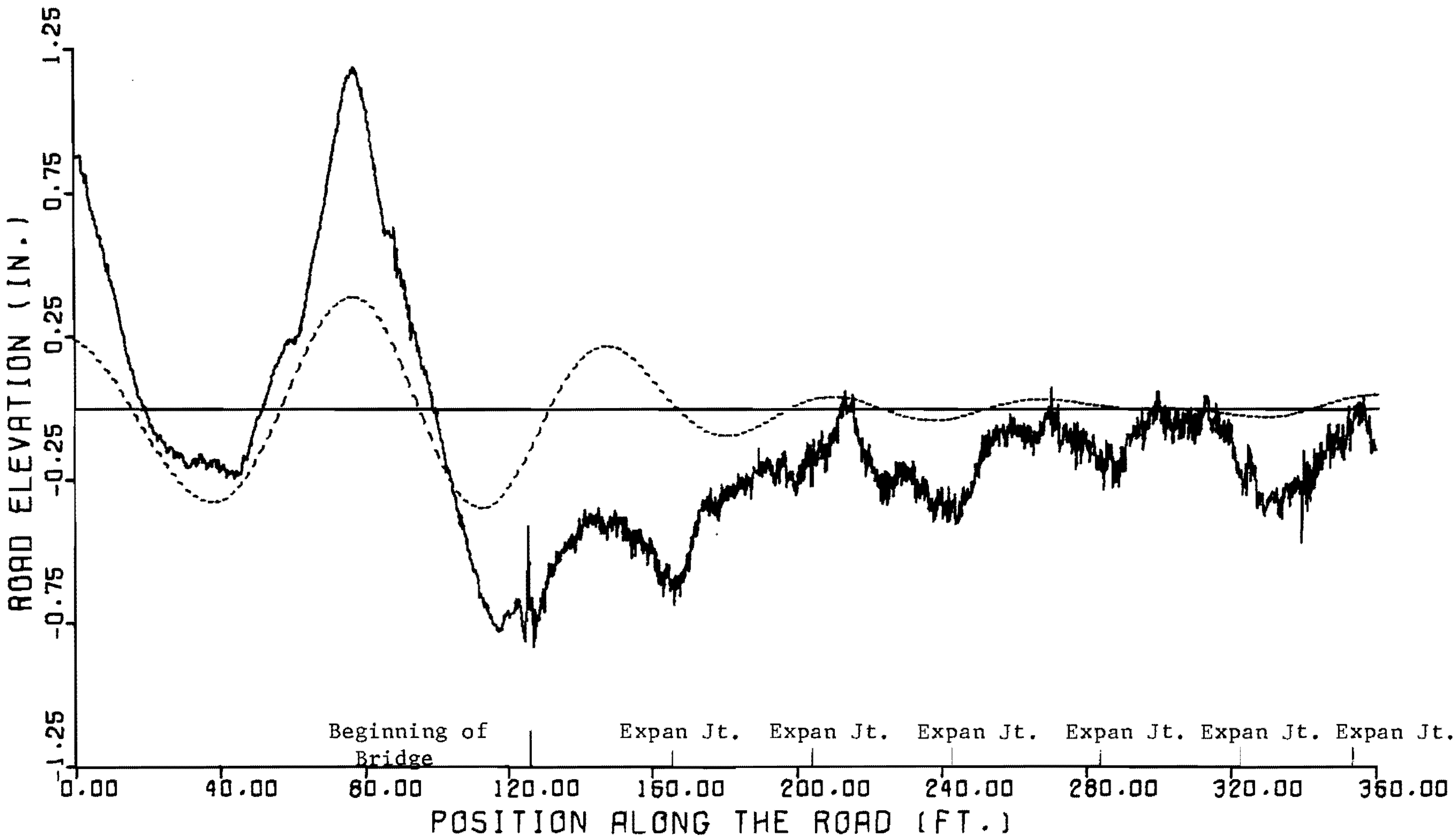

Fig. 3.8. Plum Creek Bridge

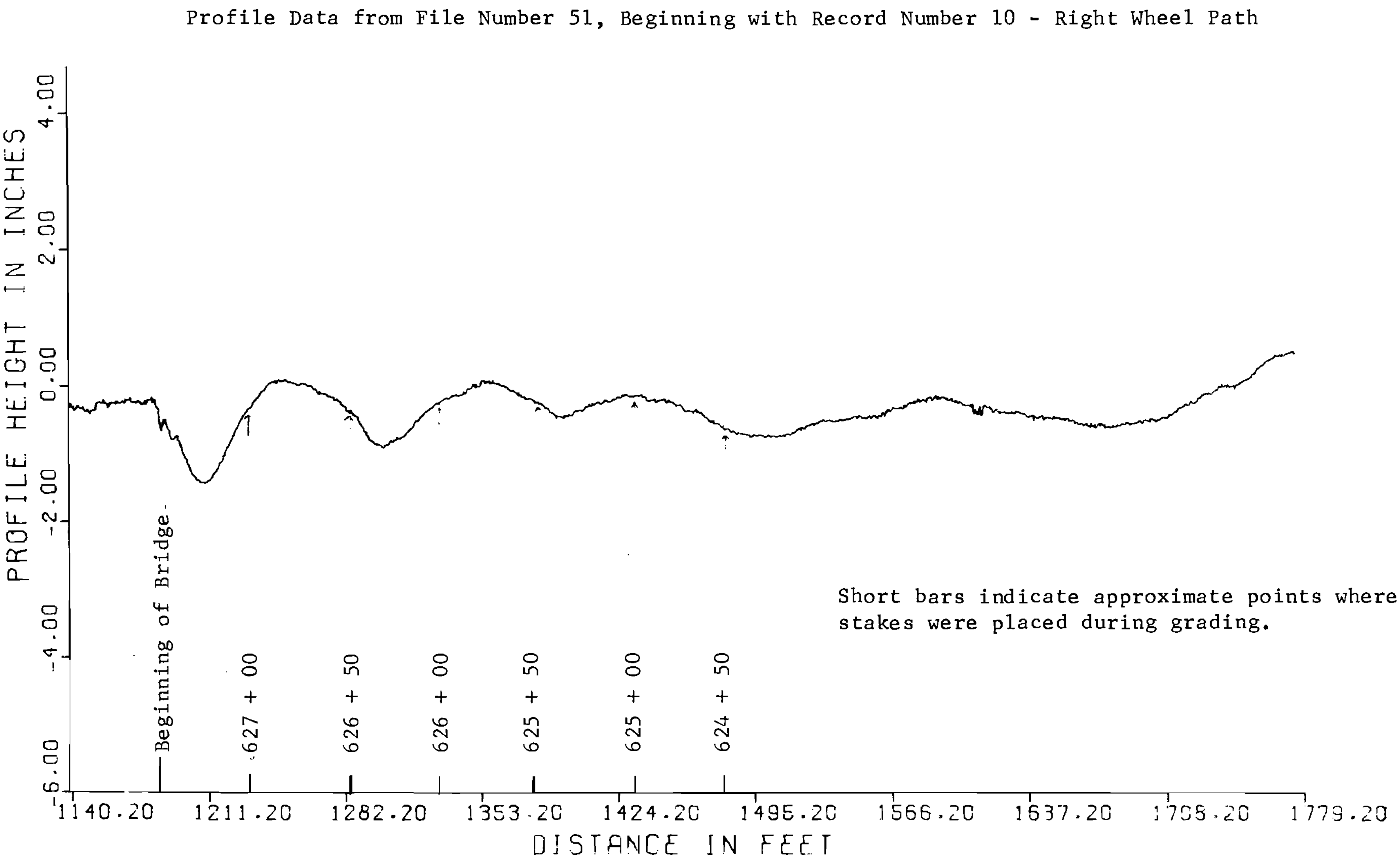

Fig. 3.9. Effect of Stationing on the MoPac Bridge Project

CHAPTER 4. QUANTITATIVE ANALYSIS OF ROAD ROUGHNESS DATA

While visual observation of road surface profile plots are very informative, several mathematical techniques are available which produce qualitative comparisons of roughness amplitudes. These comparisons enable a greater understanding of the road surface roughness present on bridge decks and the adjoining pavement. This chapter deals with these qualitative analyses.

MEAN AMPLITUDE-WAVELENGTH

In addition to visual observation of the filtered and unfiltered profile plots, useful information can be obtained from the mean amplitude-wavelength charts, Figs 4.1-4.3. On these charts, the mean of the amplitudes of the roughness observed on the bridge deck is compared to the mean observed on the pavement adjoining the bridge deck, as a function of the wavelength of the road surface irregularities. For each wavelength, the range for each pavement type (bridge deck or adjoining pavement) is indicated by bracketed bars. These bars are determined by plotting the r.m.s. amplitudes of the means of each of the two lanes studied, or of each direction in the case of the Plum Creek Project, including both wheelpaths, as well as all replications. These r.m.s. amplitudes for a given frequency are obtained from the POWER6 program, which is discussed in a later section; here we are interested in interpreting the amplitudes as measures of roughness, which increase as the road surface deformation worsens.

For the MoPac Bridge Project, greater amplitudes occur on the adjoining pavement for long wavelengths, whereas, for short wavelengths, greater amplitudes occur on the bridge deck, as seen in Fig 4.1. At these shorter wavelengths, the difference in amplitudes is very significant; for wavelengths of 10.8 feet or less, the amplitudes of the bridge deck are over twice those observed on the adjoining pavement. Also of interest is the fact that the variation in amplitude from lane to lane, which is often sizable, is never large enough to cause an overlapping in the amplitude ranges of the bridge deck and adjoining pavement. However, for wavelengths in the range of 35 feet, the mean amplitudes are approximately the same, thereby explaining why the F-test discussed in the

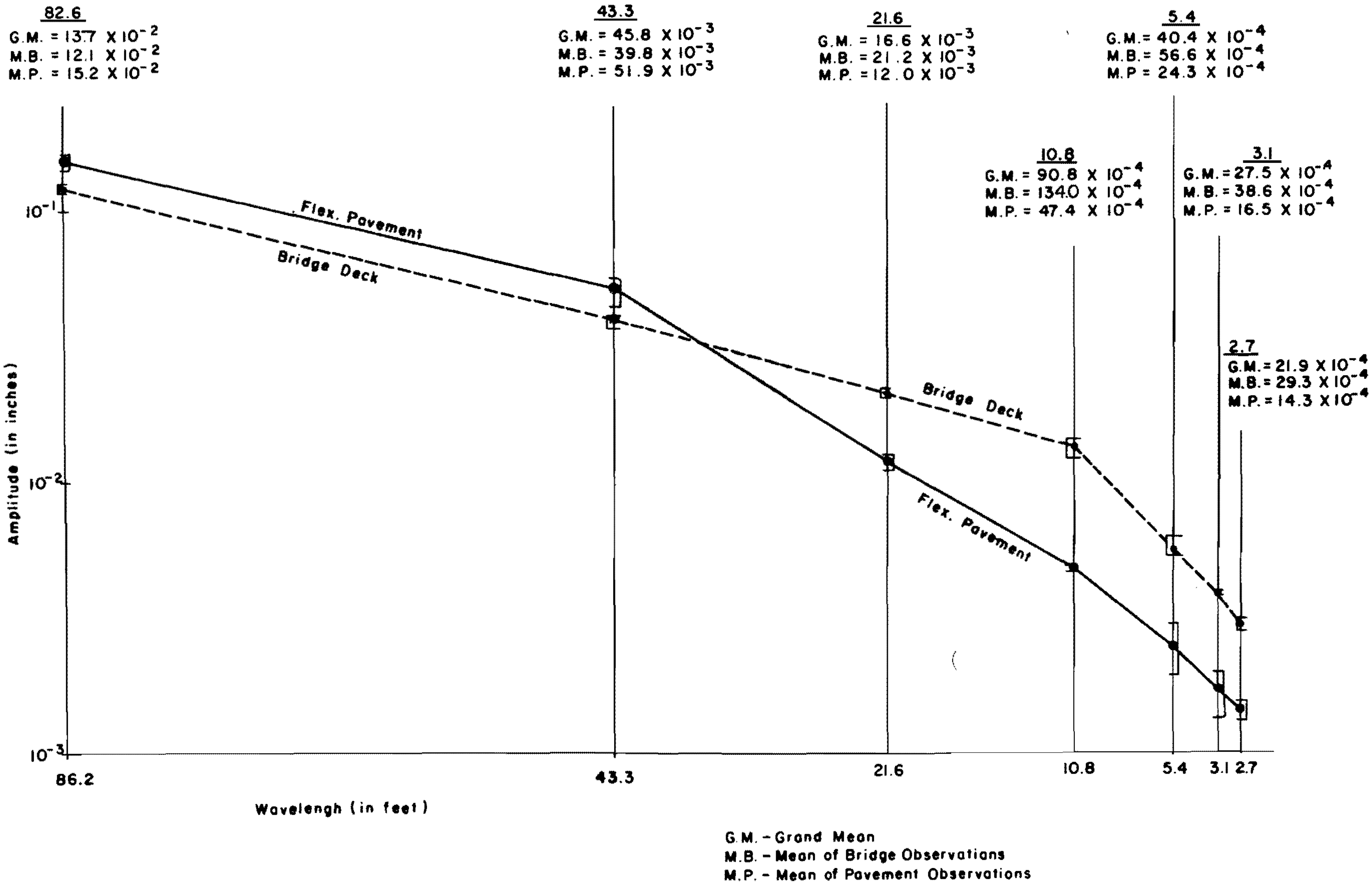

Fig 4.1. Mean Amplitude-Wavelength Chart - MoPac Bridge Project

following pages for variations between pavement and bridge deck was statistically insignificant at a wavelength of 43.3 feet but significant at the 90 percent confidence level for every other wavelength studied.

From Fig 4.2, the mean amplitude-wavelength chart for the Big Sandy Bridge Project, a different situation is presented. While, for longer wavelengths, larger amplitudes occur on the pavement section, the relationship between the shorter wavelengths and amplitude appears to be random. Although the variation from lane to lane is never enough to cause an overlapping of the amplitude ranges for the bridge deck and the pavement section for the wavelengths studied, there are four locations where the two mean amplitudes are approximately equal. Except for a wavelength of 21.6 feet, the mean amplitude observed on the bridge deck is never much larger than the mean amplitude of the pavement section. Another interesting feature is that the mean amplitude was greater for the MoPac Bridge than for the Big Sandy Bridge, in every case but two, the 43.3 and the 21.6-foot wavelengths, which was surprising. As expected, the Big Sandy project generally had larger values of mean amplitude on the pavement section than did the MoPac project since it was much older.

From Fig 4.3, the mean amplitude-wavelength chart for the Plum Creek Bridge project, a situation similar to that observed for the MoPac project occurs. Larger amplitudes occur on the pavement section for the longer wavelengths; whereas larger amplitudes occur on the bridge deck for the shorter wavelengths. However, the direction-to-direction variations are generally larger than the lane-to-lane variations of the two previous cases. Due to the fact that this project consists of two separate roadways, this feature is not unexpected. These large variations in the amplitude ranges cause an overlapping of the ranges for wavelengths of 43.3 and 21.6 feet. This explains the lack of statistical significance between the amplitudes on the bridge deck and those observed on the adjoining pavement at the 90 percent confidence level, as the F-values are 1.18 and .39 respectively, whereas F_{crit} is 8.53.

STATISTICAL ANALYSIS

Although the visual analysis of the profile plots and mean amplitude-frequency charts presented above is extremely useful, statistical techniques, particularly nested analysis of variance, are also valuable in making quantitative comparisons. While the details of the analysis techniques

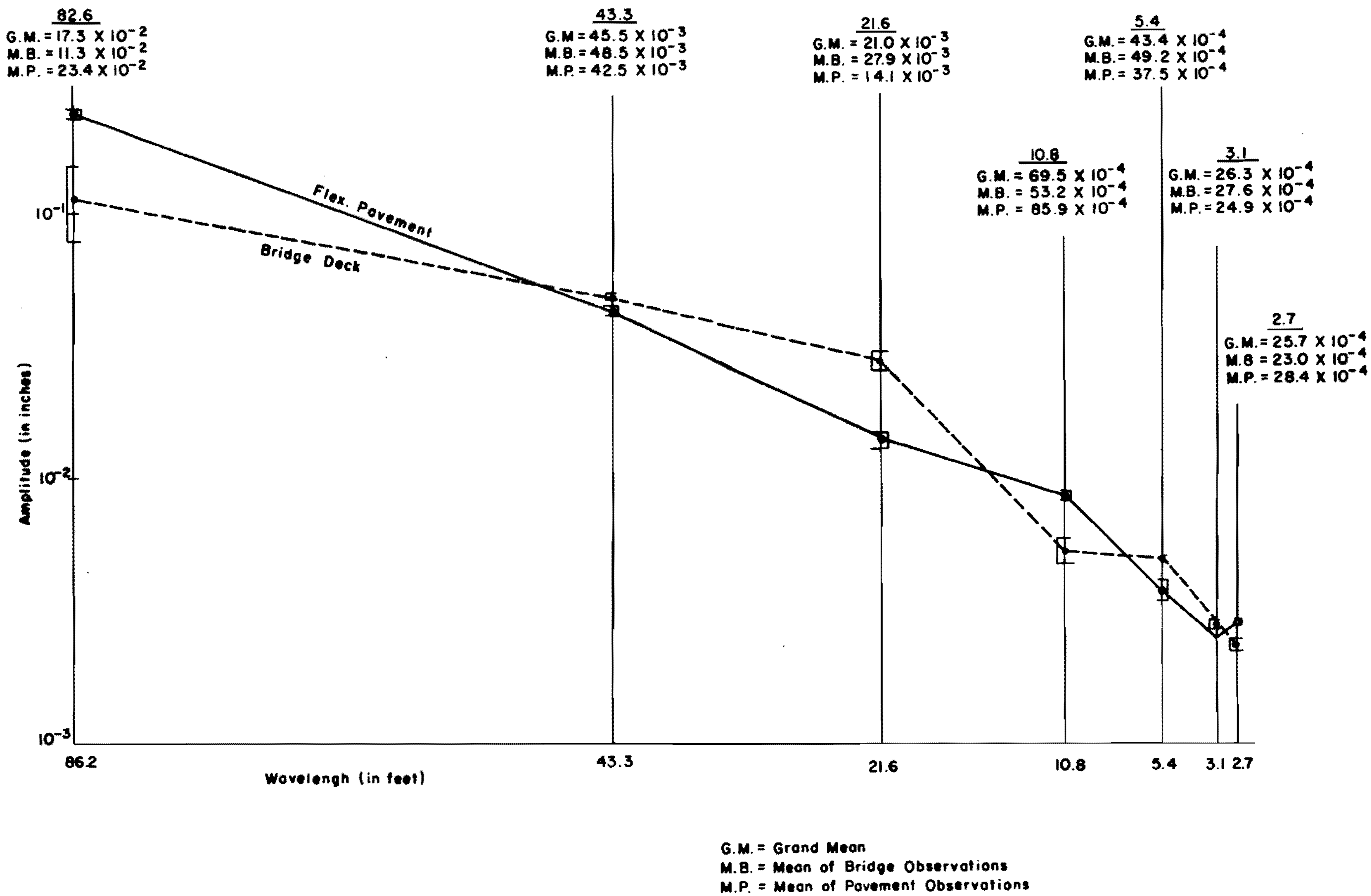

Fig 4.2. Mean Amplitude Wavelength Chart - Big Sandy Bridge Project

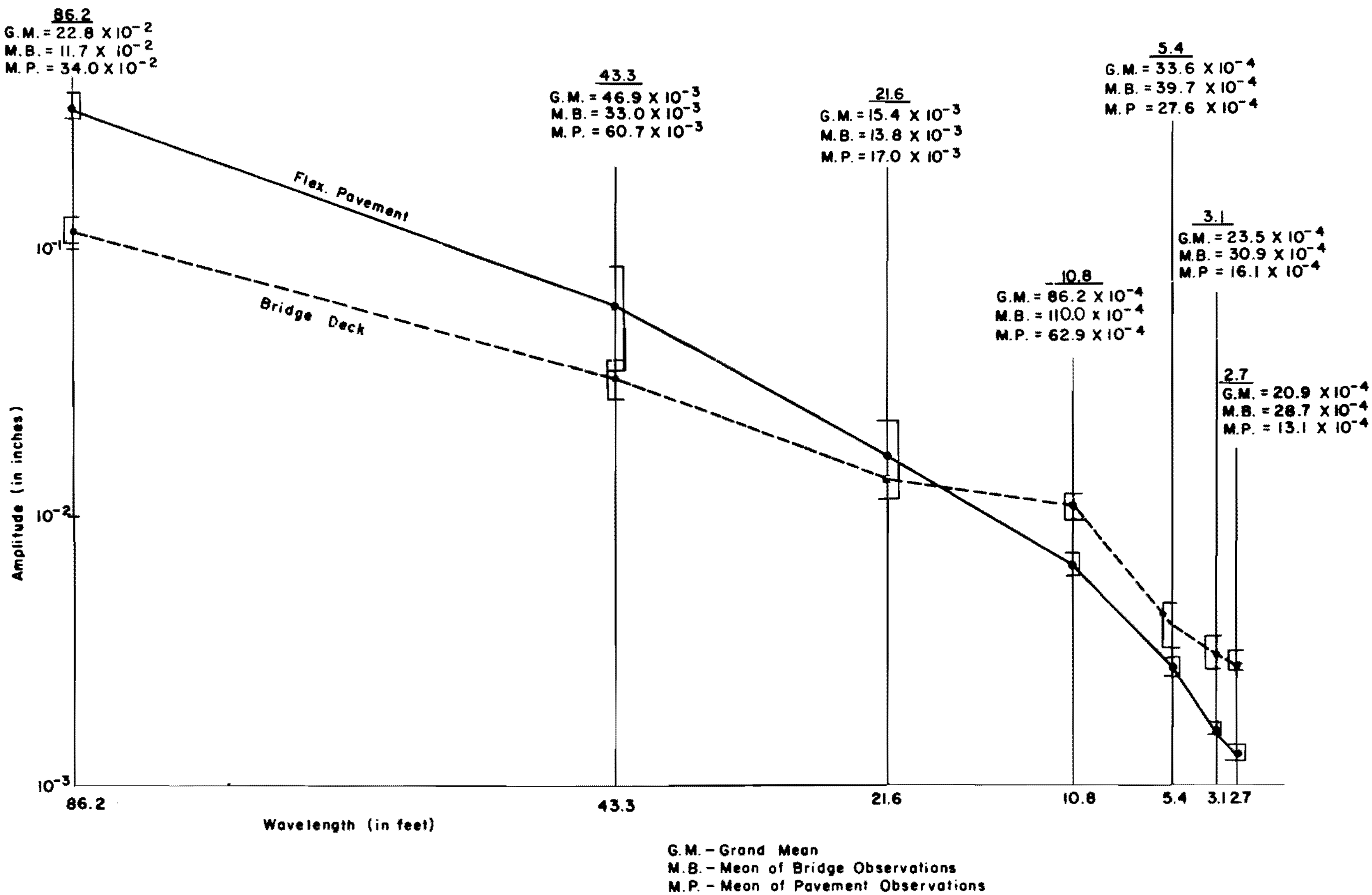

Fig 4.3. Mean Amplitude Wavelength Chart - Plum Creek Bridge Project

are included in a section of Chapter 2, the results obtained from these statistical techniques are presented in this section.

Coefficients of Variation

The coefficient of variation, defined here as the standard error of measurement divided by the r.m.s. roughness amplitude, is an indication of the relative measurement error. More commonly, the coefficient of variation is the sample standard deviation (which in some cases may be interpreted as a standard error) divided by the sample arithmetic mean.

As seen from Table 4.1, the coefficients of variation for the MoPac project are generally smaller for the bridge than for the flexible pavement, as are the standard errors. This is because the transverse surface irregularities on the bridge are smaller, and, therefore, the unavoidable variations in the wheelpaths travelled by the profilometer in replicate runs produce smaller measurement replication variances. Note from Table 4.2, however, that the variances are never significantly different at the .05 level.

Except in some cases where the r.m.s. amplitudes are very small for the flexible pavement roughness, the coefficients of variation are generally very small, indicating good measurement repeatability. This is due partly to the fact that, since MoPac had not been opened to the public at the time the measurements were made, the transverse road surface irregularities were small relative to a typical older project with surface deformations induced by traffic and weather. The coefficients of variation for the data pooled for the bridge and flexible pavement are less than .08, or 8 percent, in all but one case, as seen in Table 4.2.

The standard errors, on the order of a thousandth of an inch, appear unusually small until one realizes that

(1) the data being considered have been averaged (r.m.s.) over sections of several hundred feet and

(2) the roughness and, hence, the measurement errors have been partitioned on a frequency basis in computing the power spectrum.

No claim is being made that the elevation of the road at a given point can be measured to the accuracy of .001 inch.

TABLE 4.1. REPLICATION VARIANCES TREATED SEPARATELY FOR THE BRIDGE AND FLEXIBLE PAVEMENT

MOPAC Bridge Project

Bridge Deck Data

λ (ft.)	Standard Error (in.)	Coefficient of Variation	90% Upper Confidence for Standard Error (in.)
86.2	.00348	.0287	.00676
43.3	.00073	.0184	.00142
21.6	.00054	.0256	.00105
10.8	.00041	.0306	.00080
5.4	.00028	.0503	.00054
3.1	.00015	.0380	.00029
2.7	.00007	.0249	.00014

Flexible Pavement Data

λ (ft.)	Standard Error (in.)	Coefficient of Variation	Coefficient of Variation Using Mean of Pooled Data*	90% Upper Confidence for Standard Error (in.)
86.2	.00395	.0260	.0289	.00767
43.3	.00177	.0342	.0386	.00344
21.6	.00134	.1118	.0809	.00260
10.8	.00075	.1590**	.0826	.00146
5.4	.00063	.2600**	.1561	.00122
3.1	.00027	.1625**	.0982	.00052
2.7	.00012	.0861	.0548	.00023

*The mean of the pooled data was used, due to the fact that the shorter wavelengths had such small means for the flexible pavement

**The large coefficients of variation here are due to small means, not to large measurement replication variances. The standard errors are not out of line with the other standard errors.

TABLE 4.2. REPLICATION VARIANCES COMBINED FOR THE BRIDGE AND FLEXIBLE PAVEMENT

MOPAC Bridge Project

F - Statistics to Compare Replication Variances for the Bridge Deck and Nearby Pavement

for λ = 86.2 ft., F = 1.29

for λ = 43.3 ft., F = 5.88*

for λ = 21.6 ft., F = 6.09*

for λ = 10.8 ft., F = 3.35

for λ = 5.4 ft., F = 4.93*

for λ = 3.1 ft., F = 3.34

for λ = 2.7 ft., F = 2.79

$$F = \frac{\text{variance (flexible pavement)}}{\text{variance (bridge)}}$$

*significant for .10 percent confidence level, $F_{crit_{.10}} = 4.11$

$F_{crit_{.05}} = 6.39$

Pooled Data

λ (ft.)	Standard Error (in.)	Coefficient of Variation	90% Upper Confidence for Standard Error (in.)
86.2	.00372	.0273	.00564
43.3	.00136	.0338	.00205
21.6	.00102	.0615	.00154
10.8	.00061	.0668	.00092
5.4	.00049	.1212	.00074
3.1	.00022	.0783	.00033
2.7	.00010	.0463	.00015

The same type of information is available for the Big Sandy Bridge Project, but the results are different. From Table 4.3, it is seen that neither the bridge deck nor the adjoining pavement consistently has the larger coefficient of variation. The magnitudes clearly increase as the wavelength decreases however, indicating that the larger relative errors in smaller amplitudes correspond to the short wavelengths. By comparing the coefficients of variation for the Big Sandy Bridge, Tables 4.3 and 4.4, with those of the MoPac project, Tables 4.1 and 4.2, it can be seen that the coefficients of variation are generally larger for the Big Sandy Bridge Project, particularly for the bridge deck data. This is expected, due to the effects of weather and traffic on the Big Sandy Bridge.

For the Plum Creek Bridge Project, the coefficients of variation for the bridge deck are generally larger than those of the pavement at shorter wavelengths, as seen from Tables 4.5 and 4.6. At longer wavelengths, this relationship is generally reversed. Also noticeable is the fact that these coefficients of variation are larger than those obtained on either the MoPac or Big Sandy projects, particularly for adjoining pavement at the longer wavelengths. For the shorter wavelengths on the bridge deck (λ = 3.1 feet and λ = 2.7 feet), the coefficients of variation are roughly the same for both the Big Sandy and the Plum Creek bridges.

Analysis of Variance

From the output of the analysis of variance (AOV), we can consider several statistical comparisons among road profiles. The three questions of interest are:

(1) Is the repeat measurement variation small enough so that differences between wheelpaths in the same lane can be recognized in spite of random errors?

(2) Are the differences from lane to lane significantly greater than the differences from wheelpath to wheelpath within the individual lanes?

(3) Are the differences from structure to structure (bridge to nearby pavement) significantly greater than the differences from lane to lane within either structure?

The importance of each question is discussed in Chapter 2.

TABLE 4.3. REPLICATION VARIANCES TREATED SEPARATELY FOR THE BRIDGE AND FLEXIBLE PAVEMENT

Big Sandy Bridge Project

Bridge Deck Data			
λ (ft.)	Standard Error (in.)	Coefficient of Variation	90% Upper Confidence for Standard Error (in.)
86.2	.00443	.0394	.00861
43.3	.00273	.0563	.00530
21.6	.00046	.0165	.00089
10.8	.00040	.0752	.00078
5.4	.00050	.1016	.00097
3.1	.00060	.2176	.00117
2.7	.00060	.2608	.00117

Flexible Pavement Data			
λ (ft.)	Standard Error (in.)	Coefficient of Variation	90% Upper Confidence for Standard Error (in.)
86.2	.00560	.0240	.01088
43.3	.00279	.0656	.00542
21.6	.00104	.0738	.00202
10.8	.00021	.0245	.00041
5.4	.00045	.1200	.00087
3.1	.00049	.1964	.00095
2.7	.00040	.1410	.00078

TABLE 4.4. REPLICATION VARIANCES COMBINED FOR THE BRIDGE AND FLEXIBLE PAVEMENT

Big Sandy Bridge Project

F - Statistics to Compare Replication Variances for the Bridge Deck and Nearby Pavement
for λ = 86.2 ft., F = 1.60
for λ = 43.3 ft., F = 1.04
for λ = 21.6 ft., F = 5.21
for λ = 10.8 ft., F = 0.28
for λ = 5.4 ft., F = 0.82
for λ = 3.1 ft., F = 0.67
for λ = 2.7 ft., F = 0.46

$F_{crit_{.05}} = 6.39$

$F_{crit_{.10}} = 4.11$

Pooled Data

λ (ft.)	Standard Error (in.)	Coefficient of Variation	90% Upper Confidence for Standard Error (in.)
86.2	.00505	.0292	.00765
43.3	.00276	.0607	.00418
21.6	.00080	.0381	.00121
10.8	.00032	.0460	.00048
5.4	.00047	.1084	.00071
3.1	.00055	.2094	.00083
2.7	.00051	.1986	.00077

TABLE 4.5. REPLICATION VARIANCES TREATED SEPARATELY FOR THE BRIDGE AND FLEXIBLE PAVEMENT

PLUM CREEK BRIDGE PROJECT
Bridge Deck Data

λ (feet)	Standard Deviation (inches)*	Coefficient of Variation	90 Percent Upper Confidence For Standard Deviation
86.2	.01475	.1260	.02860
43.3	.00379	.1149	.00736
21.6	.00100	.0728	.00194
10.8	.00167	.1521	.00324
5.4	.00094	.2368	.00182
3.1	.00062	.2016	.00120
2.7	.00085	.2974	.00165
Flexible Pavement Data			
86.2	.03491	.1028	.06775
43.3	.01464	.2411	.02841
21.6	.00649	.3824	.01259
10.8	.00264	.4202	.00512
5.4	.00060	.2185	.00116
3.1	.00020	.1267	.00039
2.7	.00025	.1893	.00045

*Standard deviation based on variance including contributions from error and wheelpath-to-wheelpath effects.

TABLE 4.6. REPLICATION VARIANCES COMBINED FOR THE BRIDGE AND FLEXIBLE PAVEMENT

Plum Creek Bridge

F-Statistics to Compare Replication Variances for the Bridge Deck and Nearby Pavement

for λ = 86.2 ft., F = 4.99

for λ = 43.3 ft., F = 1.99

for λ = 21.6 ft., F = 3.02

for λ = 10.8 ft., F = 0.88

for λ = 5.4 ft., F = 1.93

for λ = 3.1 ft., F = 20.10

for λ = 2.7 ft., F = 2.08

$F_{crit_{.05}} = 19.00$ $F_{crit_{.10}} = 9.00$

Pooled Data

λ (feet)	Standard Deviation (inches) *	Coefficient of Variation	90 Percent Upper Confidence For Standard Deviation (in.)
86.2	.02680	.1174	.0404
43.3	.01069	.2281	.01614
21.6	.00465	.3023	.00702
10.8	.00221	.2563	.00334
5.4	.00079	.2347	.00119
3.1	.00046	.1972	.00069
2.7	.00063	.3007	.00095

* Standard deviation based on variance including contributions from error and wheelpath-to-wheelpath effects.

If the answer to a given one of these questions is yes, we say the result is statistically significant; that is, a difference has been identified which is large enough so that it is very unlikely that it could be explained as random sampling error. The statistical test used to address this question is called an F-test. For a more detailed explanation see pp. 9-13.

From the computed F-values for the MoPac data, it is observed that the variation between bridge deck and adjacent pavement is statistically significant for every wavelength considered except for the 43.3-foot wavelength, as seen in Table 4.7. It is also seen in Table 4.7 that the lane-to-lane variations on both the bridge deck and adjoining pavement were statistically insignificant for every case, while the variation from wheelpath to wheelpath was always statistically significant. This latter result is very important, since it indicates that the profilometer is sufficiently accurate to measure differences between wheelpaths in the same lane.

From the AOV output for the Big Sandy Bridge, the variation between pavement and bridge deck is again observed to be statistically significant, this time for every wavelength, as shown in Table 4.7. Only for the 83.3-foot wavelength is the variation between lanes statistically significant. Of particular interest is the fact that the variations between wheelpaths are again statistically significant, except for the 5.4-foot wavelength. The fact that the F-values are smaller for short wavelengths than in the case of MoPac indicates that small variations in the wheelpath traversed by the profilometer will cause large changes in mean amplitudes for the short wavelengths. This, too, is not unexpected, as the effect of traffic will cause certain distress manifestations, such as rutting, which will vary with lateral position in the lane. This effect will be greater for short wavelengths than for the longer ones.

From observation of the computed F-statistics obtained from the output of the analysis of variance program, for the Plum Creek Bridge Project, Table 4.7, no statistical difference is observed between directions. That is to say, the northbound lanes and the southbound lanes are not significantly different. This is not surprising, as the structural details were somewhat similar. The difference from lane-to-lane is not significant when compared to variations between wheelpaths within the same lane. However, the

TABLE 4.7. COMPUTED F-LEVELS FOR ROUGHNESS AMPLITUDES

	Plum Creek Project			Big Sandy Project			MoPac Project			
	Lane to Lane	Direction to Direction	Structure	Wheelpath Versus Error	Lane to Lane	Structure	Wheelpath Versus Error	Lane to Lane	Structure	λ (feet)
	2.42	3.65	31.20**	21.14**	9.44**	11.54*	13.26**	2.29	9.16*	86.2
	.03	669.26**	1.18	3.36*	.429	12.72*	26.13**	3.52	3.44	43.3
	1.84	2.67	.39	3.07*	1.07	36.00**	7.10**	.42	109.16**	21.6
	1.07	1.14	14.57*	190.90**	.09	24.64**	7.92**	2.81	36.71**	10.8
	1.94	1.85	2.64	1.37	1.43	12.45*	3.87**	2.11	21.33**	5.4
	.93	3.66	11.99*	2.95*	.03	10.79*	6.04**	1.34	51.63**	3.1
	.42	1.82	32.48**	3.60*	.05	26.33**	35.96**	.39	64.01**	2.7
$F_{crit_{.05}}$	3.84	6.94	18.50	3.84	6.94	18.50	3.84	6.94	18.50	
$F_{crit_{.10}}$	2.81	4.32	8.53	2.81	4.32	8.53	2.81	4.32	8.53	

* : significant at 90 percent confidence level

** : significant at 95 percent confidence level difference between bridge deck and adjoining pavement was significant at both the 86.2-foot wavelength, where the pavement was rougher, and the shorter wavelengths (λ = 10.8 feet, 3.1 feet, and 2.7 feet), where the bridge deck was rougher.

Components of Variance

Also available in the AOV output are the mean sums of squares. From these values, the components of variance can easily be obtained. The components of variance determine what percentage of variance among roughness amplitudes is due to measurement error, to wheelpath to wheelpath variations, to lane-to-lane variations, and to variations between bridge deck and pavement. As can be seen from Table 4.8, which contains the components of variance for the MoPac project, the percentage of the variance due to measurement error is always small, less than 4.2 percent, while the percentage of variance due to variations between pavement and bridge deck is generally very large, especially for the smaller wavelengths. Only for a wavelength of 43.3 feet is σ_s^2 less than 70 percent. In addition, the percentage of variance explained by variations from lane to lane is about the same as variations occurring from wheelpath to wheelpath.

In Table 4.9, the components of variance for the Big Sandy Bridge are presented. The percentage of variance due to variations between wheelpaths is much larger now, especially at the shorter wavelengths. The variation from lane to lane contributes very little to the total variation. However, the replication error contributes a sizable percentage of the total variance for very short wavelengths, where components range from 24.12 at 5.4 feet to 48.16 when λ = 3.1 feet. This is, as discussed earlier, most likely due to the effects of traffic upon the pavement, as the replication variance is very small for the long wavelengths.

The Plum Creek Bridge, due to its separate roadways, was analyzed in a slightly different manner, as discussed previously. Because of the lack of replications for each lane, the components of variance due to measurement error and variations between wheelpaths had to be combined.

The components of variance for the Plum Creek Bridge are presented in Table 4.10. The percentage of variance attributed to differences between pavement and bridge deck is generally very high, whereas this percentage

TABLE 4.8. COMPONENTS OF VARIANCE FOR THE MOPAC BRIDGE PROJECT

Variance Component	Wavelength (feet) 86.2	43.3	21.6	10.8	5.4	3.1	2.7
$\hat{\sigma}_e^2$	1.38×10^{-5} (2.35)	1.84×10^{-6} (1.72)	1.04×10^{-6} (2.24)	3.69×10^{-7} (0.93)	2.40×10^{-7} (4.12)	4.66×10^{-8} (1.81)	1.02×10^{-8} (0.77)
$\hat{\sigma}_w^2$	8.50×10^{-5} (14.45)	2.31×10^{-5} (21.58)	3.18×10^{-6} (6.85)	1.28×10^{-6} (3.23)	3.44×10^{-7} (5.91)	1.17×10^{-7} (4.54)	1.79×10^{-7} (13.47)
$\hat{\sigma}_L^2$	5.94×10^{-5} (10.10)	3.04×10^{-5} (28.40)	0 (0)	1.32×10^{-6} (3.33)	2.58×10^{-7} (4.43)	2.40×10^{-8} (0.93)	0 (0)
$\hat{\sigma}_s^2$	4.30×10^{-4} (73.10)	5.17×10^{-5} (48.30)	4.22×10^{-5} (90.91)	3.67×10^{-5} (92.52)	4.98×10^{-6} (85.54)	2.39×10^{-6} (92.72)	1.14×10^{-6} (85.77)

Components are given in $(\text{in.})^2$ and percent of total (in parentheses) for each wavelength.

$\hat{\sigma}_e^2$ = standard error

$\hat{\sigma}_L^2$ = lane-to-lane variance

$\hat{\sigma}_w^2$ = wheelpath-to-wheelpath variance

$\hat{\sigma}_s^2$ = bridge to flexible pavement variance

TABLE 4.9. COMPONENTS OF VARIANCE FOR THE BIG SANDY BRIDGE PROJECT

Components given in $(in)^2$ and % of total (in parenthesis) for each wavelength

λ (ft.)	86.2	43.3	21.6	10.8	5.4	3.1	2.7
$\hat{\sigma}_e^2$	2.55×10^{-5} (0.31)	7.63×10^{-6} (23.33)*	6.45×10^{-7} (0.62)	1.02×10^{-7} (0.68)	2.24×10^{-7} (24.12)	3.03×10^{-7} (48.16)*	2.61×10^{-7} (35.37)*
$\hat{\sigma}_w^2$	2.57×10^{-4} (3.16)	9.03×10^{-6} (27.48)	9.56×10^{-6} (9.25)	9.70×10^{-6} (64.96)	4.15×10^{-8} (4.47)	2.95×10^{-7} (46.88)	3.39×10^{-7} (45.93)
$\hat{\sigma}_1^2$	1.14×10^{-3} (14.04)	0 (0)	3.50×10^{-7} (0.34)	0 (0)	3.32×10^{-8} (3.57)	0 (0)	0 (0)
$\hat{\sigma}_s^2$	6.70×10^{-3} (82.49)	1.62×10^{-5} (49.30)	9.28×10^{-5} (89.79)	5.13×10^{-6} (34.36)	6.30×10^{-7} (67.84)	3.12×10^{-8} (4.96)	1.38×10^{-7} (18.70)

$\hat{\sigma}_e^2$ = standard error

$\hat{\sigma}_w^2$ = wheelpath-to-wheelpath variance

$\hat{\sigma}_1^2$ = lane-to-lane variance

$\hat{\sigma}_s^2$ = bridge to flexible pavement variance

*Note that the sizable percentage here is largely due to a small bridge deck-to-adjoining pavement variance. The error variance is not out of line.

TABLE 4.10. COMPONENTS OF VARIANCE FOR THE PLUM CREEK BRIDGE PROJECT

	Wavelength (feet)						
	86.2	43.3	21.6	10.8	5.4	3.1	2.7
$\hat{\sigma}_e^2 + \hat{\sigma}_w^2$	7.18×10^{-4} (2.73)	1.14×10^{-4} (13.90)	2.16×10^{-5} (45.80)	4.88×10^{-6} (31.83)	6.23×10^{-7} (38.26)	2.15×10^{-7} (15.88)	3.94×10^{-7} (24.58)
$\hat{\sigma}_L^2$	5.10×10^{-4} (1.94)	0 (0)	9.03×10^{-6} (19.15)	1.76×10^{-7} (1.15)	2.92×10^{-7} (17.94)	0 (0)	0 (0)
$\hat{\sigma}_D^2$	1.15×10^{-3} (4.38)	6.49×10^{-4} (78.96)	1.65×10^{-5} (35.04)	1.836×10^{-7} (1.20)	2.56×10^{-7} (15.69)	1.33×10^{-7} (9.83)	3.36×10^{-8} (2.10)
$\hat{\sigma}_s^2$	2.40×10^{-2} (90.97)	5.87×10^{-5} (7.14)	0 (0)	1.01×10^{-5} (65.84)	4.58×10^{-7} (28.12)	1.01×10^{-6} (74.32)	1.18×10^{-6} (73.32)

components are given in $(\text{in.})^2$ and percent of total (in parenthesis) for each wavelength.

$\hat{\sigma}_e^2$ = standard error

$\hat{\sigma}_L^2$ = lane-to-lane variance

$\hat{\sigma}_w^2$ = wheelpath-to-wheelpath variance

$\hat{\sigma}_D^2$ = direction-to-direction variance

$\hat{\sigma}_s^2$ = bridge to flexible pavement variance is much smaller for variations due to differences in lanes or differences in directions. However, a fairly high component of variance does exist for the variation due to differences in wheelpaths pooled with measurement error. This is understandable when it is realized that these two categories, σ_e^2 and σ_w^2, have been combined due to the physical nature of the Plum Creek Bridge.

ROUGHNESS AMPLITUDE DISTRIBUTION MEASURES

While the methods discussed above are ideal for comparisons of overall roughness measures, additional information in the form of roughness amplitude distribution measures is very beneficial. Through these measures, both mean amplitude and measures of the worst roughness in a given section can be determined for each pavement type. It is these extreme areas of pavement roughness that are most likely to affect a driver, yet these isolated effects tend to average out over a long enough section so that their effect upon overall roughness amplitude is minimal. By means of numerical comparisons of the roughness amplitude distribution measures, the type of road roughness on each pavement type can be better characterized. For this study, the 50th, 75th, 90th, 95th, and 99th percentile points were used, in addition to the mean. A percentile point is used as a measure of what amplitude exists such that a given percentage of observations have values less than or equal to this value. The 90th percentile amplitude, for example, is the value greater than or equal to 90 percent of all the local roughness amplitudes for a given road section. Local roughness measures are computed at discrete steps throughout the section.

<u>MoPac Bridge Project</u>

It is observed that the span length appears to have virtually no effect upon the roughness present on the bridge deck. In fact, the amplitudes were larger on the adjoining pavement than they were on the bridge deck. This feature is not surprising, however, when it is recalled that the span length was 97 feet, while prominent 100 foot waves existed on the adjoining pavement, caused by the stationing of the project. It must also be remembered that the bridge had yet to be subjected to the effects of traffic and time. For the bridge deck section, the 81 to 120 foot passband indicates that, for the right profile, a rather uniform roughness distribution exists, as the 99th percentile amplitude is only .01 inch larger than the 50th percentile point. The difference profile, on the other hand, contains several waves of much larger amplitudes than the average roughness amplitude. These extreme transverse roughness amplitudes approach the amplitudes of the longitudinal roughness.

For the short wavelength roughness, 0 to 20 feet, the bridge deck much rougher for the right profile, particularly for the extreme roughness measures, than is the adjoining pavement. These extreme measures differ vastly from the mean and 50th percentile roughness measures. The difference profile roughness measures indicate that the rolling effect is more severe than the longitudinal roughness for the short wavelengths on the bridge deck, 0 to 9 feet. This transverse roughness is also generally more severe on the bridge deck than it is on the adjoining pavement for the shorter wavelengths.

The standard deviations of the two sections indicate that the roughness on the bridge deck is less uniform and therefore contains a larger variety of roughness amplitudes than the adjoining pavement for the short wavelengths, while the opposite holds true for the larger wavelengths.

Big Sandy Bridge Project

The span length of the bridge, 48 feet, plays a definite role in determining the type of roughness present on the bridge deck. For both lanes of the bridge, the 40 to 60-foot waves have greater amplitudes than do the 60 to 81-foot waves, which differs from the trend of increasing amplitude with increasing wavelength. It is also noted that the longitudinal roughness corresponding to the span length tends to be fairly uniform, that is, the 99th percentile amplitude is only .015 inch greater than the 50th percentile amplitude, whereas, on the adjoining pavement, the roughness contains a wider range of amplitudes.

For short wavelength roughness, 0 to 9 feet, the bridge deck tends to be rougher, particularly for the extreme roughness measures, than the adjoining pavement. These extreme measures differ greatly from the mean amplitude.

The difference profile indicates that the transverse roughness is more severe than the longitudinal roughness for the short wavelengths. This transverse roughness is also generally more severe on the bridge deck than it is on the adjoining pavement for the 0 to 3-foot wavelengths. It is also seen that these transverse roughness measures decrease with increasing wavelength on the bridge deck, while they increase on the adjoining pavement.

The standard deviations of the sections indicate that for short wavelength roughness, 0 to 9 feet, the bridge deck longitudinal roughness varies to a greater extent than that of the adjoining pavement, while for the longer wavelengths, 9 to 81 feet, the situation is reversed. For the transverse roughness, only the 0 to 9-foot wavelength roughness has large variations in amplitude on the bridge deck, while large variations always occur on the adjoining pavement.

Plum Creek Bridge Project

Once again, the span length influences the type of roughness present on the bridge. It is observed that, for wavelengths corresponding to the span length, the bridge deck is rougher than the adjoining pavement, particularly for the lower percentile points. It is also noted, that, unlike the other two projects, the higher percentile amplitudes are larger than the mean roughness amplitude. This is not surprising when it is realized that the span length varies somewhat over the length of the bridge. From observation of the roughness amplitudes, it is apparent that the amplitudes of this span length induced roughness is much greater than it would be for a longer span length.

For the short wavelengths, the bridge deck is generally rougher. Because different roadways are used for each direction, larger variations occur between directions than existed for the Big Sandy Bridge project. On the bridge deck, the higher percentile amplitudes are much greater than the mean amplitude. As can be seen from the standard deviations of the roughness measures, the bridge deck roughness is more diverse for short wavelength roughness, whereas the adjoining pavement roughness is more diverse for the longer wavelengths.

From the transverse roughness measures, it is observed that the amplitudes generally decrease with increasing wavelength for the bridge deck, while these amplitudes tend to increase with wavelength on the adjoining pavement.

CHAPTER 5. SUMMARY OF RESULTS AND CONCLUSIONS

It has been shown that several methods of analysis are available for characterizing and comparing road roughness on bridge decks and the adjoining pavement. Such methods include power spectral analysis, analysis of variance, components of variance, and visual observation of filtered road profile plots. Through the use of these techniques, it is felt that a better understanding of road roughness can be obtained, both for bridge decks and the adjoining pavement. Once a thorough understanding of the problem exists, meaningful steps can be taken towards alleviating the problem of road roughness associated with the presence of bridges.

While, with the aid of the methods mentioned previously, bridge deck roughness can be characterized and contrasted to the roughness existing on the adjoining pavement, it is impossible to arrive at widely applicable, conclusive findings due to the limited nature of this pilot study. Within the scope of a pilot study, however, results are presented, and several methods of obtaining these roughness characterizations have been presented and demonstrated for three pavement projects. The results of the study are summarized below.

SUMMARY OF RESULTS

Qualitative Analysis

Long wavelength roughness on the adjoining pavement tends to increase appreciably before the beginning of a bridge and then dies out on the bridge deck itself. However, a significant increase in short wavelength, 0 to 10 feet, roughness amplitudes on the adjoining pavement occurs about 50 feet, or 150 feet in the case of the MoPac Bridge project, from the beginning of the bridge. This short wavelength roughness is also extremely prevalent on the bridge deck itself.

The span length of a bridge has a major effect upon the type of roughness present on a bridge deck, as large amplitude waves corresponding to the span length occur on the bridge. While this effect is fairly insignificant for very long span lengths, span lengths on the order of 30 to 50 feet lead to very noticeable roughness, as witnessed on both the Big Sandy and Plum Creek bridges. This problem also is not as objectionable to a car passenger on short bridges as it is on longer ones.

The most severe areas of roughness related to bridges are the bumps at the ends of the bridge. While the asphaltic concrete pavement on either side of the bridge will generally compact with time due to the loads applied by the traffic, or expand due to the presence of swelling clay, the Portland Cement Concrete bridge deck remains virtually unaffected by compaction, thus causing bumps due to the unequal settlement. These bumps have an amplitude of approximately .25 inch. Other factors that have an influence on the roughness at the end of the bridge include the presence of an approach ramp and/or a 12-inch wide concrete abutment. Both of these structures create a bump themselves, while reducing somewhat the magnitude of the bumps at the actual ends of the bridge deck.

The surveying layout of the project may tend to induce 100-foot waves onto the pavement immediately adjoining a bridge deck. This is most likely due to construction problems such as difficulties in grading and compacting the soil. This effect increases near the beginning of a bridge, probably because the construction crew does not have enough grade stakes just ahead of the bridge to "aim for" in the grading process. Difficulties are also encountered in properly compacting the soil in these areas.

Mean Amplitude-Wavelength

From the mean amplitude-wavelength charts, several general observations are noteworthy. For each of the three cases studied, the adjoining pavement section has larger amplitudes for the longest wavelength than does the bridge deck. As the amplitude decreases, so do the r.m.s. amplitudes for both section types. For the shorter wavelengths, 15 feet of less, the amplitudes on the bridge deck are generally larger than the corresponding amplitudes on the adjoining pavement, which can also be observed from the plots of the filtered profiles. Whether or not the span length has any effect on determining the zone where the two lines cross remains to be seen, as only a small sample has been used for this pilot study. This feature might be of possible future interest, however.

Statistical Analysis

From the observations of the statistical comparisons of the roughness data, it is very important to realize that the repeat measurement variations have been shown to be small enough to allow differences between wheelpaths in the same lane to be recognized, as seen in Table 4.7. Since the profilometer is capable of obtaining information this accurately, it is accurate enough for most practical purposes. Also of note is the fact that the difference in roughness amplitudes between bridge deck and adjoining pavement was significant in nearly every case. Thus, different types of roughness occur on each structural type. Lane-to-lane variations were found to be insignificant.

Components of Variance

From the components of variance tables (Tables 4.8, 4.9, and 4.10), it is observed that both wheelpath-to-wheelpath variations and measurement error for replicate runs of the same wheelpath are generally greater for the older bridge for which replicate runs were made (Big Sandy) than for the new (MoPac). This is understandable due to the effects of traffic and time, which cause irregularities in the road surface. Because of these irregularities, there are small differences in the wheelpaths traversed by the profilometer in replicate runs and the result is larger measurement differences in older pavements as compared to newer ones. However, age seemed to have surprisingly little effect on the lane-to-lane variations for the projects studied, relative to wheelpath variations. The variation between structures, bridge deck and adjoining pavement, consistently explains more of the total roughness variance for the new project, MoPac, than for the older sections for the shorter wavelengths. This is most likely because other variations, such as measurement error due to pavement distress varying with lateral location, increase with age. Table 4.7 reinforces the information mentioned above.

Roughness Amplitude Distribution Measures

From the roughness amplitude distribution tables presented in Appendix A, it is seen that the type of long wavelength roughness present on a bridge deck depends upon the span length. The greater the span length, the less objectionable is the road roughness. For the short wavelength roughness, the amplitudes on the bridge tend to be both more severe and more diverse, while for long wavelength roughness, the amplitudes on the bridge tend to be less severe and fairly uniform in comparison to the roughness present on the adjoining pavement. The transverse roughness (rolling effect) is worse than the longitudinal roughness for very short wavelengths. On the bridge deck, this transverse roughness tends generally to decrease with increasing wavelength and is fairly uniform at these longer wavelengths while being more diverse at the shorter wavelengths.

CONCLUSIONS AND RECOMMENDATIONS

The results of this study show that an appreciable amount of roughness is associated with the presence of bridge decks, both on the bridge decks themselves and the adjoining pavement. Although it would be virtually impossible to eliminate this roughness, several methods, involving both design and construction techniques, could be employed in order to reduce this effect.

As mentioned earlier, the span length of a bridge tends to induce roughness of similar wavelength on the bridge deck. In order to minimize this effect, the possibility of constructing new bridges with either very long (greater than 80 feet) or varying span lengths should be considered. Long span lengths, while inducing definite roughness, would not be as detrimental to the riding quality as would roughness caused by shorter span lengths. Previous studies (see Reference 6) have indicated that short wavelength roughness tends to have more effect upon ride quality than does long wavelength roughness. Varying span lengths, on the other hand, could be used much in the same manner as variable joint spacing is sometimes used in jointed concrete pavements. These variable distances between contraction joints are used to eliminate the steady rhythm of the tires hitting the joint filler at regular time intervals. Similarly, varying span lengths would eliminate the steady rhythm caused by roughness of a constant wavelength.

The problem of 100-foot waves created by the surveying layout of the roadway section within about 300 feet of a bridge could easily be eliminated by increasing the frequency at which cut or fill stakes are placed. If these stakes were placed every 25 feet or so, rather than only every half-station as is currently the practice, the operators of the grading equipment would be better able to accurately grading the roadway section, as more stakes would be available for the operators to "aim" for. However, near the end of the bridge, this interval might need to be decreased to prevent the creation of 50-foot waves in the same manner as 100-foot waves are currently built in, as these shorter waves would only serve to worsen the existing situation.

The bump at the end of the bridge, due primarily to differential settlement, is generally the worst type of bridge-related roughness. This roughness could be reduced somewhat if the compaction of the soil in the area were improved. Care should therefore be taken to see that the area immediately next to the bridge is compacted as well as possible, using whatever methods are available to the construction crew. Soils susceptible to swelling should be removed if feasible. Another possible means of reducing this roughness might be the addition of a fairly short length of rigid pavement, called an approach slab, on either side of the bridge. The purpose of this strip would be to reduce the stress caused by dynamic loading due to vehicles "falling" off the end of the bridge deck. Since Portland cement concrete pavements are less subject to rutting and consolidation than asphaltic concrete pavements, the differential settlement between bridge and adjoining pavement may be reduced by using rigid pavement on either side of the bridge. The length of these rigid pavement sections would be dependent on the distance necessary for the vehicles to lose the vertical acceleration caused by the remaining bump at the end of the bridge; several districts currently use 20 foot approach slabs. In this way, the large bump at the end of the bridge would be replaced by two smaller, and consequently less objectionable, bumps: one at the end of the bridge and the other at the end of the rigid pavement strip. It is recommended that further study be conducted to compare roughness between bridges with and without approach slabs.

REFERENCES

1. Carey, W. N., Jr., and P. E. Irick, "The Pavement Serviceability-Performance Concept," Highway Research Board Bulletin No. 250, 1960.

2. Walker, R. S., and W. R. Hudson, "The Use of Spectral Estimates for Pavement Characterization," Research Report 156-2, Center for Highway Research, The University of Texas at Austin, August 1973.

3. Roberts, F. L., and W. R. Hudson, "Pavement Serviceability Equations Using the Surface Dynamics Profilometer," Research Report 73-3, Center for Highway Research, The University of Texas at Austin, April 1970.

4. Hudson, W. R., "High-Speed Road Profile Equipment Evaluation," Highway Research Record 189, 1967.

5. Wine, R. L., Statistics for Scientists and Engineers, Prentice-Hall, Englewood Cliffs, New Jersey, 1964.

6. Holbrook, L. F., and J. R. Darlington., "Analytical Problems Encountered in the Correlation of Subjective Response and Pavement Power Spectral Density Functions," Highway Research Record 471, 1973.

7. Walker, R. S., and W. R. Hudson, "A Correlation Study of the Mays Road Meter with the Surface Dynamics Profilometer," Research Report 156-1, Center for Highway Research, The University of Texas at Austin, February 1973.

8. Williamson, H. J., and W. R. Hudson, "Analysis of Characteristic Roughness Patterns in Pavements and the Relationship Between Roughness and Pavement Distress," Research Report 156-3, Center for Highway Research, The University of Texas at Austin, October 1974.

APPENDIX A

A DETAILED QUALITATIVE ANALYSIS OF ROAD ROUGHNESS DATA

APPENDIX A. A DETAILED QUALITATIVE ANALYSIS OF ROAD ROUGHNESS DATA

Road surface profiles of both the right and left wheelpaths can be accurately measured by the General Motors profilometer currently owned by the Texas Highway Department and operated by the Center for Highway Research. These road profiles are in the form of road surface elevations observed at equally spaced distances and are an essential tool for the development of a better understanding of the changes in roughness caused by the presence of any physical structure, in this case bridge decks. From the plots of both the filtered and unfiltered profiles, a great amount of information can be obtained by visual observation.

Here, digital filtering is referred to simply as a method for computing a new profile from the original road profile in order to isolate the type of roughness which is of specific interest, e.g., that with wavelengths from 0 to 15 feet. Thus, the components of the road roughness can be observed and analyzed separately, thereby enabling a more thorough investigation into roughness characterization.

Included in this appendix is a discussion of the profile plots of the three projects studied in detail, the MoPac project, the Big Sandy project, and the Plum Creek project. The second part of this appendix contains the profile plots of these projects. To aid the reader in better understanding the profile plots, vertical lines have been placed along the position scale of these plots to indicate features of the bridge deck that are of interest. A long mark is used to indicate either the beginning or end of the bridge deck, while a short mark is used to indicate the location of an expansion joint.

As was mentioned previously, in Chapter 3, the operation of the electronic measuring system aboard the profilometer requires certain processing (analog filtering) of the road profile data which introduces a frequency dependent "phase shift." In order to more accurately interpret the road surface profile plots, the reader should be aware that, while short waves are virtually unaffected, roughness with wavelength longer than 32 feet is shifted to the right on the profile plots; the longer the wavelength, the greater this phase shift. The effect of this is to cause some of the long waves of the adjoining pavement to appear to extend onto the bridge by a fraction of a wavelength in some cases. Despite this disadvantage, much meaningful information can be obtained from the present data.

The reader who is interested in studying the characteristics of the frequency response to phase shift should see pages 8-10 of Ref 3. The chart on page 9 of Ref 3 requires a vehicle speed of 20 mph and use of filter two, which were also used for all road measurement by the profilometer during this study.

MOPAC BRIDGE PROJECT

From visual observation of the profile plots of the MoPac Bridge Project, the following features are apparent.

It is observed from the plots of the right profile, Figs. A.1 through A.3, that the profile is much smoother on the adjoining pavement than it is on the bridge. This is due to the increased amplitudes of the short waves that occur after passing onto the bridge deck, which begins at about 290 feet. On the adjoining pavement, the profile consists of very short waves having very small amplitudes. These wavelengths, and the corresponding amplitudes, begin to increase gradually at about 150 feet before the bridge. The crossing onto the bridge deck itself is marked by a distinct spike (an extremely short wave having a relatively large amplitude). While other spikes are noticeable at 97-foot increments, due to the expansion joints of the bridge, they are not as severe. There are pronounced 5 to 10-foot-long waves on the bridge, along with shorter waves of smaller amplitude. The 0 to 5-foot waves have much larger amplitude than those observed on the approaching pavement. Another feature that is noticeable is the long wavelength roughness, which increases greatly just before the bridge and then tends to die out once onto the bridge deck itself.

The same trends exist for the right-left difference plots, as seen in Figs. A.4 through A.6. While short waves with very small amplitudes occur on the pavement section, slightly longer waves, on the order of 6 feet, with larger amplitudes, for the most part, occur on the bridge. The crossing onto the bridge deck itself is marked by a severe spike. Spikes marking the expansion joints are noticeable but often difficult to detect due to the surrounding roughness. The amplitudes of the long wavelengths, 30 feet or more, tend not to be significant on the bridge deck, although the amplitude of these long wavelengths becomes much greater just before the bridge.

Another interesting feature that appears on the MoPac Bridge project is the effect of stations. Stations and half-stations are used by surveyors to indicate at 50-foot intervals the correct grade at which the project is to be constructed. On the flexible pavement between the two bridges, it is observed, in Figs. A.7 and A.8, that several 100-foot waves appear as the shorter bridge deck is approached. The amplitudes of these waves also increase as the distance to the shorter bridge decreases. This feature is most likely due to the fact that the operators of the grading equipment have difficulty grading accurately near the beginning of a bridge because they have too few grade stakes, one at every half-station, to "aim" for. The nearer they approach the bridge deck, the fewer grade stakes they have to use, which explains why the amplitudes become greater.

Observation of the bump at the end of the bridge shows that the beginning of the bridge deck is very noticeable.

As seen in Fig. A.4, the right-left difference profile for the MoPac Bridge project, the bump at the beginning of the bridge is characterized by a spike with an amplitude of approximately .25 inch, followed by a slightly smaller spike a foot later. This second spike is the actual beginning of the bridge deck, while the first spike marks the end of the approaching flexible pavement. In between these two points rests a 12-inch concrete abutment, which serves to support the bridge beam, as well as provide a transition from pavement to bridge deck. From Fig. A.1, the right profile for MoPac, it is observed that these two spikes have amplitudes of about .20 inch and .17 inch respectively. Another feature observed is that the right profile and the right-left difference profile are very similar in the area of the beginning of the bridge deck. In both cases, the spike points upward, indicating that the bridge deck is at a slightly higher level.

BIG SANDY BRIDGE PROJECT

From visual observation of the profile plots of the Big Sandy Bridge project, the following information is obtained.

For the 0 to 15-foot passband for the right profiles, noticeable differences exist between the profiles of the bridge deck and the pavement, as seen in Figs. A.9 through A.12. The waves on both sections are normally very short, so that they appear as "bumps." Both before and after the bridge deck, which begins at about 170 feet and ends at around 650 feet, these "bumps" are generally of small magnitude, particularly on the western side of the bridge. However, on the bridge deck, these "bumps" are usually of much larger amplitude and occur far more frequently, resulting in a darker and thicker plot for the bridge deck. The spikes which mark expansion joints on the bridge deck are very noticeable.

From the right-left difference profiles for the 0 to 15-foot passband, it is observed, in Figs. A.13 through A.16, that the bridge deck is somewhat rougher than the approaching pavement. Spikes on the bridge deck denoting expansion joints usually are noticeable, as are both ends of the bridge deck. Short wavelengths generally tend to occur more frequently, and with larger amplitudes, on the bridge deck than on the approaching pavement, although there is very little difference in the eastbound lane.

For the 30 to 60-foot passband for the right profiles of the Big Sandy Bridge project, it is observed that no wavelengths with significant amplitudes appear on the western side of the bridge, as seen in Figs. A.17 through A.20. On the eastern side, however, some waves having sizable amplitudes do occur, particularly on the eastbound lane after leaving the bridge deck. On the bridge deck itself, these waves, which closely correspond to the span length of 48 feet, are definitely noticeable, and generally appear to have larger amplitudes when nearer the center of the bridge deck.

For the right-left difference profiles for the 30-foot to 60-foot passband, shown in Figs. A.21 through A.24, the bridge deck contains no waves having an appreciable amplitude. However, waves do exist on the approaching pavements and the amplitudes are usually noticeable. The amplitude of these waves tends to die out once the bridge deck is reached.

For the 80 to 110-foot passband for the right profiles, it is observed, from Figs. A.25 through A.28, that only waves with very small amplitudes occur on the bridge deck and on the western part of the approaching pavement. However, on the eastern side of the bridge deck, waves possessing considerable amplitude exist. The amplitudes of these waves which have a length of approximately 85 feet, die out once the bridge deck is encountered.

For the right-left difference plots of the 80 to 110-foot passband, seen in Figs. A.20 through A.32, very little difference exists between those for bridge deck and the western side of the adjoining pavement, as the roughness waves for both sections have fairly short wavelengths. However, the section of adjoining pavement to the east of the bridge deck contains longer waves, about 90 feet in length, with much larger amplitudes, as it also does for the 30 to 60-foot passband. This feature of distinct differences in roughness patterns on opposite sides of Big Sandy Bridge indicates a strong possibility that a non-uniformity exists in the soil conditions between the two sides of the bridge.

As seen in Figs. A.13 through A.16, the plots of the right-left difference profile of the Big Sandy Bridge, the ends of the bridge deck are very difficult to detect. Although the spikes marking these ends are of fairly large amplitude, approximately .25 inch, there is enough short wave roughness on the adjoining pavement to camouflage the actual ends. In Figs. A.9 through A.12, the right profile plots of Big Sandy Bridge, spikes marking the ends of the bridge deck stand out clearly, particularly at the western end of the bridge. The amplitudes of these spikes vary from .52 inch to .28 inch at the beginning of the bridge to .22 inch to .32 inch at the end of the bridge.

The profile plots were also examined for roughness patterns near the ends of the bridge, which could be explained in terms of the different directions of traffic flow. While the two bumps at the eastern end of the bridge consisted of very sharp spikes, the bumps at the western end consisted of a distinct length, of about one foot. Thus, it is apparent for the Big Sandy Bridge that proximity plays a more dominant role than direction of traffic in determining the roughness cuased by the end of the bridge deck.

PLUM CREEK BRIDGE PROJECT

Since this project consisted of two separate roadways and bridges, a description of the visual observations of each is presented independently in this section. The discussion of the bumps at the ends of the bridge is combined, however.

Southbound Lane

From the plots of the 0 to 15-foot passband of the right profile, it is observed that the roughness before the bridge consists of very short waves with fairly small amplitudes, in addition to the long wavelengths which appear to extend onto the bridge deck, as seen in Figs. A.33 through A.38. This effect is due to "phase shift," which is mentioned at the beginning of the chapter.

About 50 feet before the bridge deck, which begins at 165 feet (Fig A.33), the wavelengths and amplitudes of these short waves start increasing. A large spike occurs at about 14 feet before the bridge deck, which coincides with the beginning of the approach ramp. Another large spike marks the beginning of the bridge deck itself; other spikes, indicating expansion joints, are also generally noticeable. Once onto the bridge deck, it appears that the roughness tends to remain the same for about the first 100 feet. However, the waves then tend to become shorter and have larger amplitudes than the roughness waves on the adjoining pavement. The beginning of the metal trestle bridge, which occurs at 315 feet (Fig A.36), is marked by an extremely large spike, having an amplitude of over .5 inch. The expansion joints on this bridge are not noticeable, nor is the end of this metal trestle. The overall patterns of roughness on the two different bridges are not appreciably different. Past the bridge deck, which ends at approximately 470 feet (Fig. A.37), no change in type of roughness occurs for about 25-30 feet. After this, however, the roughness assumes longer wavelengths with rather large amplitudes for several cycles. These waves quickly die out and are replaced with the familiar short waves with small amplitude.

The plots of the 60 to 100-foot passband of the right profile are presented in Figs. A.39 through A.41. Long waves having significant amplitudes exist before the bridge, but the amplitudes of these waves diminish gradually on the bridge deck itself. The amplitudes of these waves on the adjoining pavement, which have a length of about 65-70 feet, tend to increase just before the beginning of the bridge. Occasionally these wavelengths appear on the bridge deck with noticeable amplitude, but they generally are insignificant, except at the very beginning of the bridge, where "phase shift" occurs, causing long wavelength roughness present on the adjoining pavement to appear to be on the bridge deck.

It is observed from the plots of the 15 to 60-foot passband that waves having significant amplitudes are generally very scarce on the bridge deck, particularly on the metal trestle. However, waves having large amplitudes do occur right at the end of the bridge deck, and for the next 100 feet or so, after which the amplitudes of these waves decrease significantly. No pattern of roughness is discernible for this particular passband.

Northbound Lanes

When observing the filtered profile plots of the two northbound lanes, it should be realized that the vertical scales, signifying road surface elevation, are different for the two lanes. It appears that the inner lane is much rougher, but the vertical scale has been automatically enlarged by the computer, and, in reality, the two lanes experience similar roughness amplitudes.

It is observed from the plots of the two northbound lanes for the 0 to 15-foot passband, seen in Figs. A.45 through A.50, that the bridge deck is much rougher than the adjoining pavement. On the adjoining pavement, the short wavelength roughness possesses rather small amplitudes, thereby providing a relatively smooth appearance. At approximately 40 feet before the beginning of the bridge, however, the amplitudes of the pavement roughness increase. Once onto the bridge deck itself, which begins at approximately 125 feet, the roughness is characterized by very short waves having large amplitudes. Spikes indicating expansion joints are occasionally difficult to detect, but generally these joints stand out clearly.

For the 60 to 100-foot passband, it is observed that the longer waves have fairly large amplitudes before the bridge, as seen in Figs. A.51 through A.56. Once onto the bridge deck, however, the amplitudes of these longer waves tend to die out, although an occasional wave does exist with appreciable amplitude. For the most part, though, these wavelengths on the bridge are not significant. It must be remembered that the effects of "phase shift" cause a partial cycle of the long wavelength roughness on the adjoining pavement to appear as if it were actually on the bridge deck.

Additional information is available for the outer northbound lane. The plot of the right profile of the first part of the northbound bridge for the 20 to 40-foot passband is presented in Figs. A.57 through A.59. It is readily apparent that there is an absence of waves corresponding to this passband, with appreciable amplitudes on the adjoining pavement. However, such waves are extremely prominent on the bridge deck, having amplitudes on the order of .1 inch. These waves correspond directly to the expansion joints of the bridge deck, which are spaced at 30-foot intervals. Furthermore, waves with significant amplitudes are not present on the section of the bridge where the span length is 39 feet, although roughness in the form of slightly shorter wavelengths with sizable amplitude does exist near the transition from a 39-foot span length to a 30-foot span length, which occurs at approximately 320 feet.

From the plot of the 50 to 70 foot passband for the outer northbound lane, Figs. A.60 through A.62, very little difference is observed between the bridge deck and the adjoining pavement. While the amplitudes of these waves on the bridge deck are generally larger, the difference in magnitude is not enough to appear significant.

Ends of Bridge

For the northbound bridge, the beginning of the bridge deck is marked by a single large spike having an amplitude of approximately .40 inch. Once again, it must be realized that the vertical scales for the two lanes are different. For both lanes, the surrounding road profile is very rough, as seen in Figs. A.45 and A.48, particularly the latter plot, due to the enlarged vertical scale. The surface is extremely rough for about 2 feet in front of the beginning of the bridge deck.

For the southbound lane, a comparison of the bumps at the two ends of the bridge reveals several interesting features. Due to the presence of the 15-foot approach ramp, the beginning of the bridge is marked by two spikes, a .35 inch spike at the beginning of the approach ramp and a .40 inch spike at the beginning of the bridge deck. The two spikes are very similar, as seen in Fig. A.33. At the end of the bridge, the end of the approach ramp is extremely difficult to detect, as no spike is present. The end of the bridge deck itself consists of a spike with amplitude of about .35 inch.

Filter Passband: 0.0 to 15.0 ft. Wavelengths - Outer Lane - Right Profile Frame 1

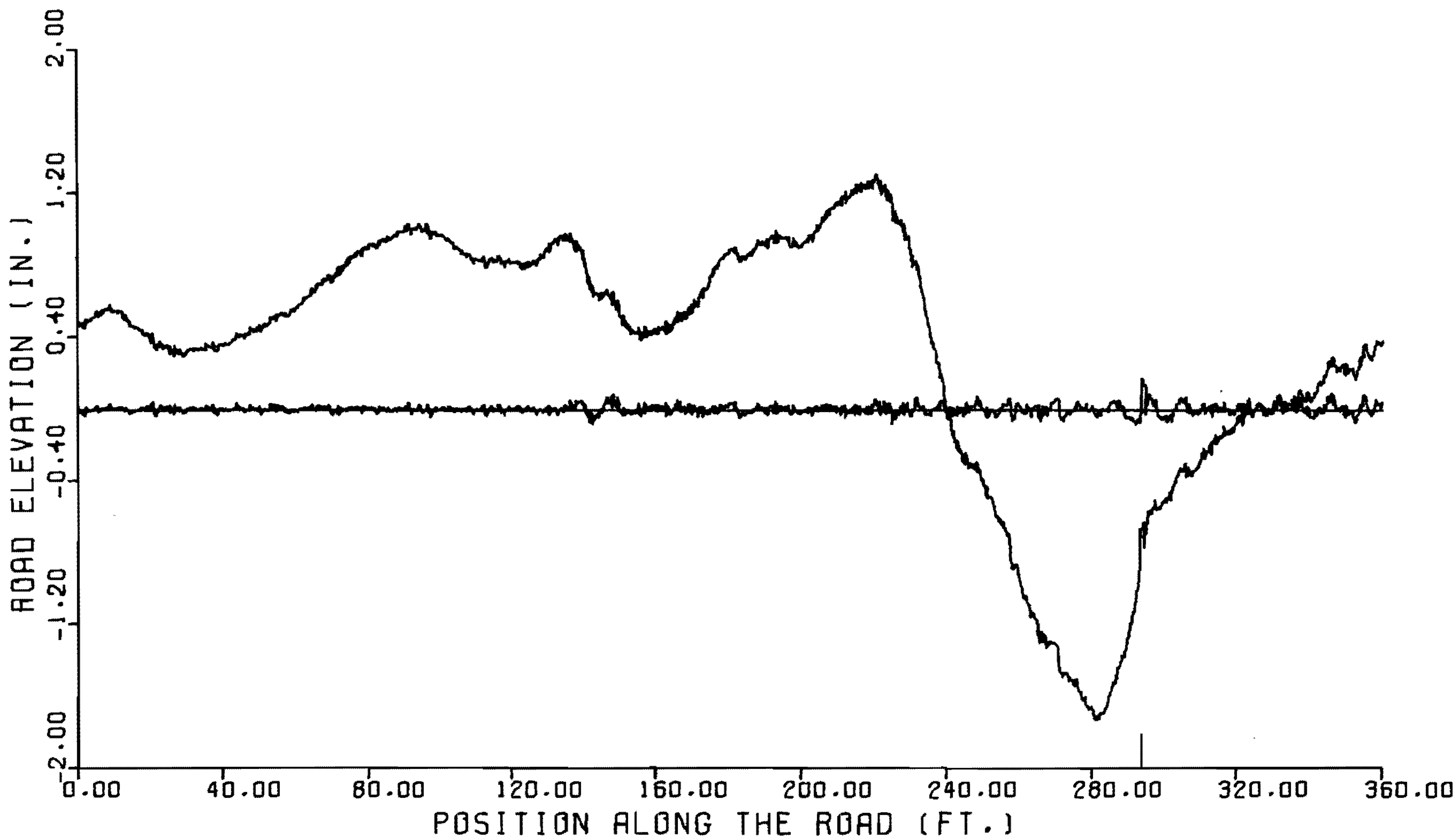

Fig A1.1. MoPac Bridge

Filter Passband: 0.0 to 15.0 ft. Wavelengths - Outer Lane - Right Profile Frame 2

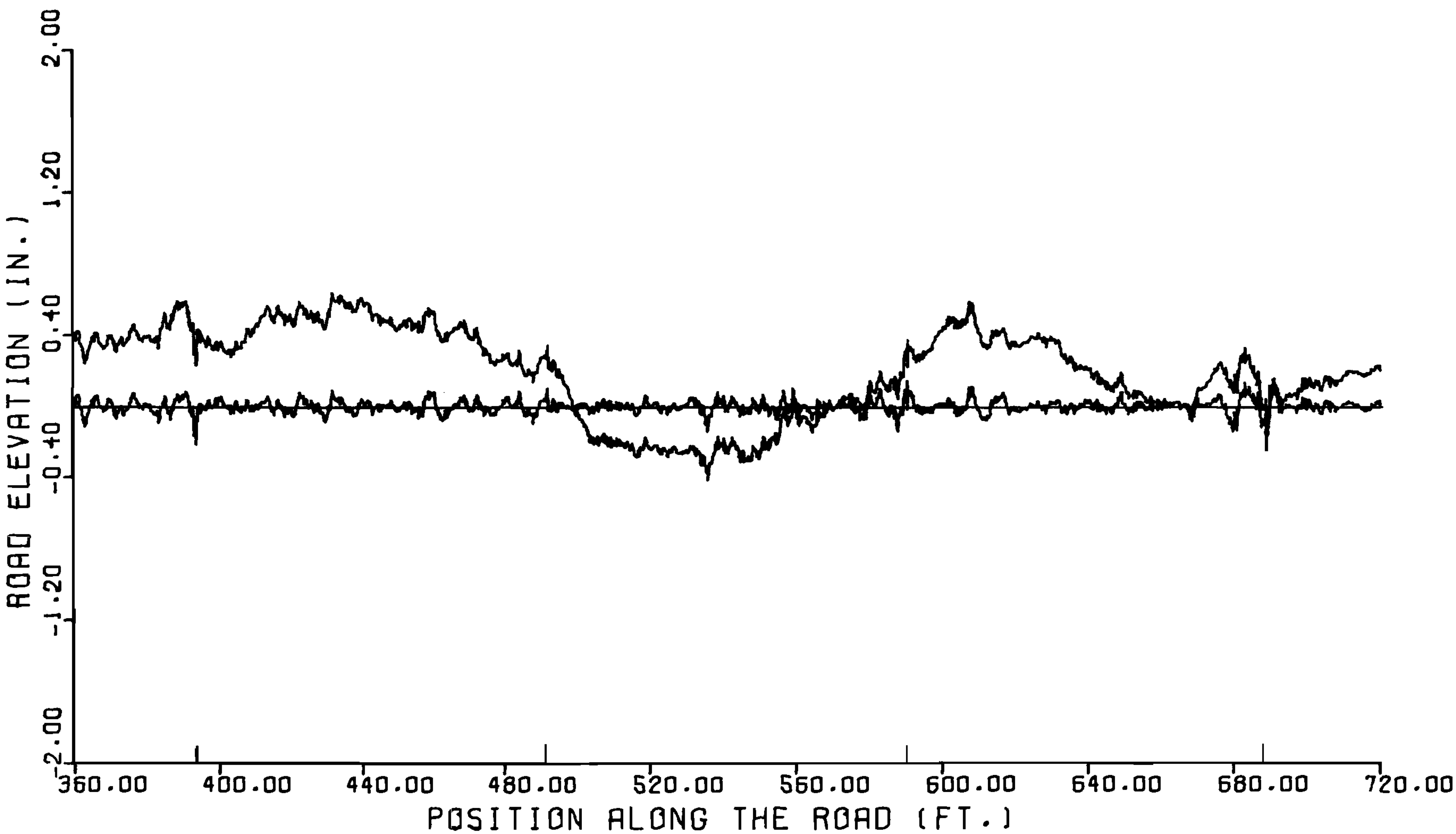

Fig A1.2. MoPac Bridge

Filter Passband: 0.0 to 15.0 ft. Wavelengths - Outer Lane - Right Profile Frame 3

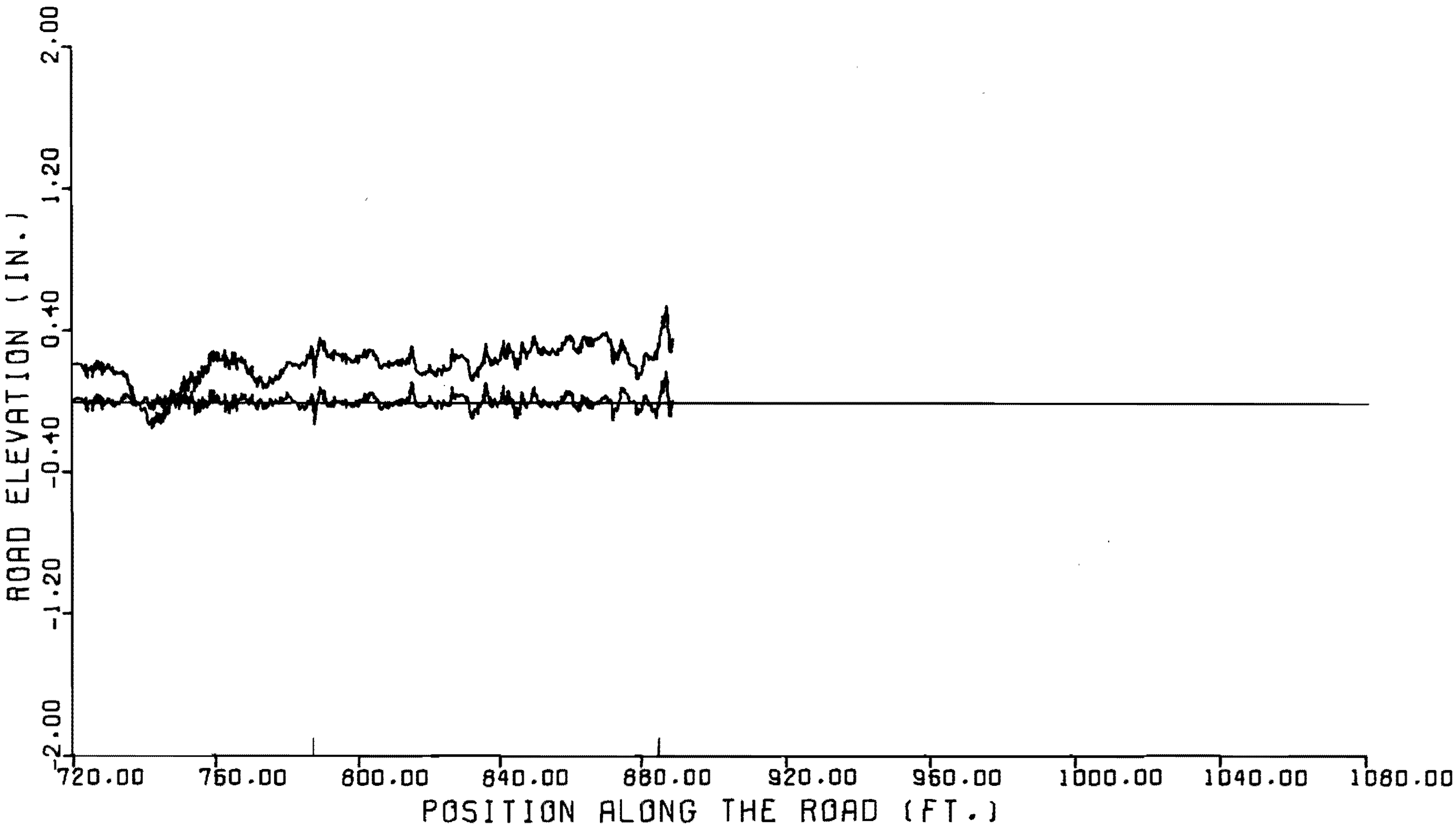

Fig A1.3. MoPac Bridge

Filter Passband: 0.0 to 15.0 ft. Wavelengths - Outer Lane - Right-Left Profile Frame 1

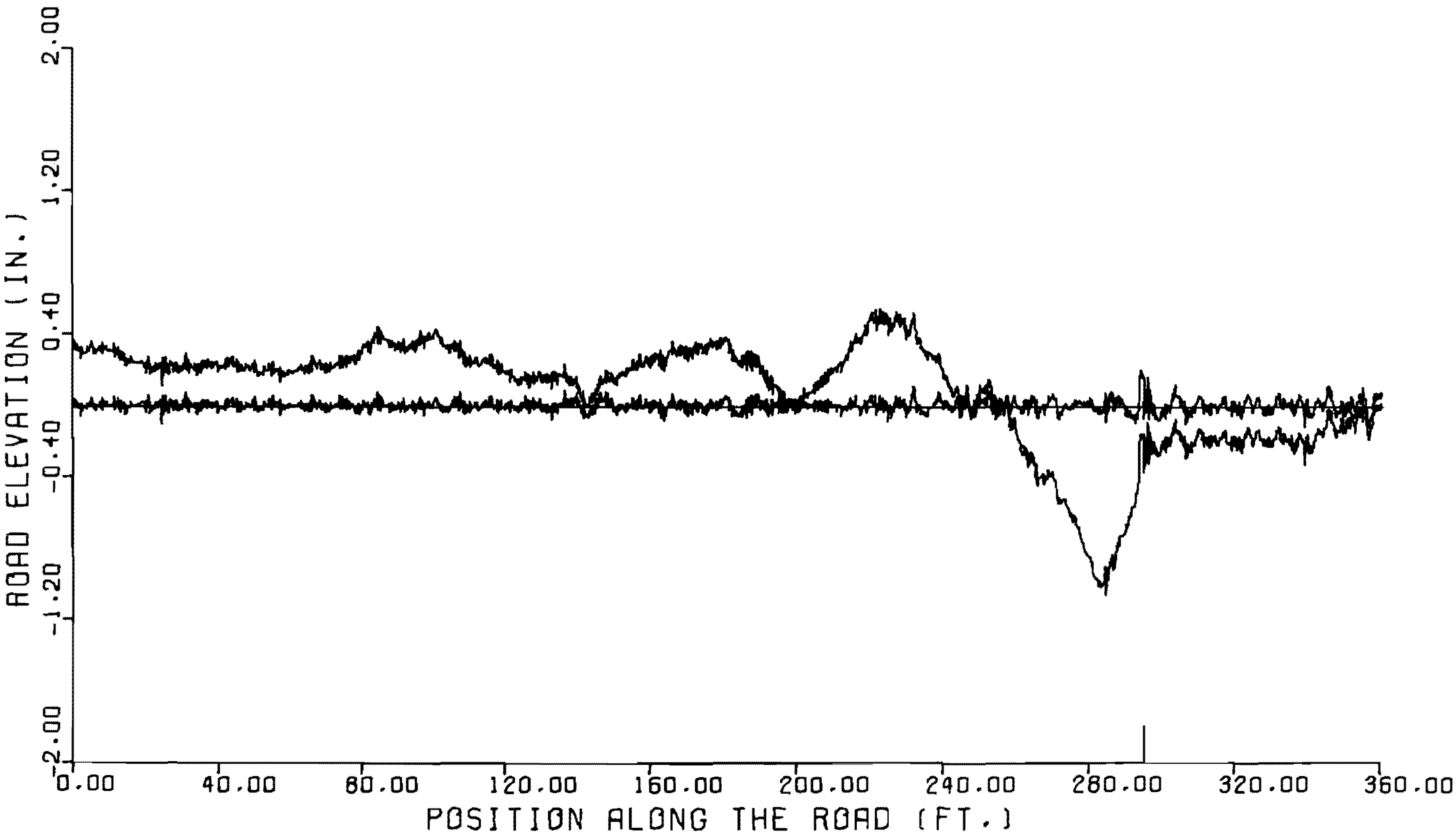

Fig A1.4. MoPac Bridge

Filter Passband: 0.0 to 15.0 ft. Wavelengths - Outer Lane - Right-Left Profile Frame 2

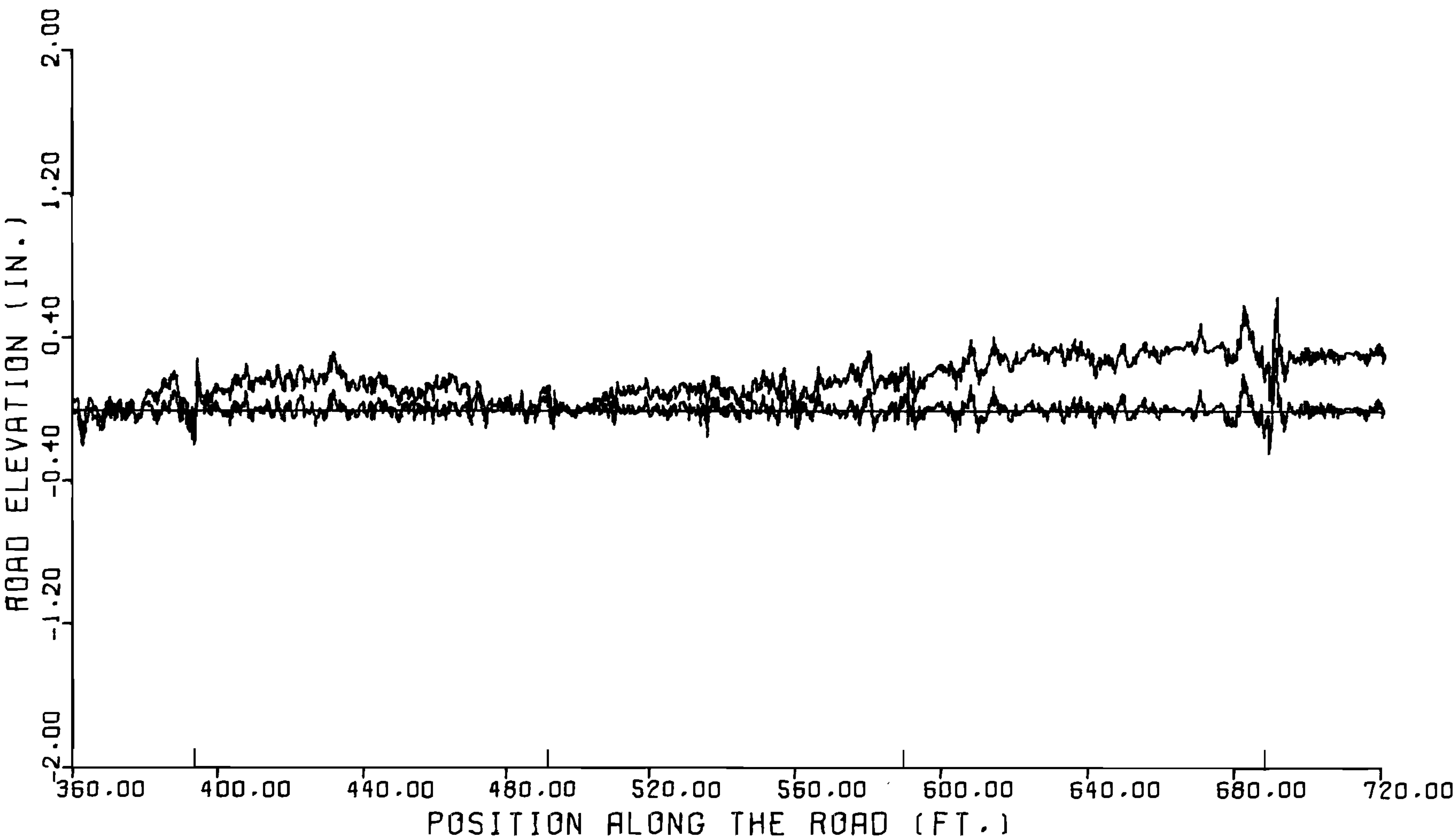

Fig A1.5. MoPac Bridge

Filter Passband: 0.0 to 15.0 ft. Wavelengths - Outer Lane - Right-Left Profile Frame 3

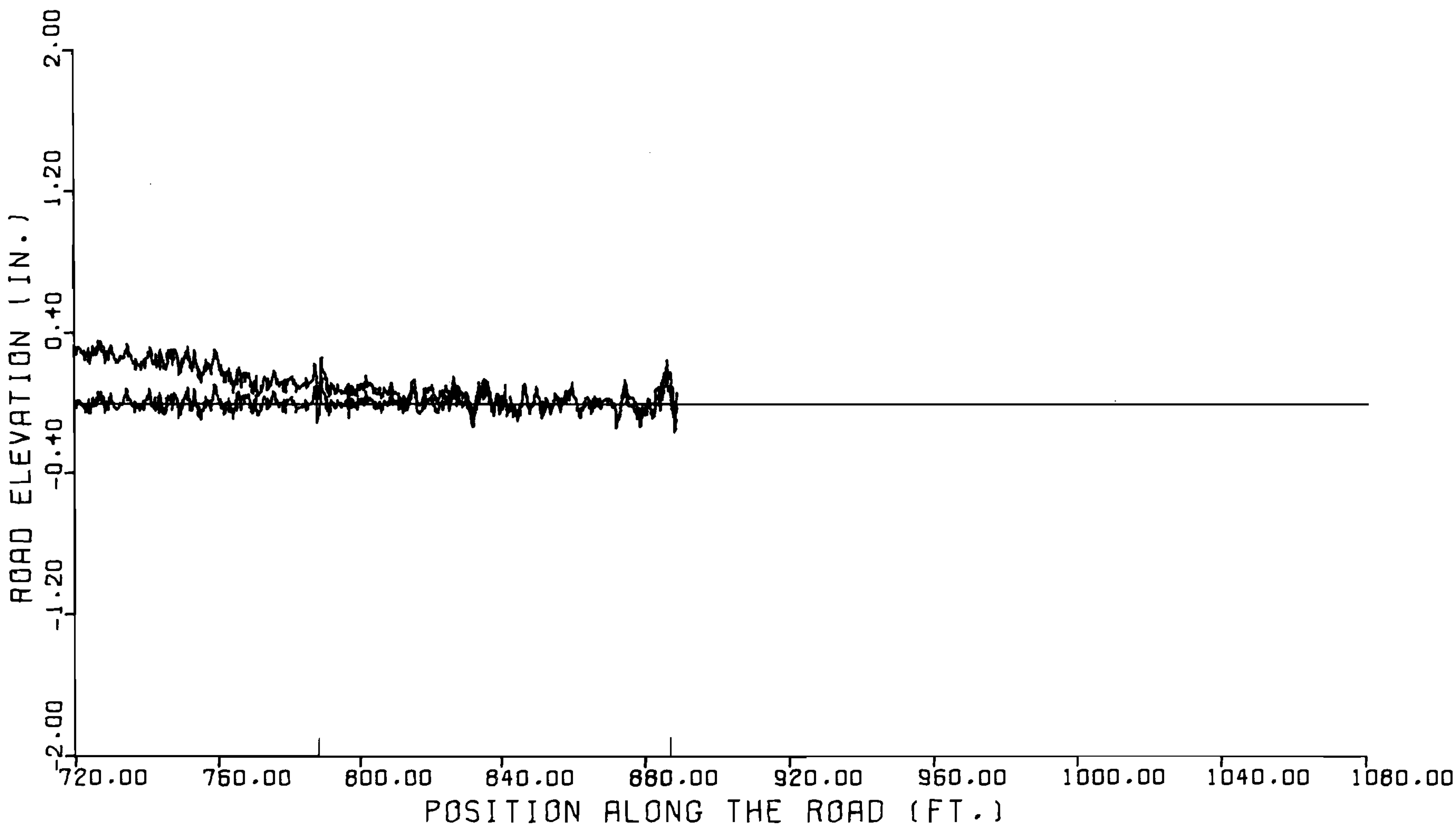

Fig A1.6. MoPac Bridge

Profile Data from File Number 51 beginning with Record Number 10. Right Wheel Path.
5 Records were used for plotting. Frame 1.

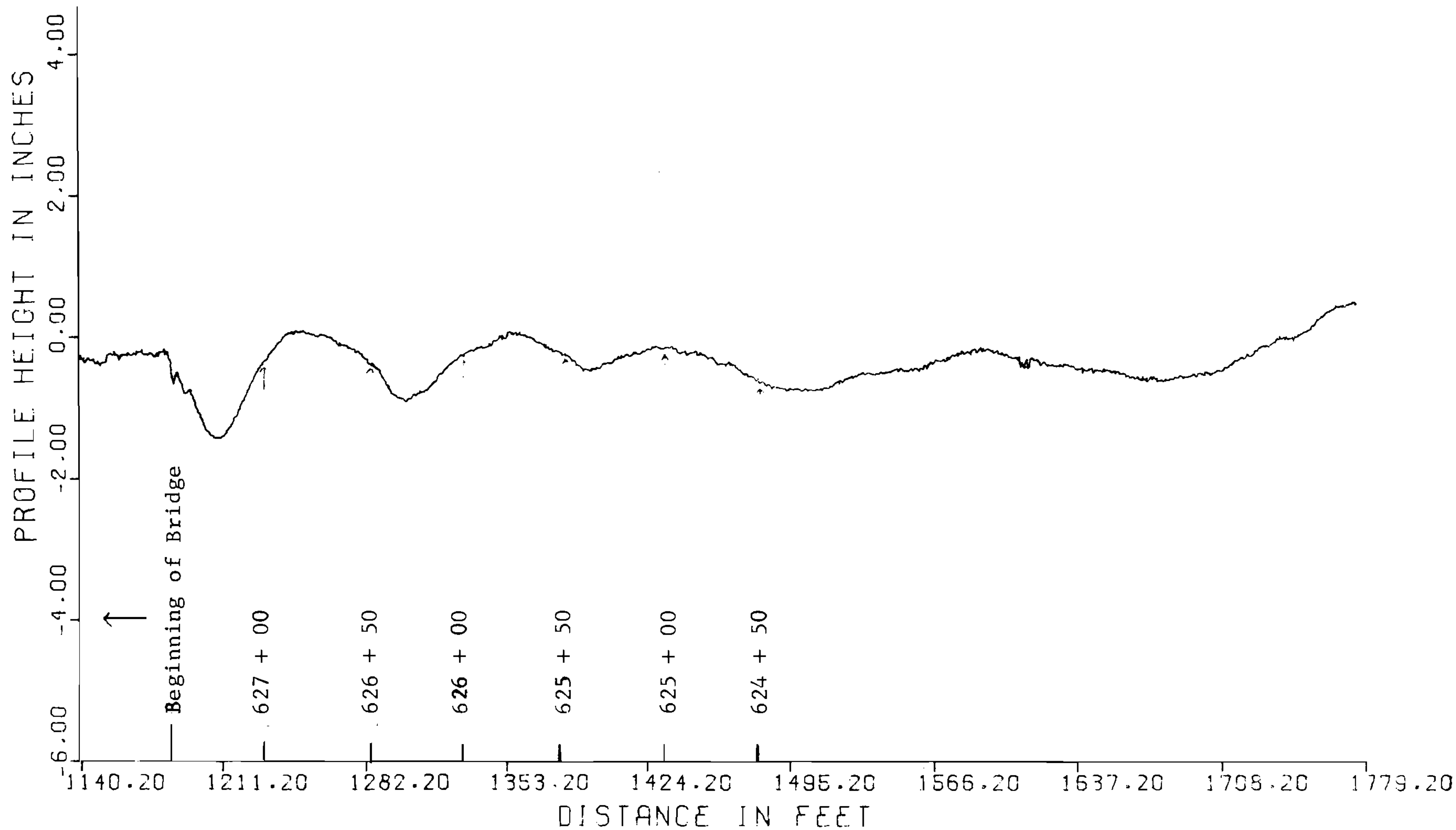

Fig A1.7. MoPac Bridge Project Unfiltered Profile

Profile Data from File Number 51 beginning with Record Number 15. Right Wheel Path.
5 records were used for plotting. Frame 2.

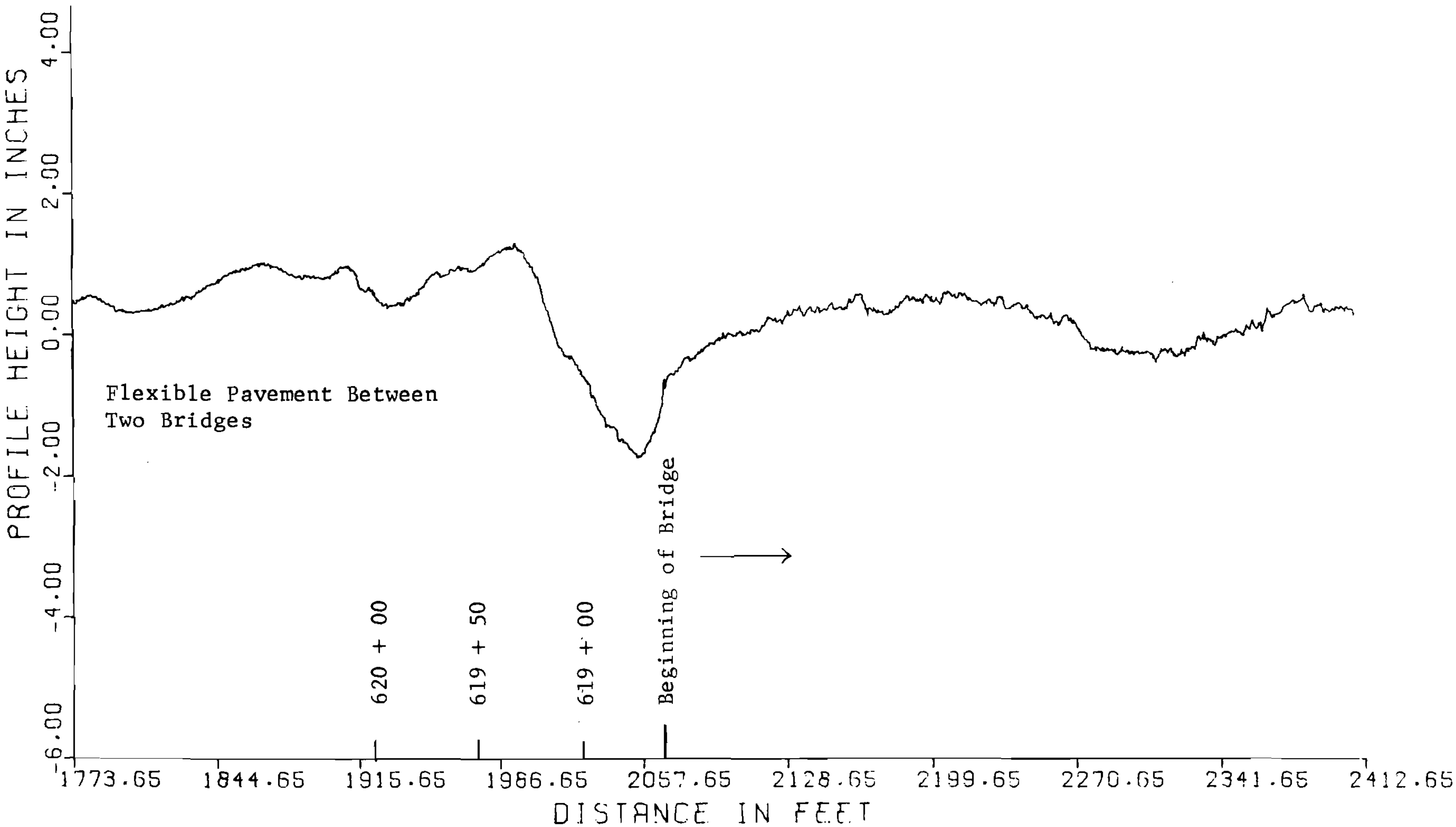

Fig A1.8. MoPac Bridge Project Unfiltered Profile

Filter Passband: 0.0 to 15.0 ft. Wavelengths - Westbound Lane - Right Profile Frame 1

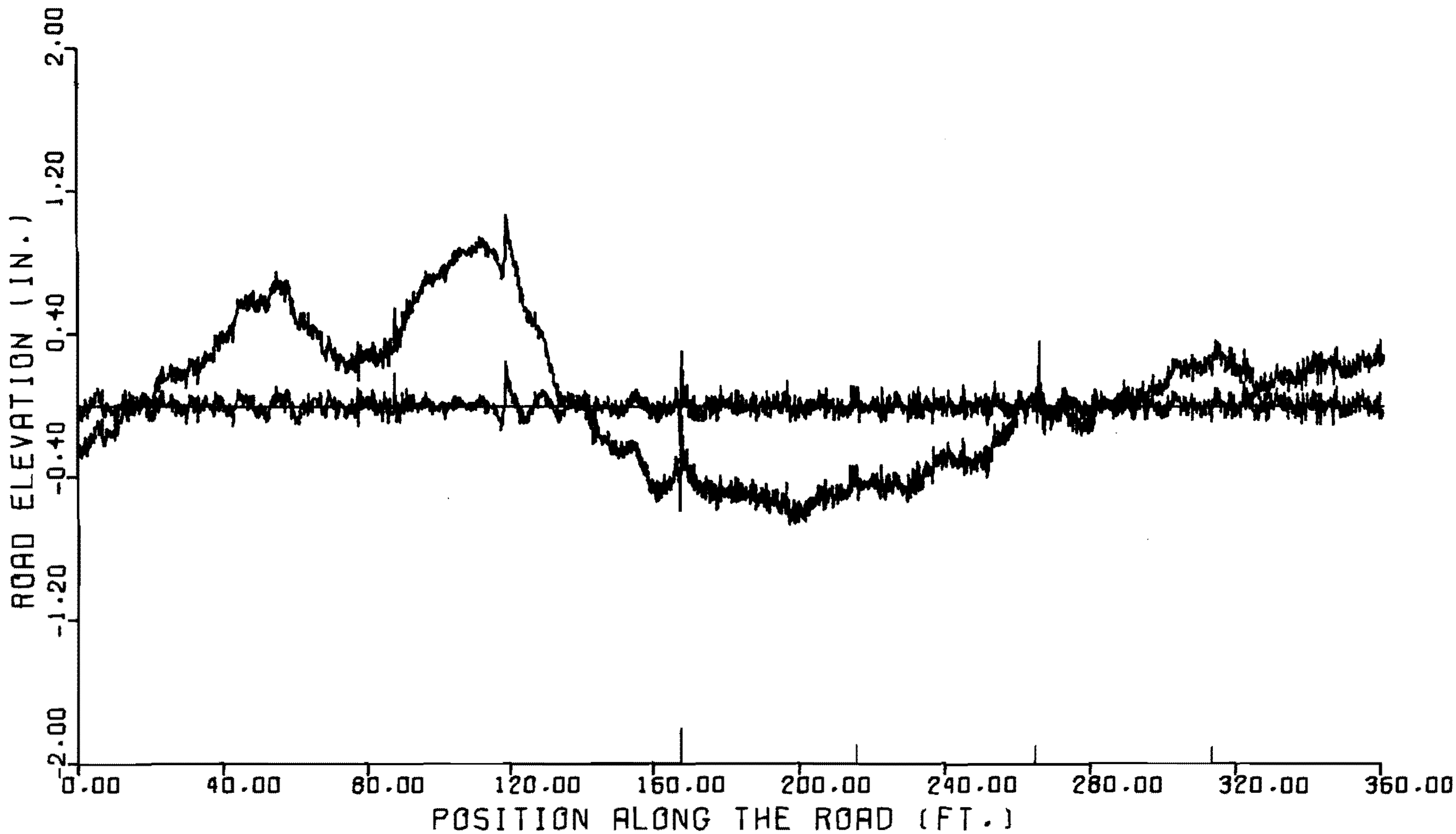

Fig A1.9. Big Sandy Bridge

Filter Passband: 0.0 to 15.0 ft. Wavelengths - Westbound Lane - Right Profile Frame 2

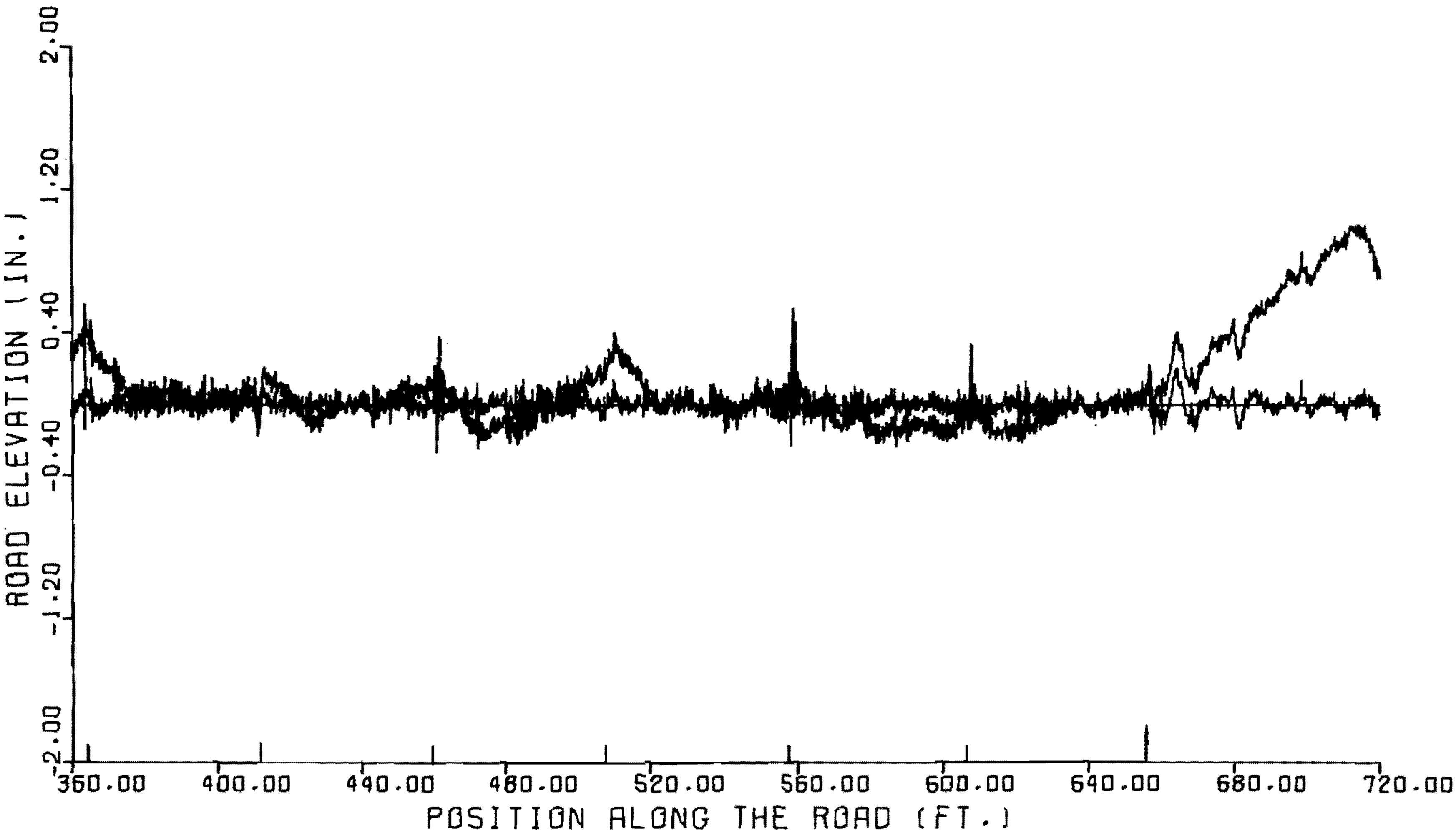

Fig A1.10. Big Sandy Bridge

Filter Passband: 0.0 to 15.0 ft. Wavelengths - Eastbound Lane - Right Profile Frame 1

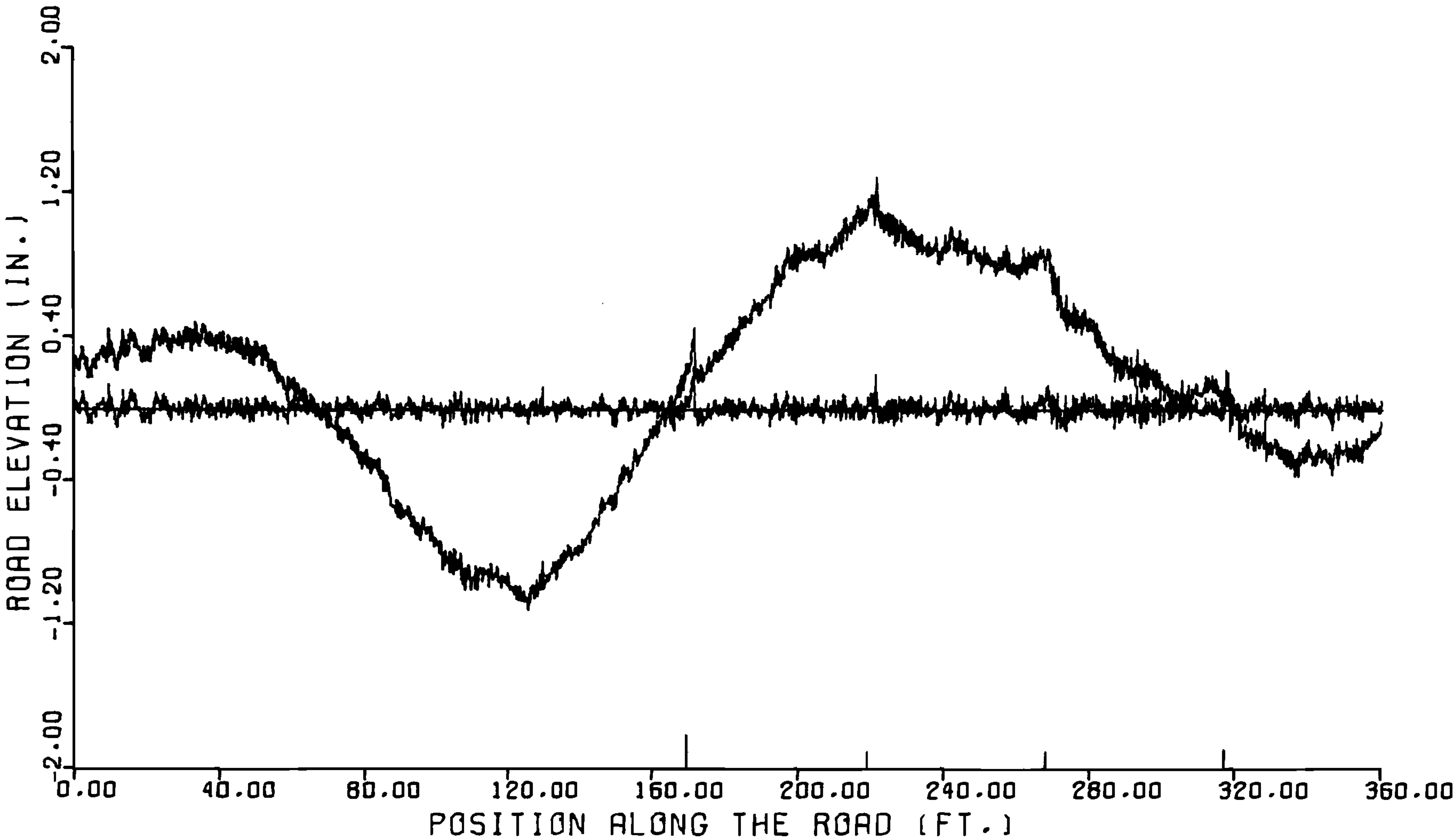

Fig A1.11. Big Sandy Bridge

Filter Passband: 0.0 to 15.0 ft. Wavelengths - Eastbound Lane - Right Profile Frame 2

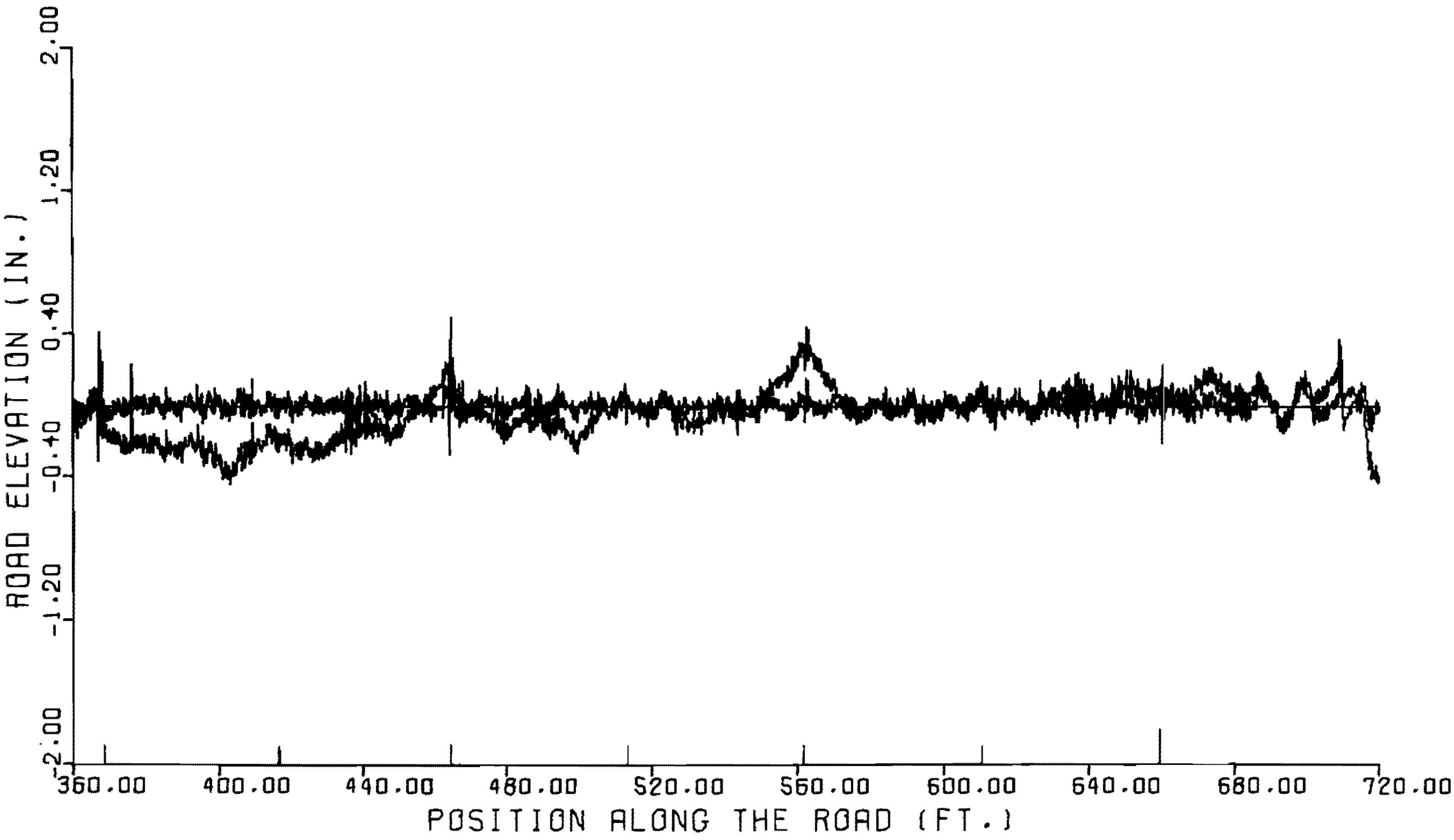

Fig A1.12. Big Sandy Bridge

Filter Passband: 0.0 to 15.0 ft. Wavelengths - Westbound Lane - Right-Left Profile Frame 1

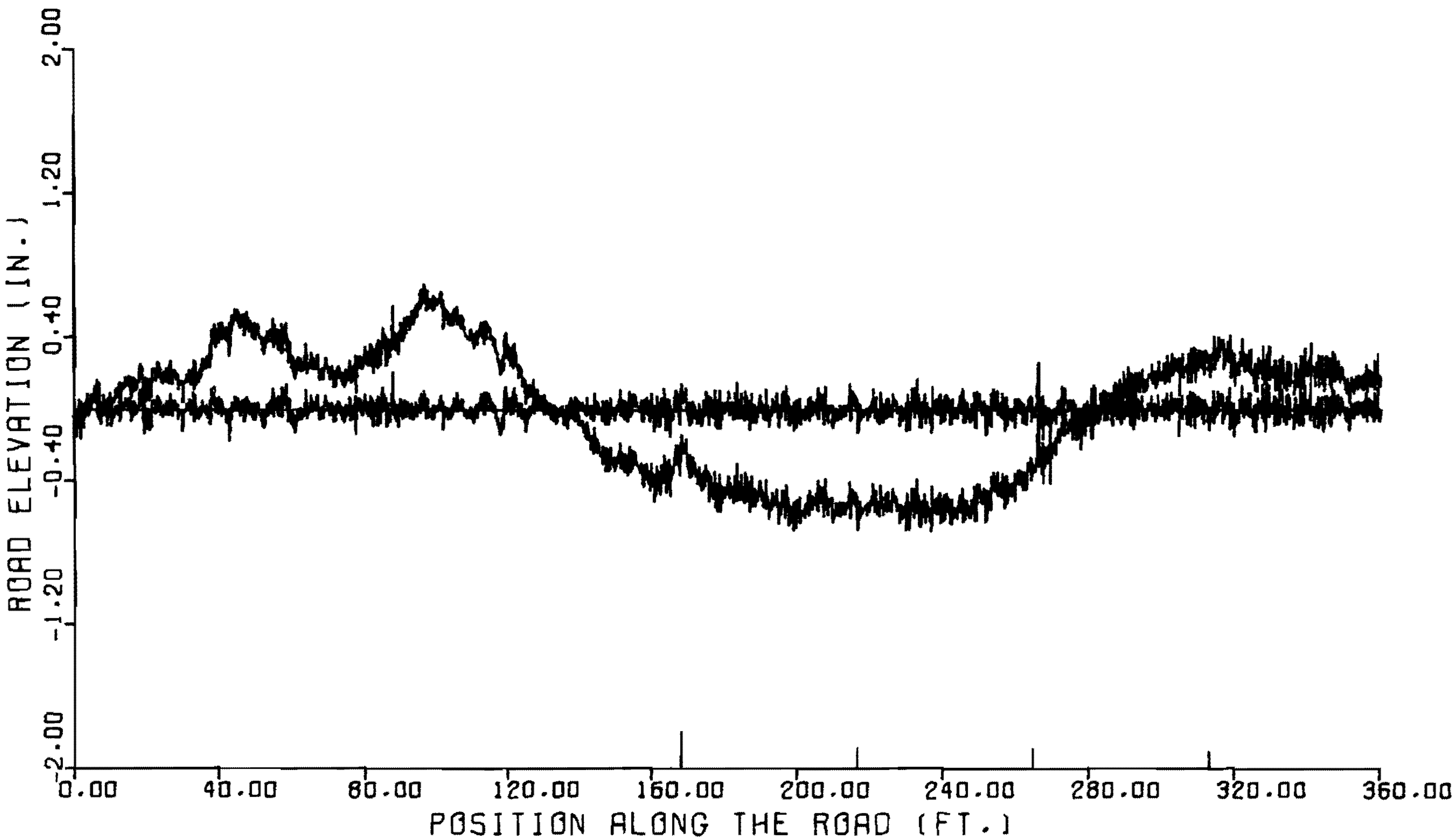

Fig A1.13. Big Sandy Bridge

Filter Passband: 0.0 to 15.0 ft. Wavelengths - Westbound Lane - Right-Left Profile Frame 2

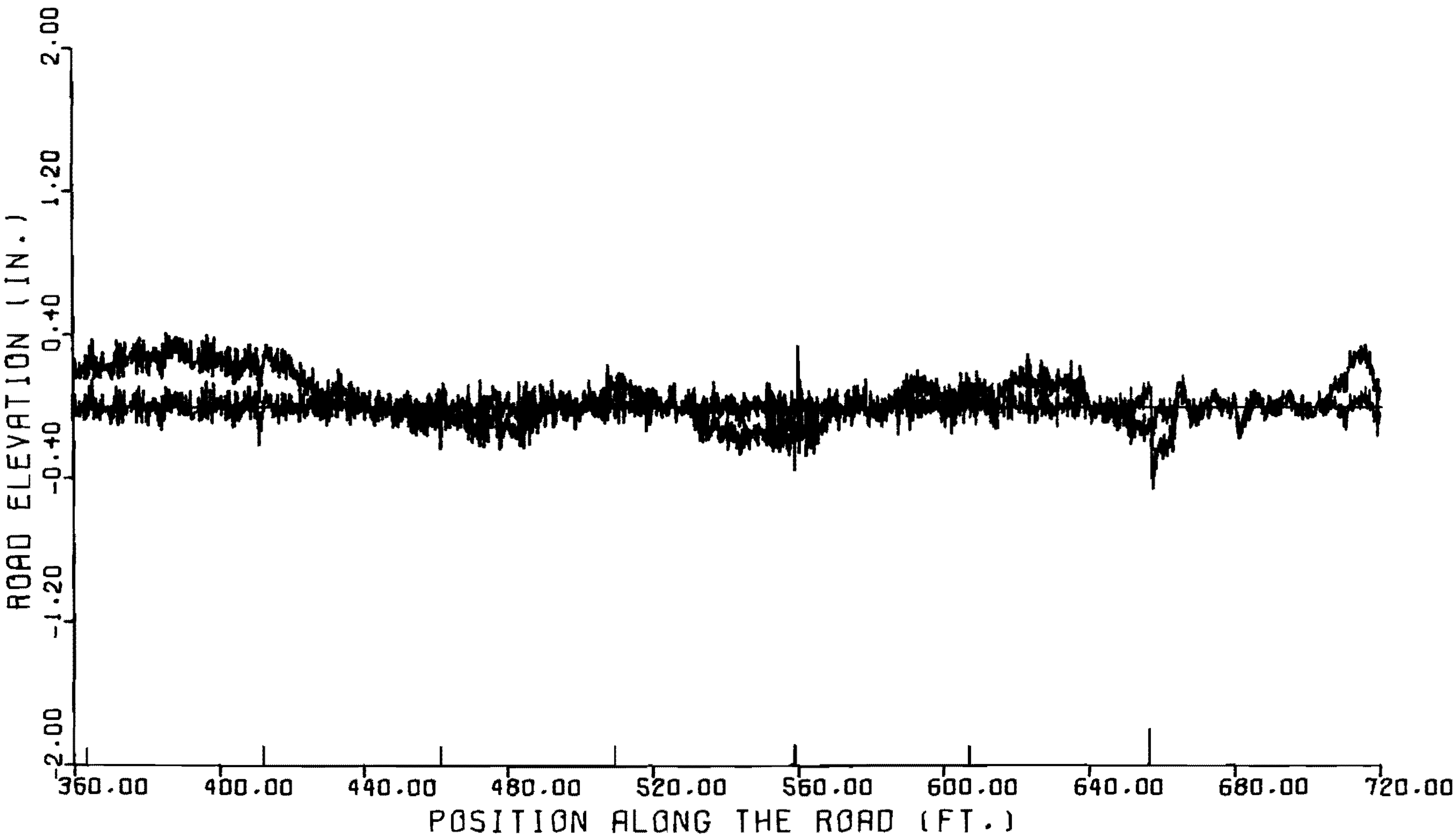

Fig A1.14. Big Sandy Bridge

Filter Passband: 0.0 to 15.0 ft. Wavelengths - Eastbound Lane - Right-Left Profile Frame 1

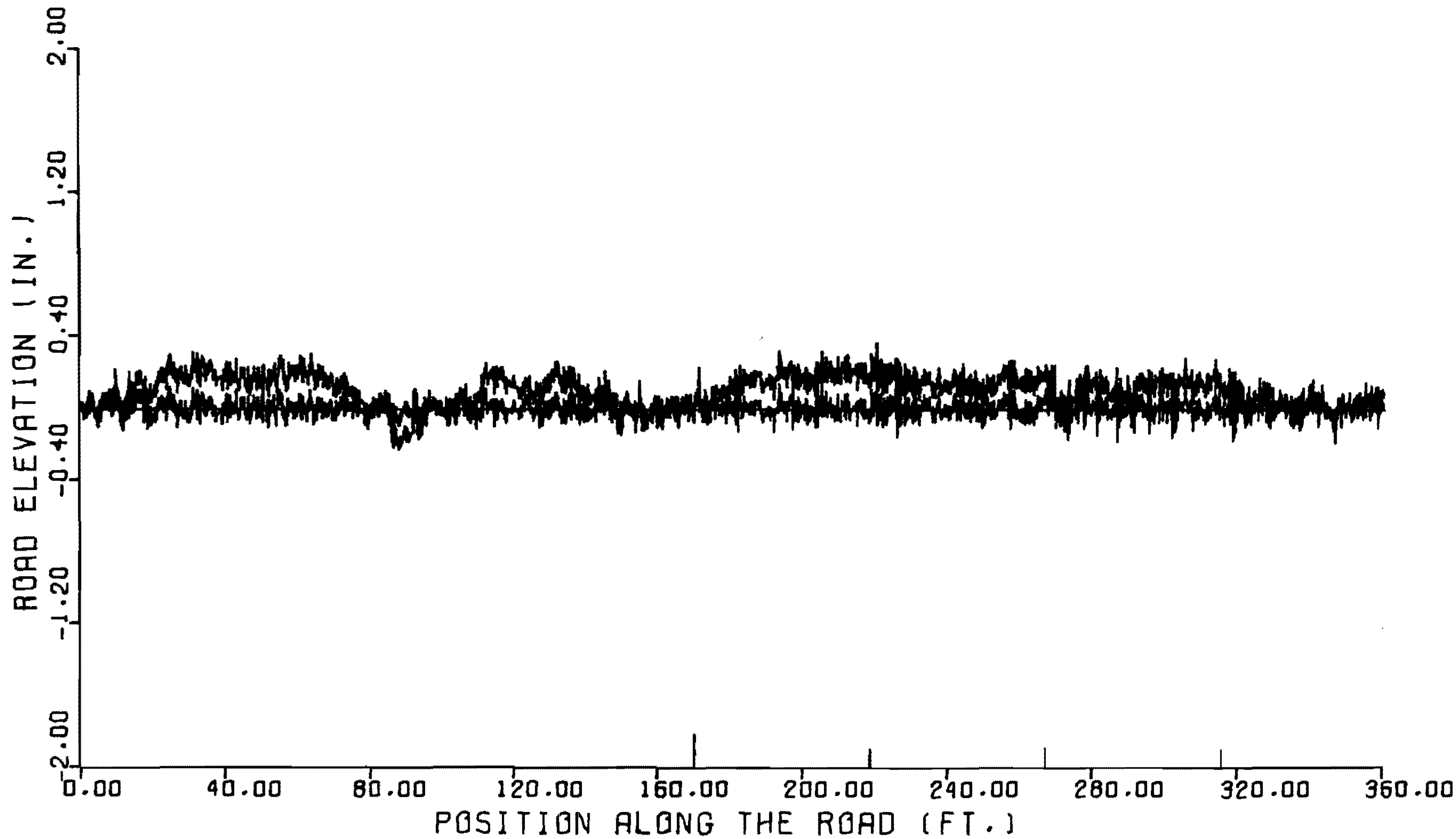

Fig A1.15. Big Sandy Bridge

Filter Passband: 0.0 to 15.0 ft. Wavelengths - Eastbound Lane - Right-Left Profile Frame 2

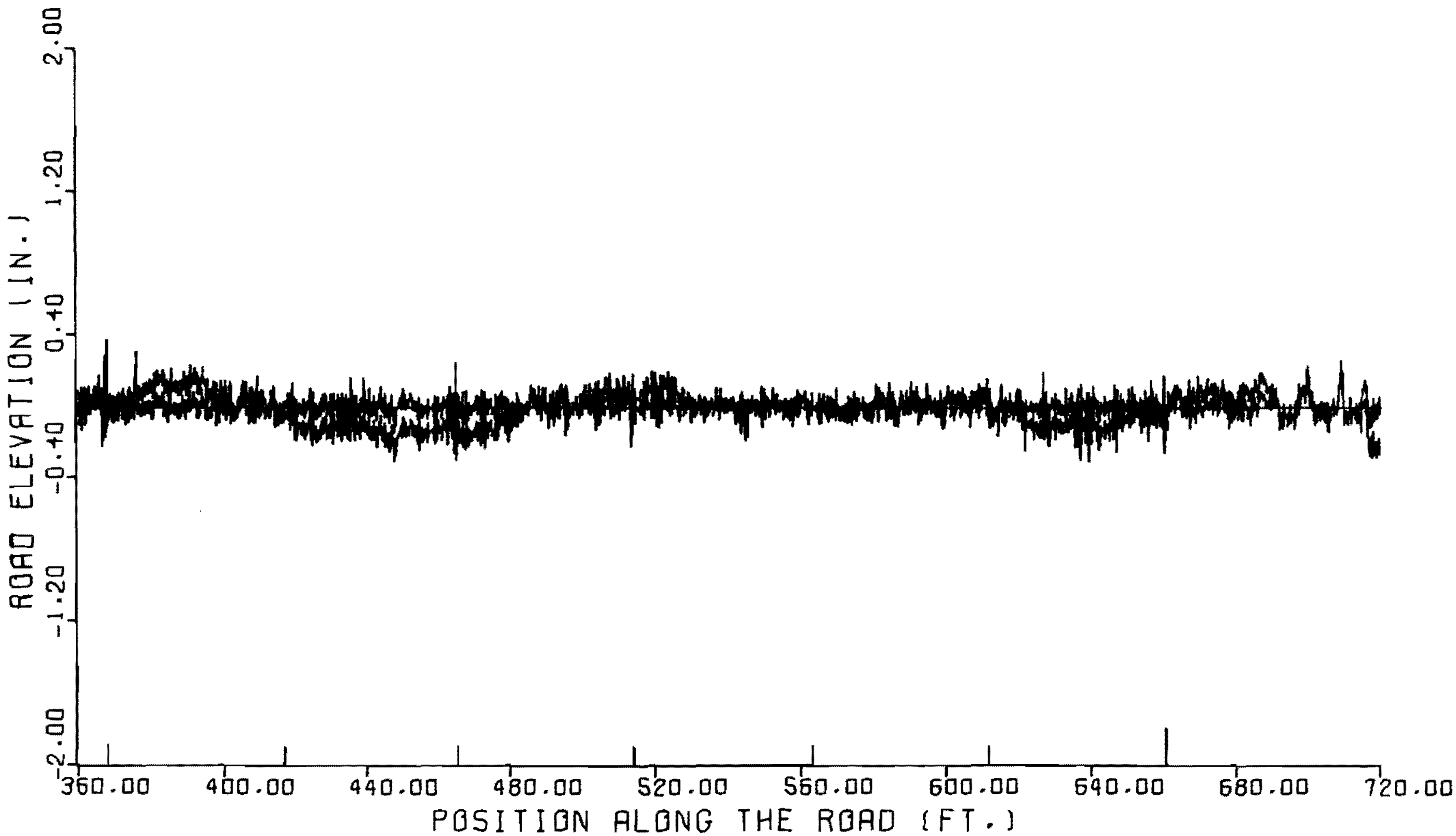

Fig A1.16. Big Sandy Bridge

Filter Passband: 0.0 to 15.0 ft. Wavelengths - Eastbound Lane - Right Profile Frame 1

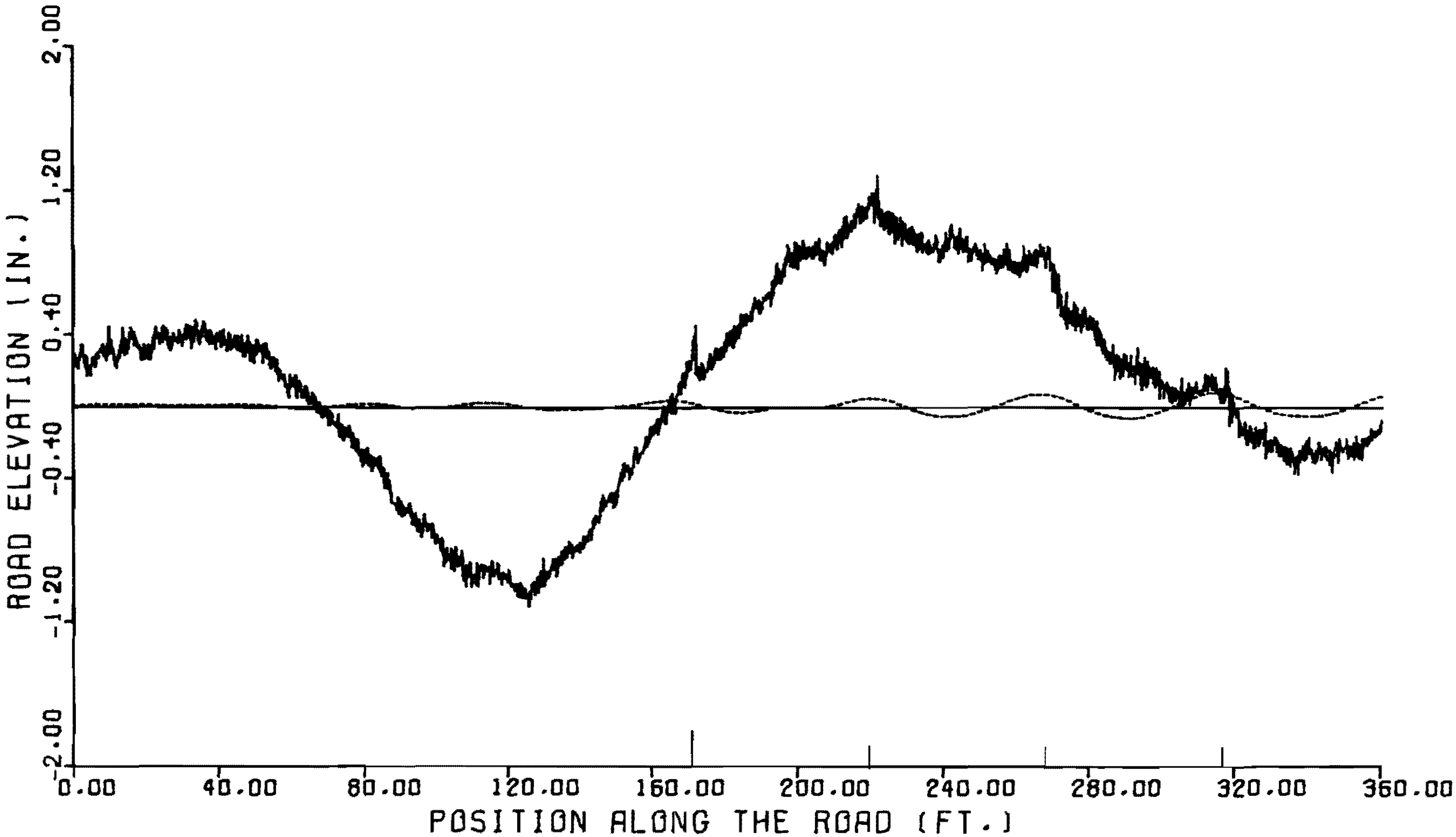

Fig A1.17. Big Sandy Bridge

Filter Passband: 0.0 to 15.0 ft. Wavelengths - Eastbound Lane - Right Profile Frame 2

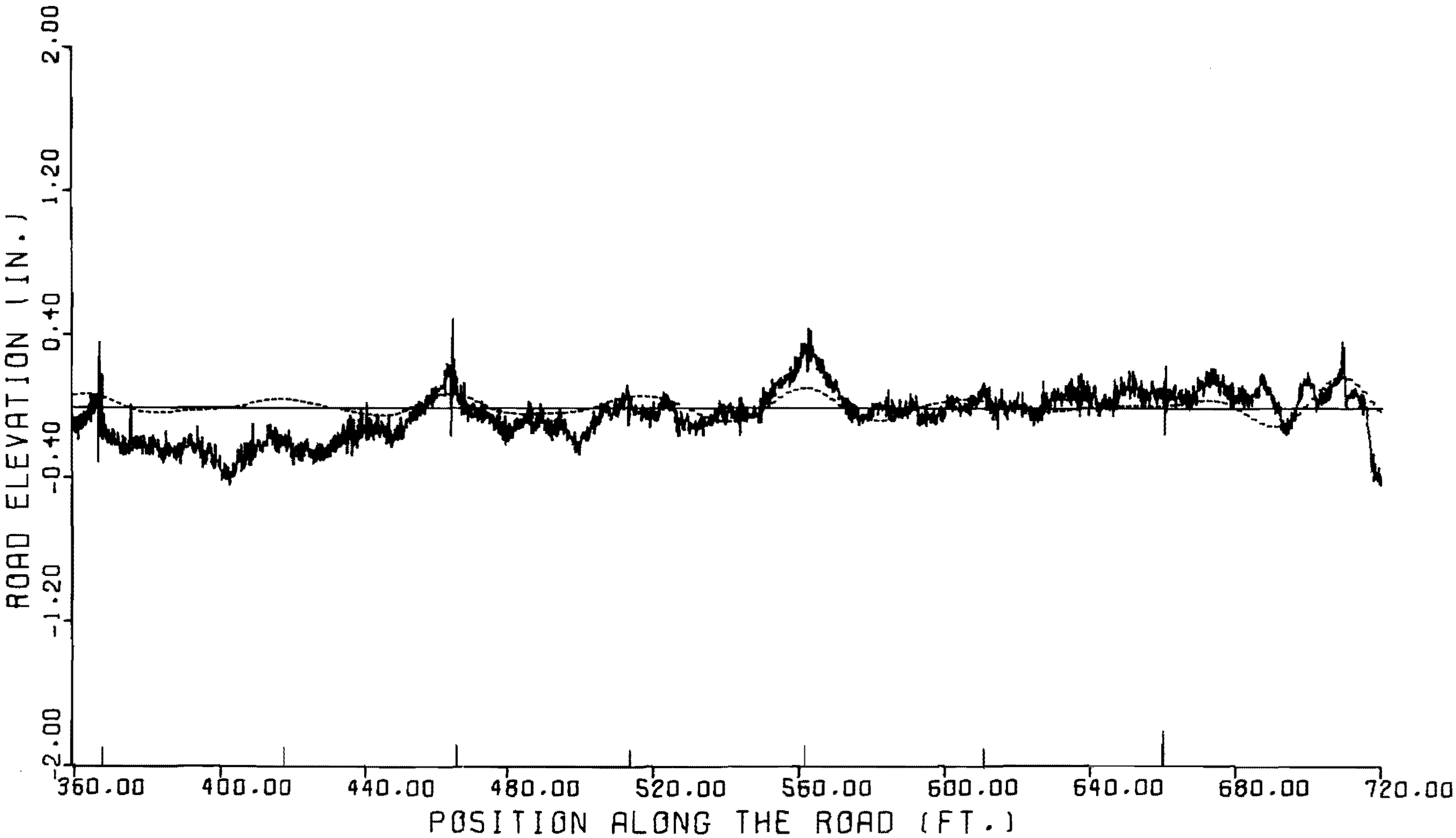

Fig A1.18. Big Sandy Bridge

Filter Passband: 0.0 to 15.0 ft. Wavelengths - Westbound Lane - Right Profile Frame 1

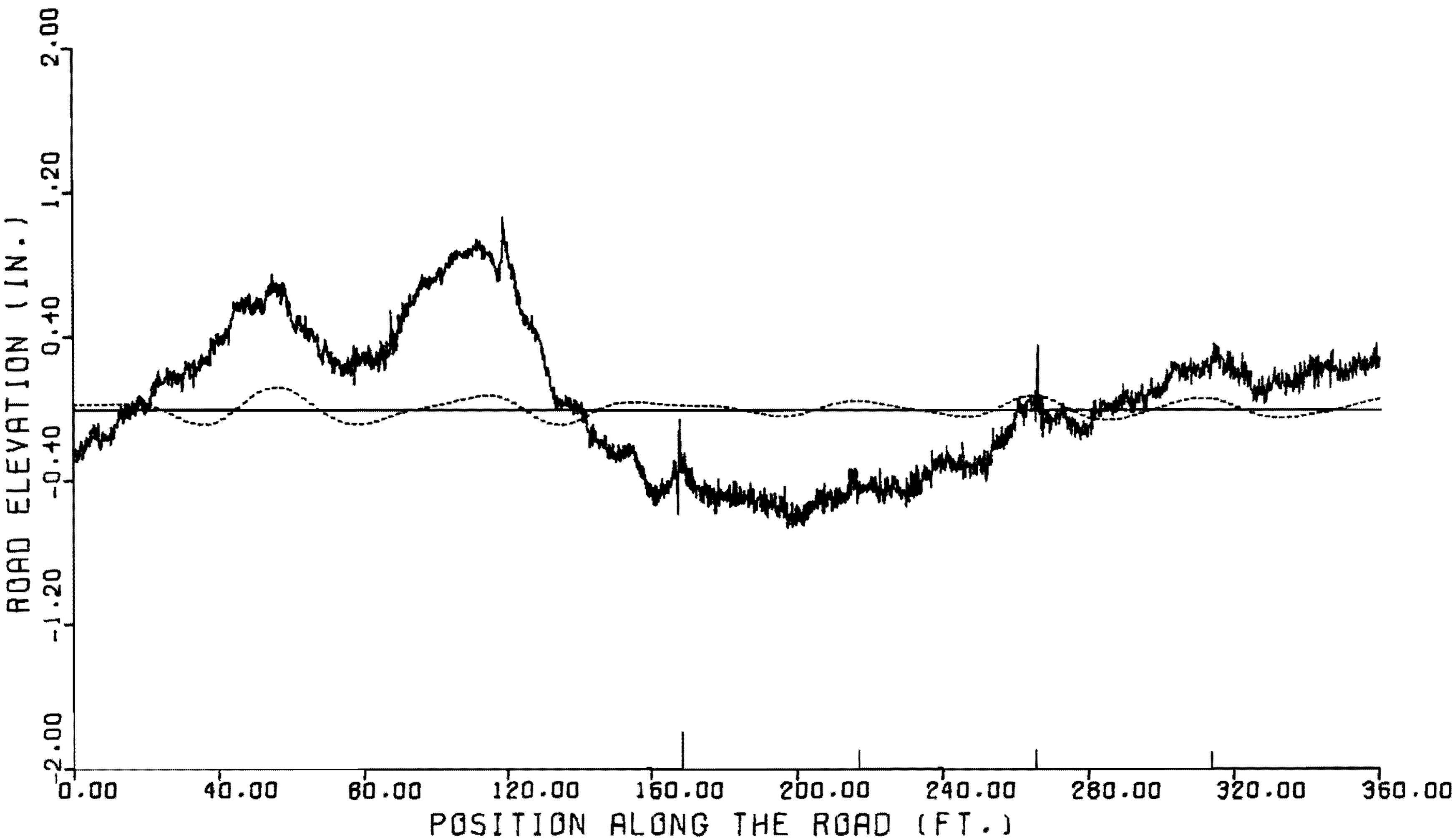

Fig A1.19. Big Sandy Bridge

Filter Passband: 30.0 to 60.0 ft. Wavelengths - Westbound Lane - Right Profile Frame 2

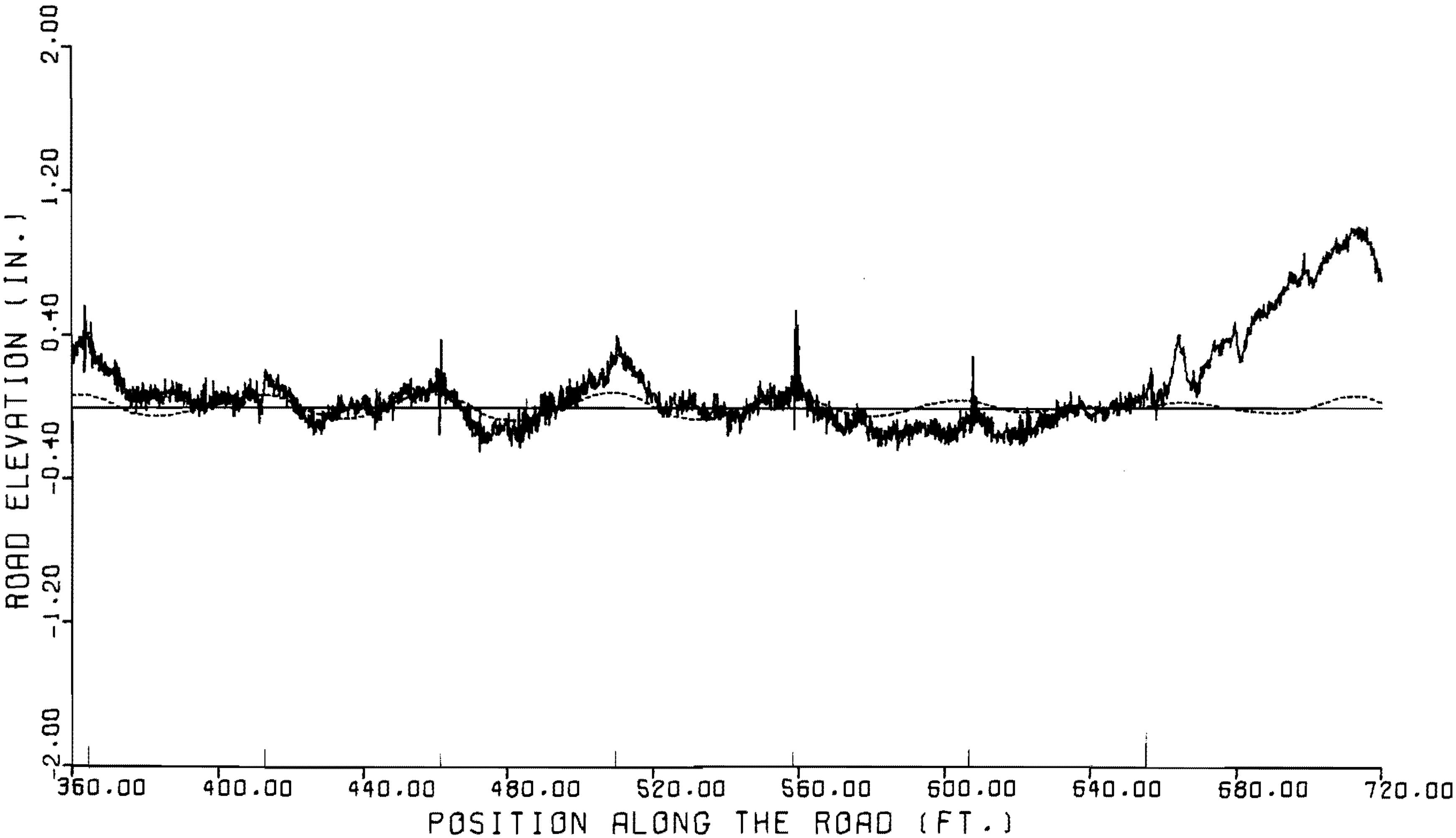

Fig A1.20. Big Sandy Bridge

Filter Passband: 30.0 to 60.0 ft. Wavelengths - Eastbound Lane - Right Profile Frame 1

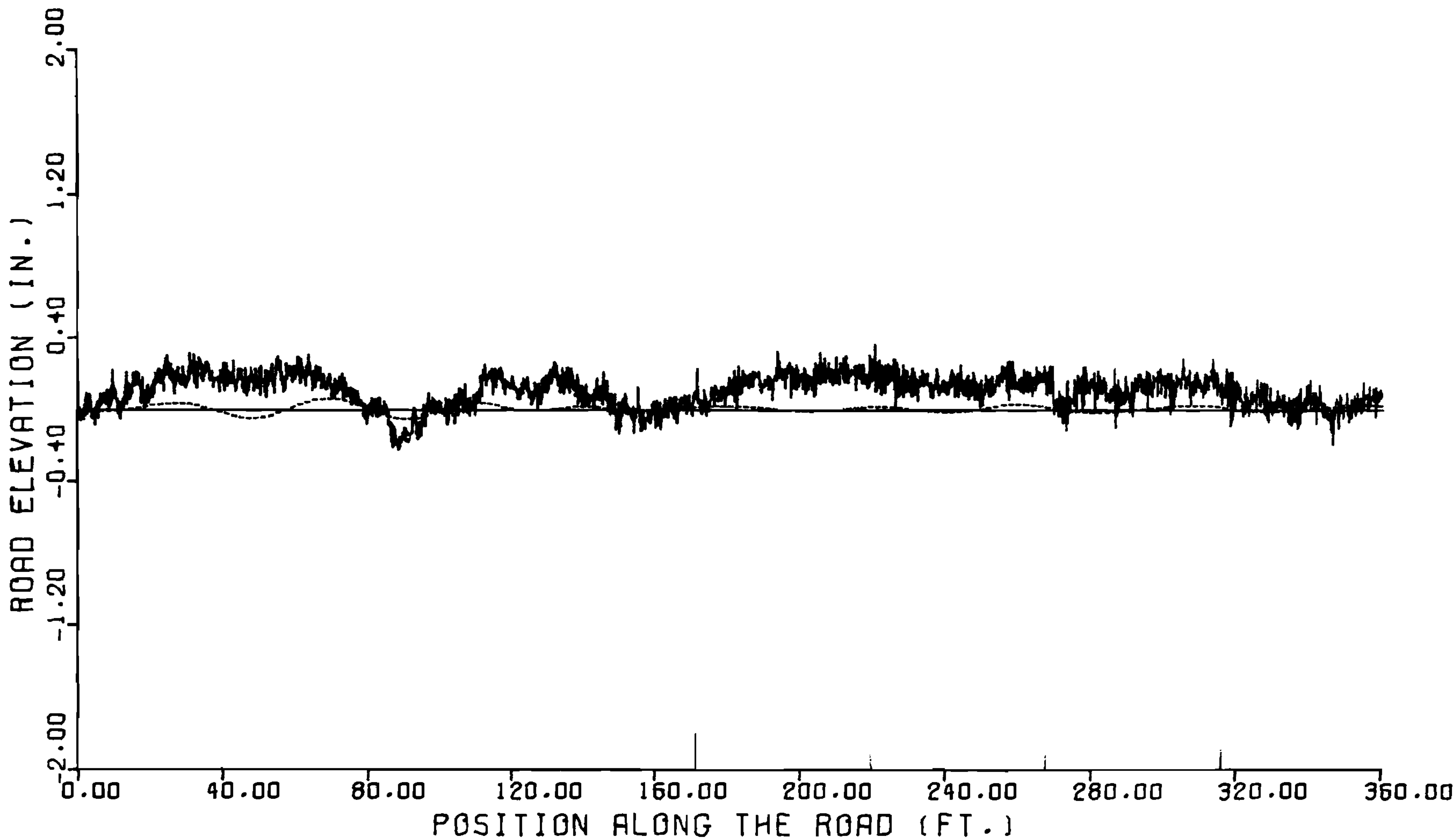

Fig A1.21. Big Sandy Bridge

Filter Passband: 30.0 to 60.0 ft. Wavelengths - Eastbound Lane - Right-Left Profile Frame 2

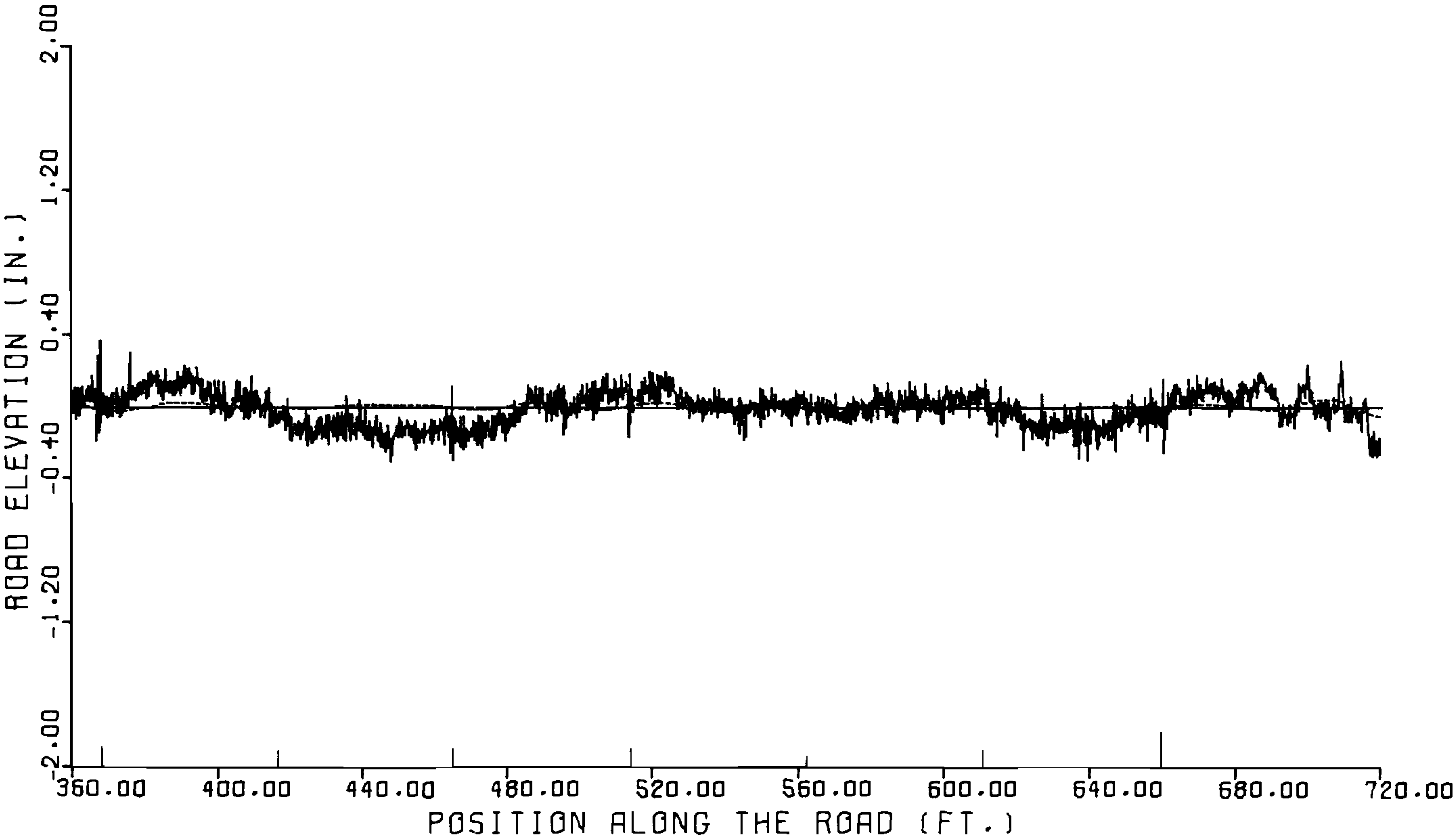

Fig A1.22. Big Sandy Bridge

Filter Passband: 30.0 to 60.0 ft. Wavelengths - Westbound Lane - Right-Left Profile Frame 1

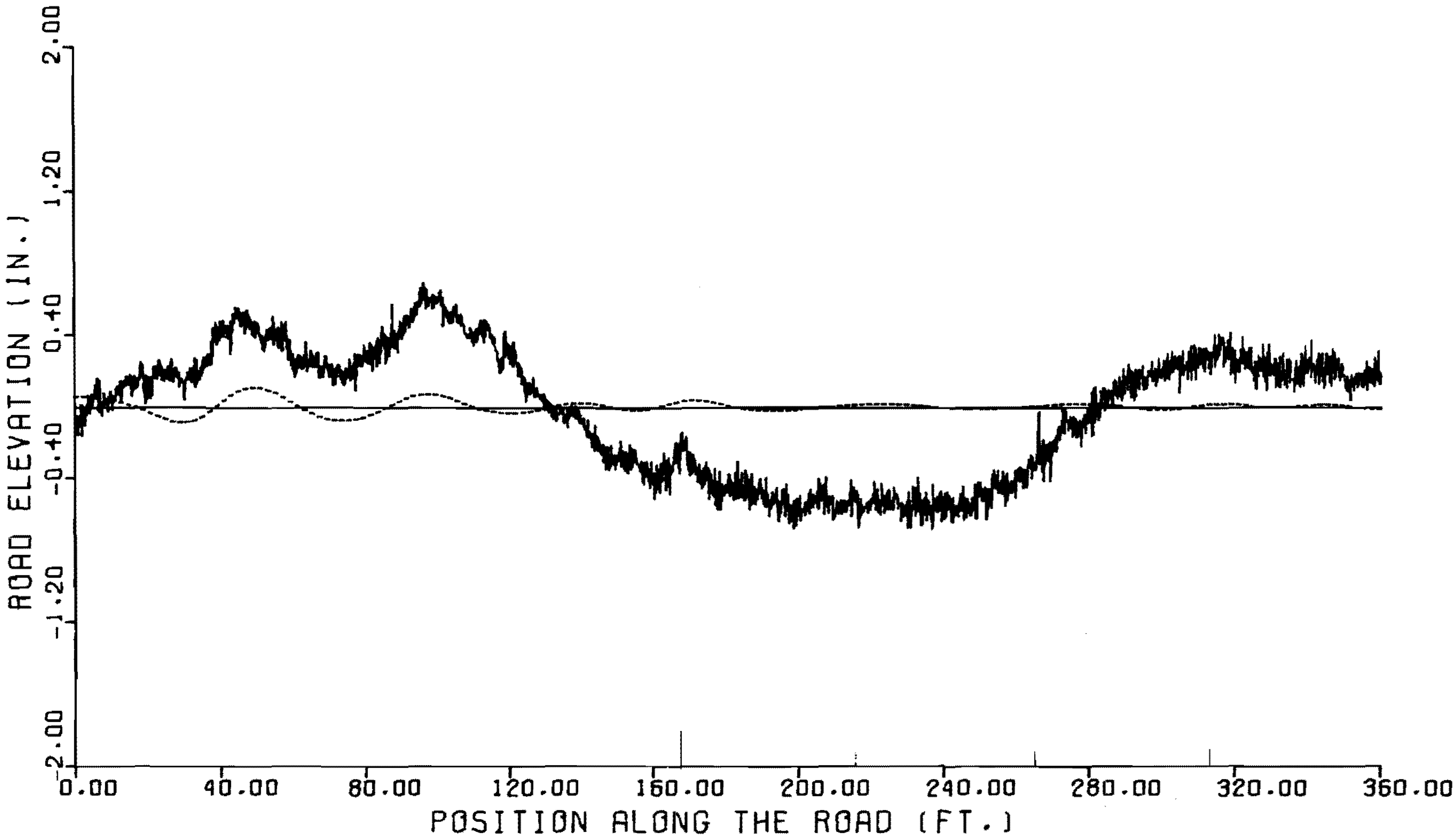

Fig A1.23. Big Sandy Bridge

Filter Passband: 30.0 to 60.0 ft. Wavelengths - Westbound Lane - Right-Left Profile Frame 2

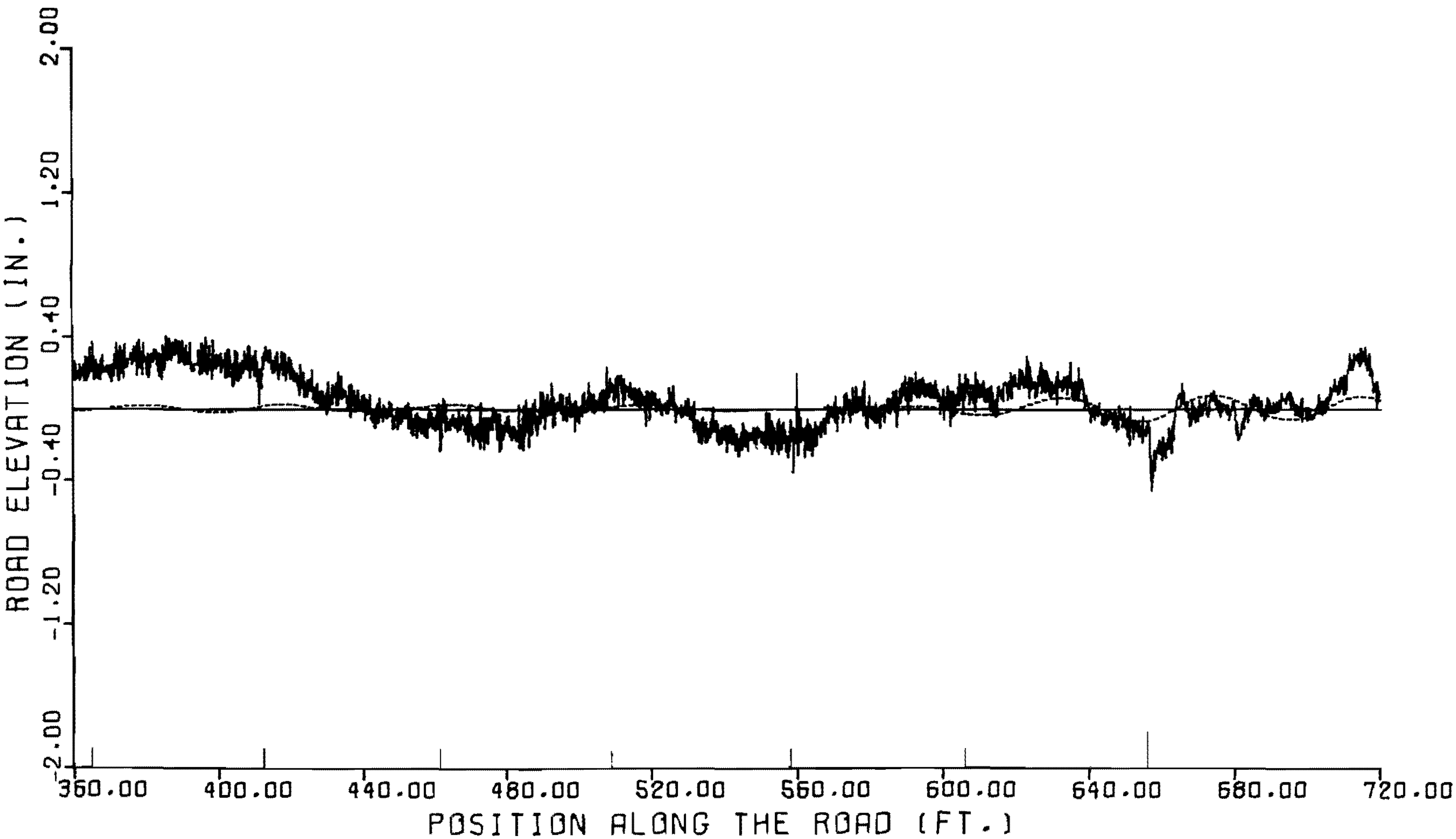

Fig A1.24. Big Sandy Bridge

Filter Passband: 80.0 to 110.0 ft. Wavelengths - Eastbound Lane - Right Profile Frame 1

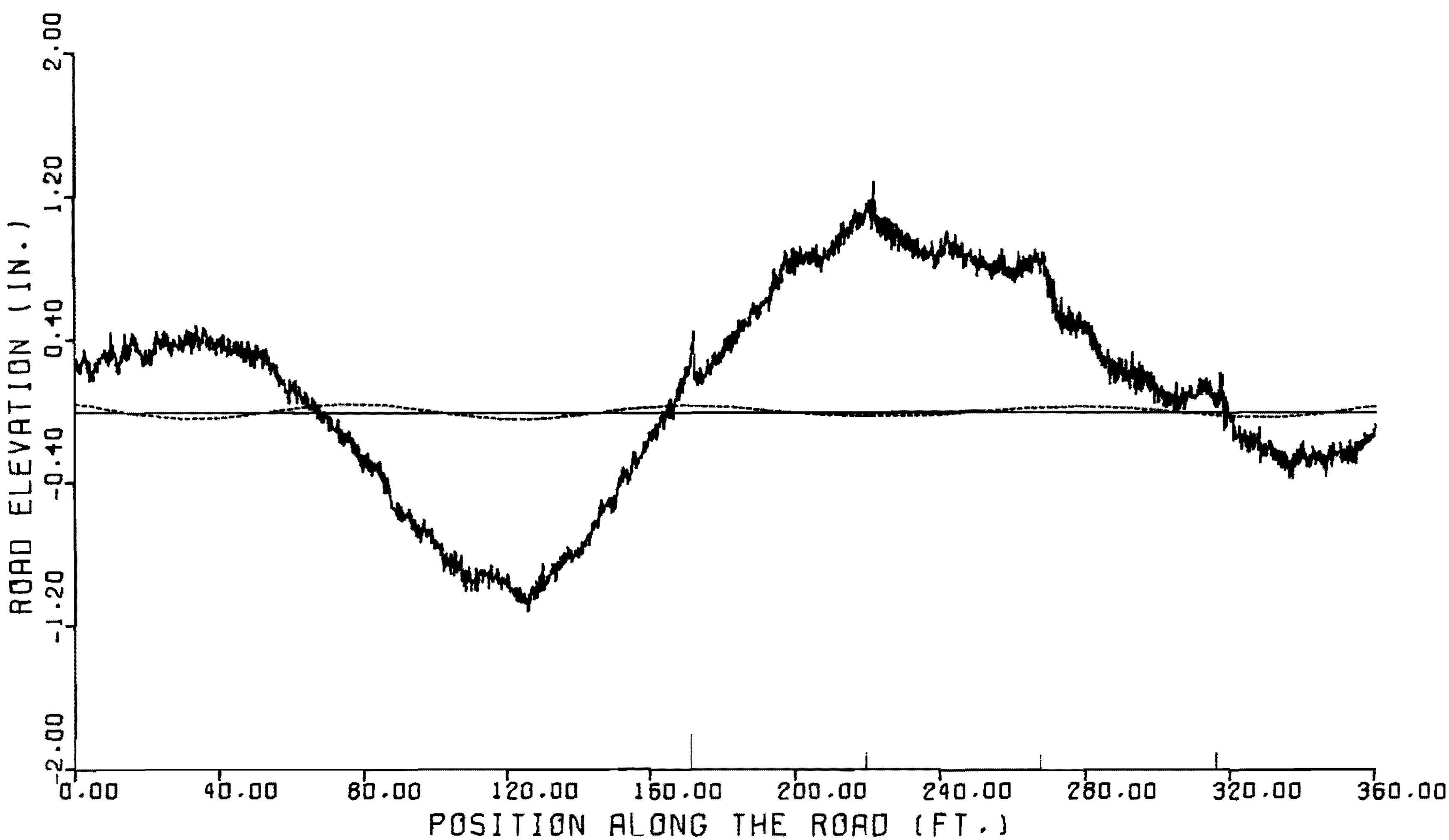

Fig A1.25. Big Sandy Bridge

Filtered Passband: 80.0 to 110.0 ft. Wavelengths - Eastbound Lane - Right Profile Frame 2

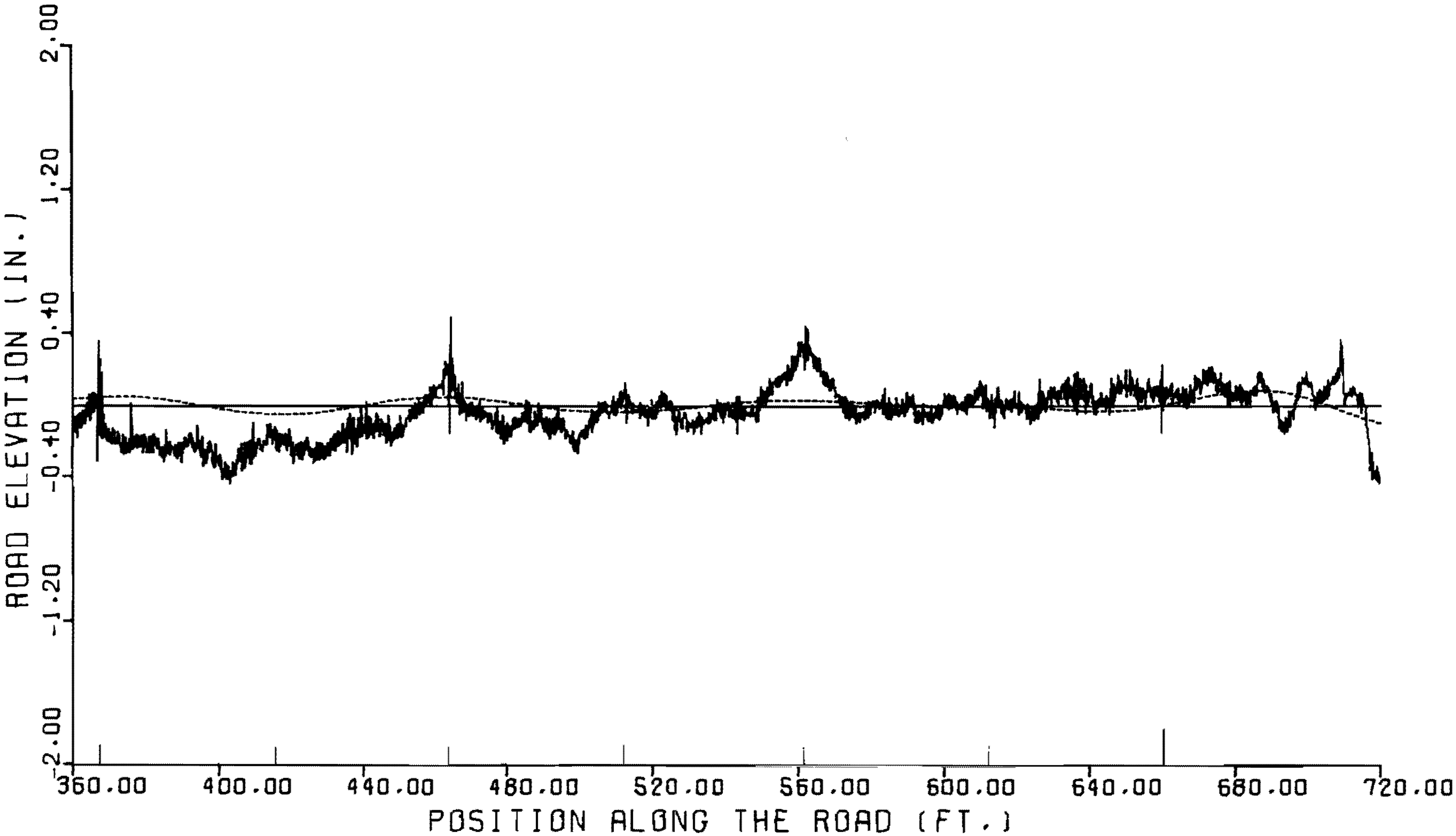

Fig A1.26. Big Sandy Bridge

Filter Passband: 80.0 to 110.0 ft. Wavelengths - Westbound Lane - Right Profile Frame 1

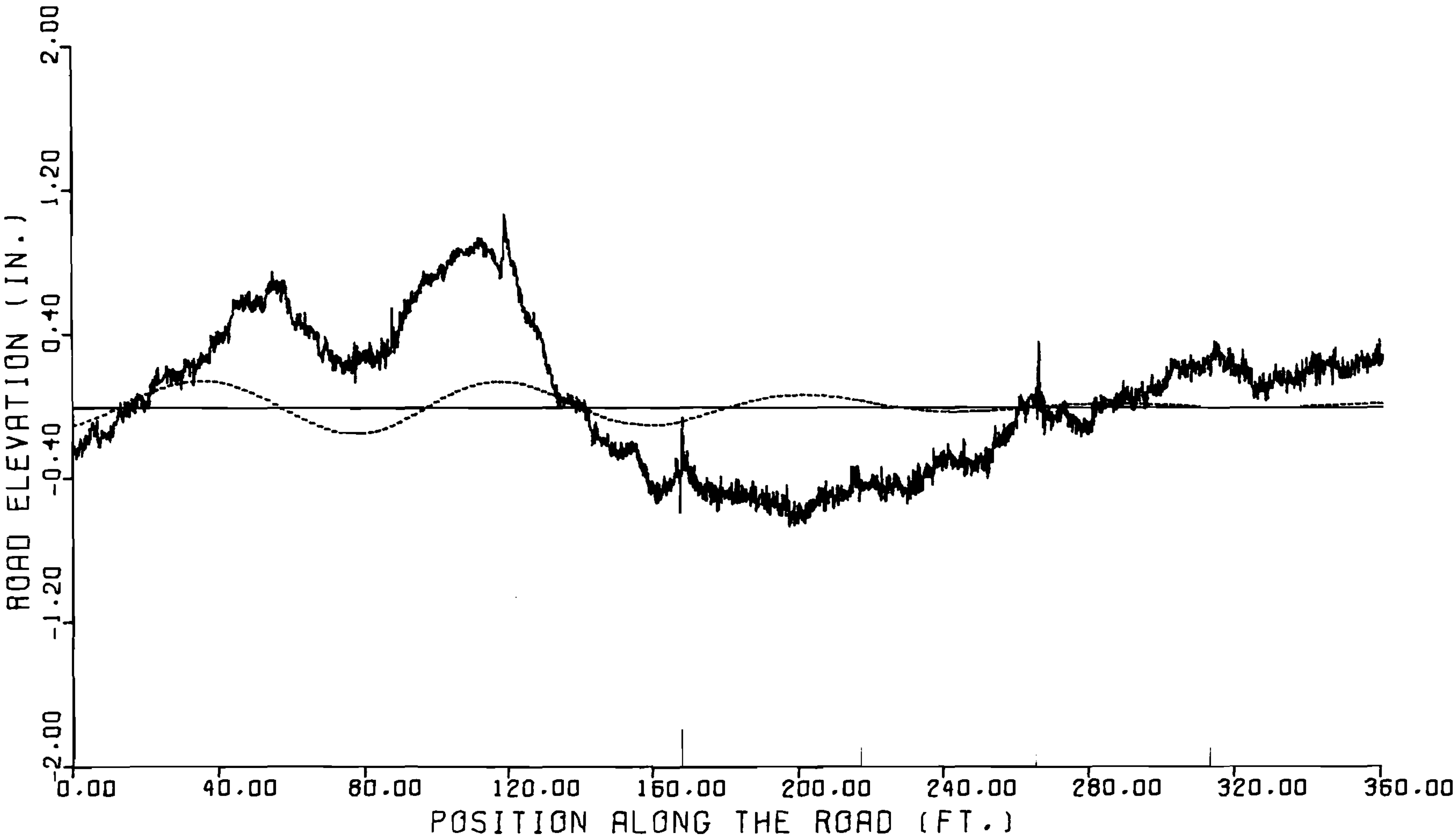

Fig A1.27. Big Sandy Bridge

Filter Passband: 80.0 to 110.0 ft. Wavelengths - Westbound Lane - Right Profile Frame 2

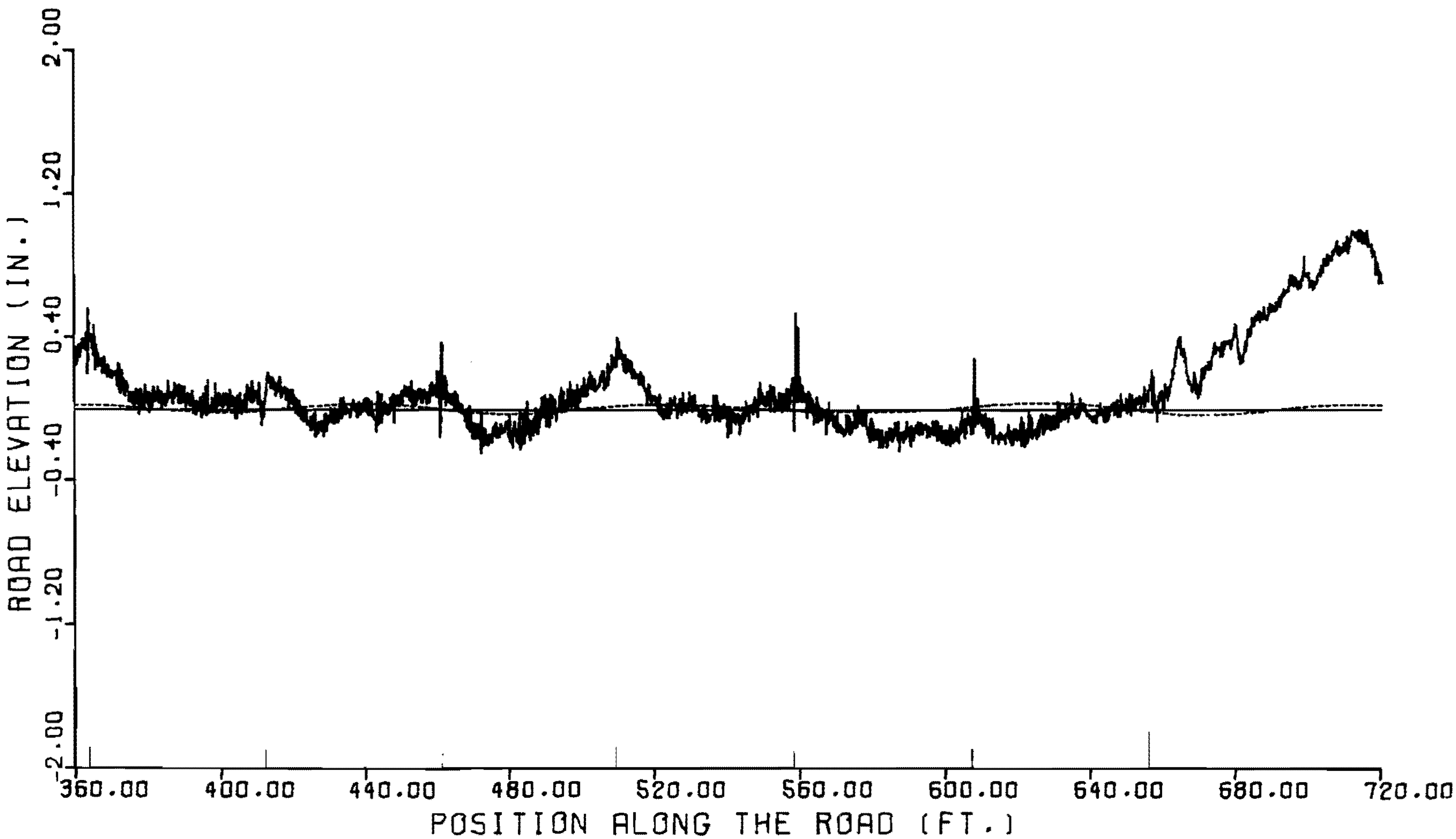

Fig A1.28. Big Sandy Bridge

Filter Passband: 80.0 to 110.0 ft. Wavelengths - Eastbound Lane - Right-Left Profile Frame 1

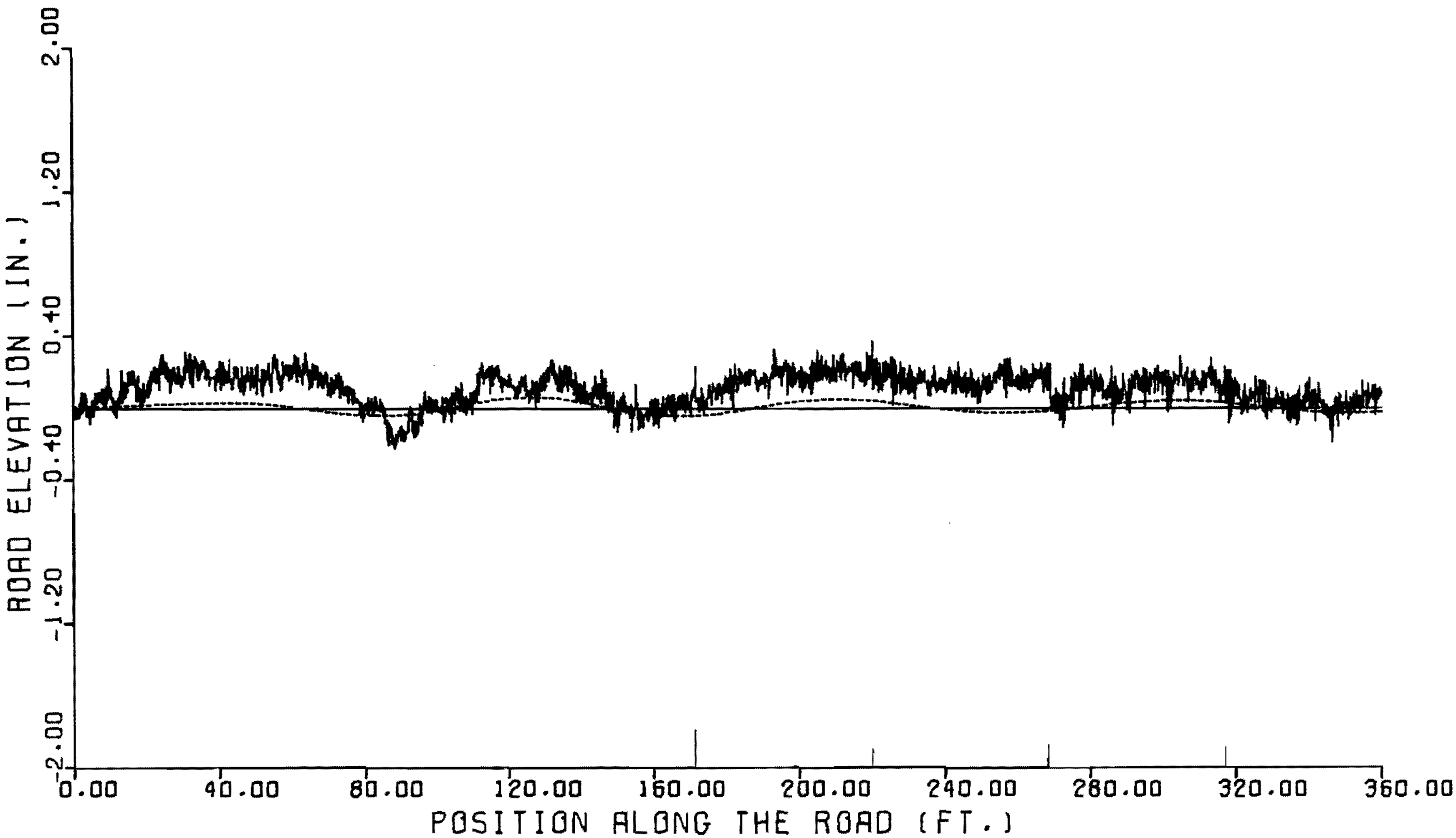

Fig A1.29. Big Sandy Bridge

Filter Passband: 80.0 to 110.0 ft. Wavelengths - Eastbound Lane - Right-Left Profile Frame 2

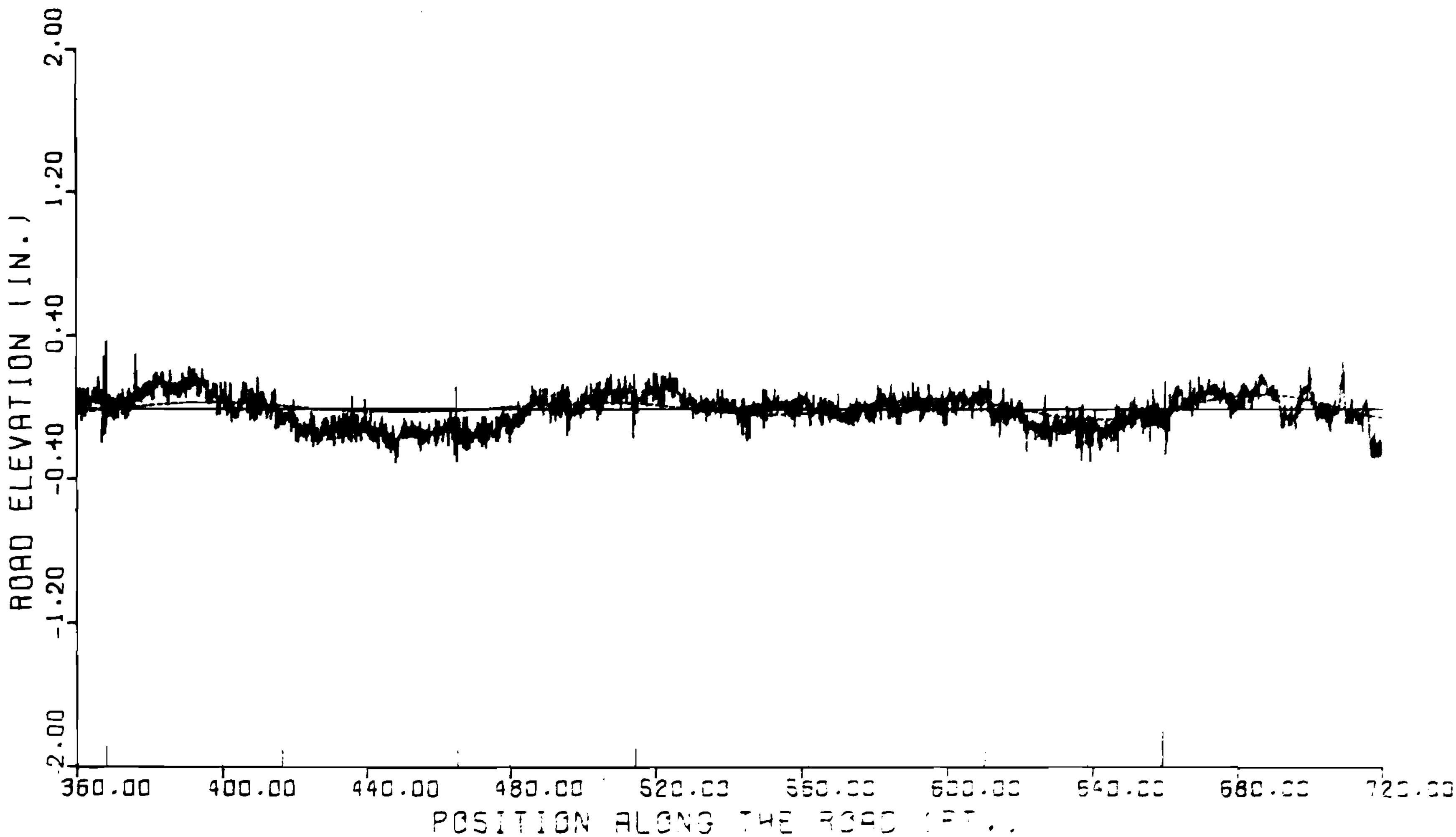

Fig A1.30. Big Sandy Bridge

Filter Passband: 80.0 to 110.0 ft. Wavelengths - Westbound Lane - Right-Left Profile Frame 1

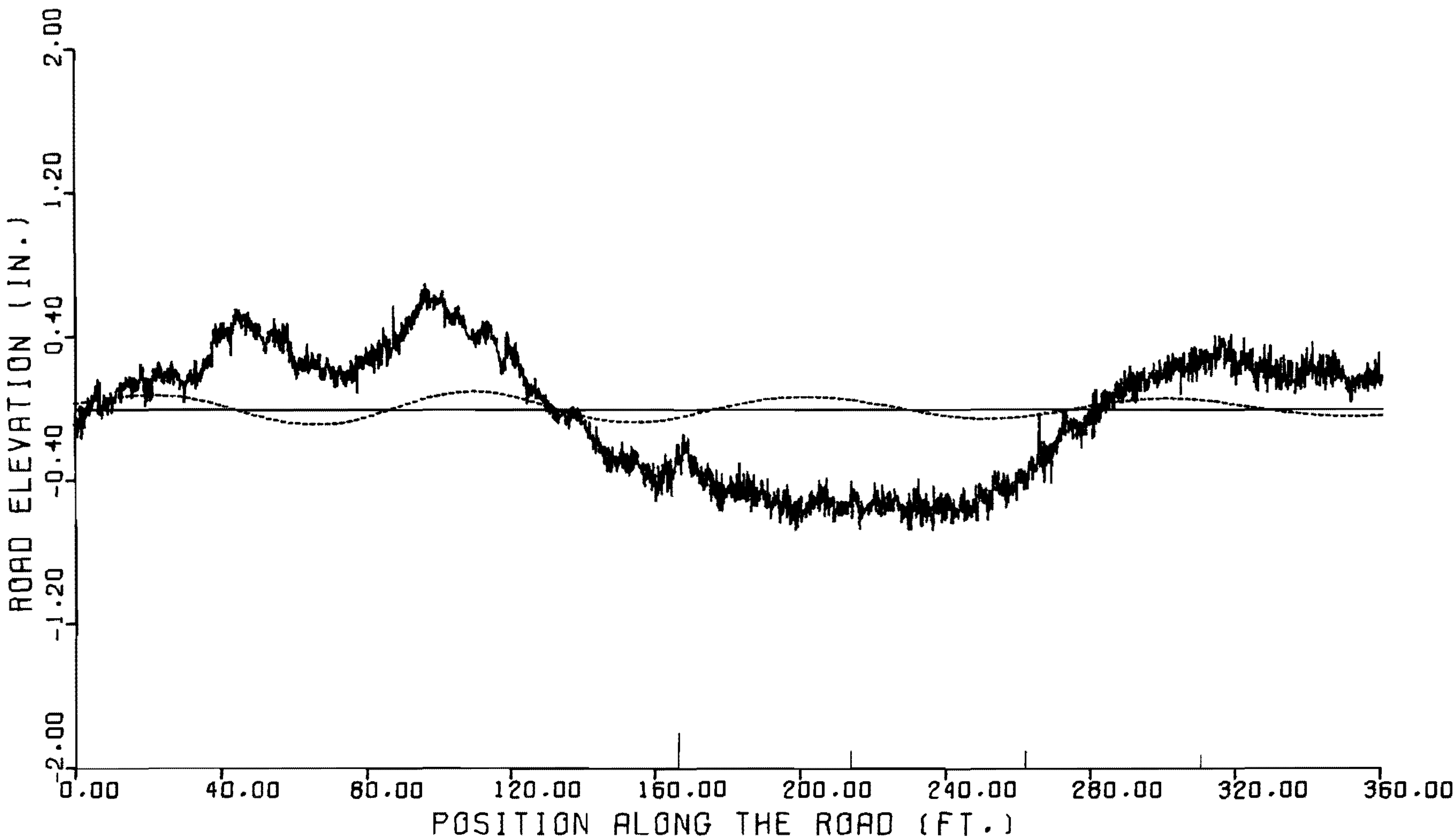

Fig A1.31. Big Sandy Bridge

Filter Passband: 80.0 to 110.0 ft. Wavelengths - Westbound Lane - Right-Left Profile Frame 2

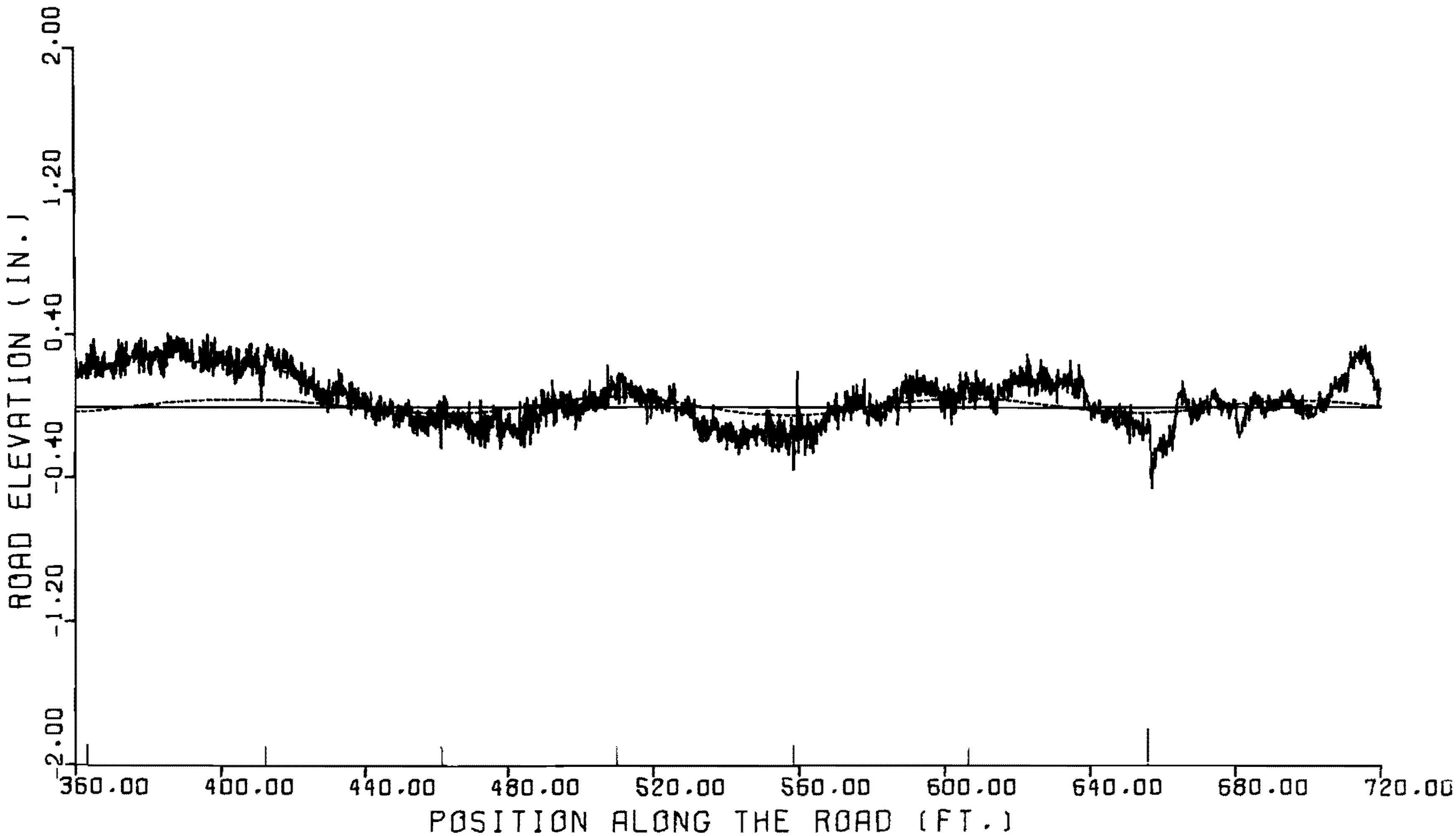

Fig A1.32. Big Sandy Bridge

Filter Passband: 0.0 to 15.0 ft. Wavelengths - Southbound Lane - Right Profile Frame 1

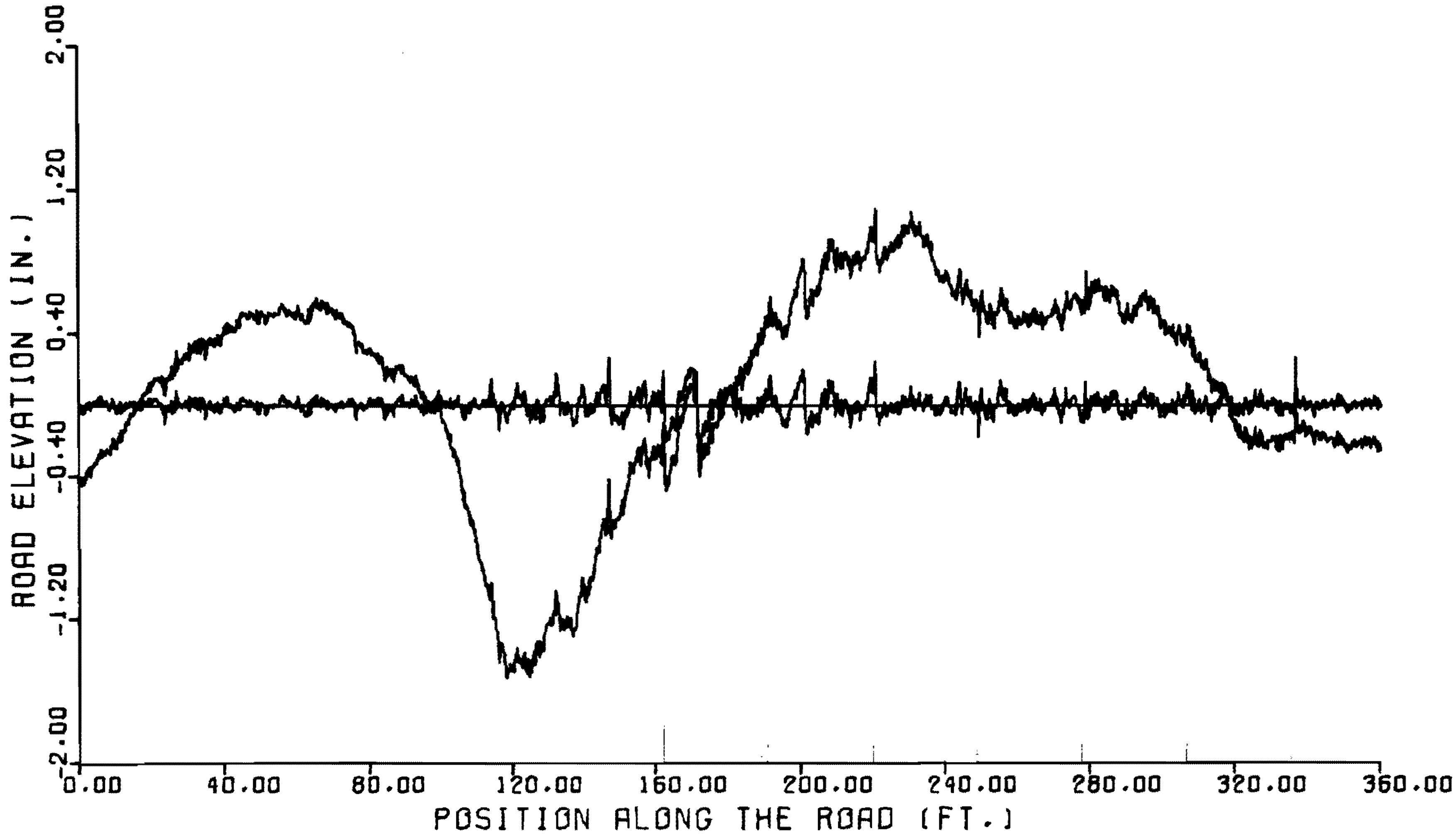

Fig A1.33. Plum Creek Bridge

Filter Passband: 0.0 to 15.0 ft. Wavelengths - Southbound Lane - Right Profile Frame 2

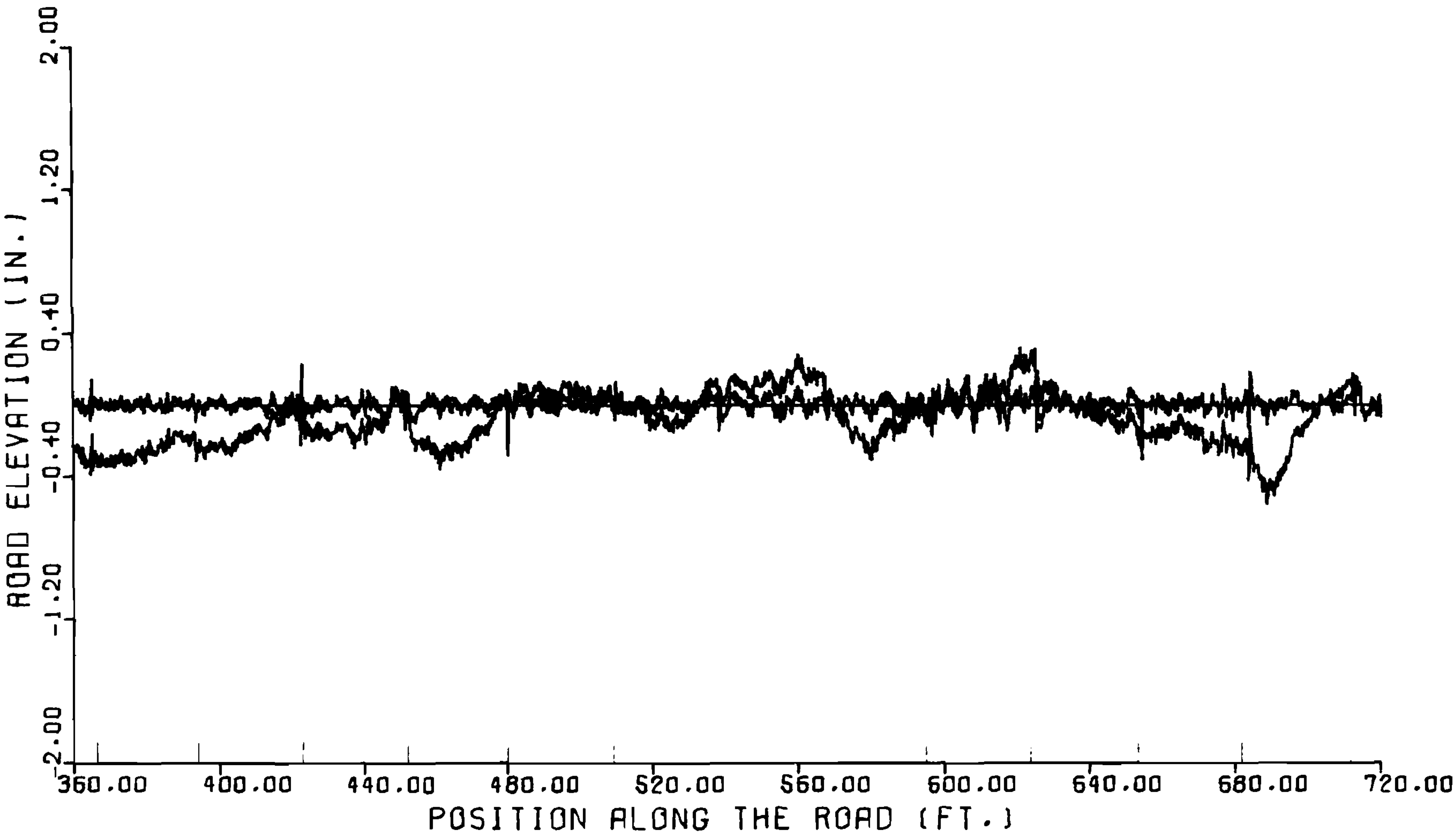

Fig A1.34. Plum Creek Bridge

Filter Passband: 0.0 to 15.0 ft. Wavelengths - Southbound Lane - Right Profile Frame 3

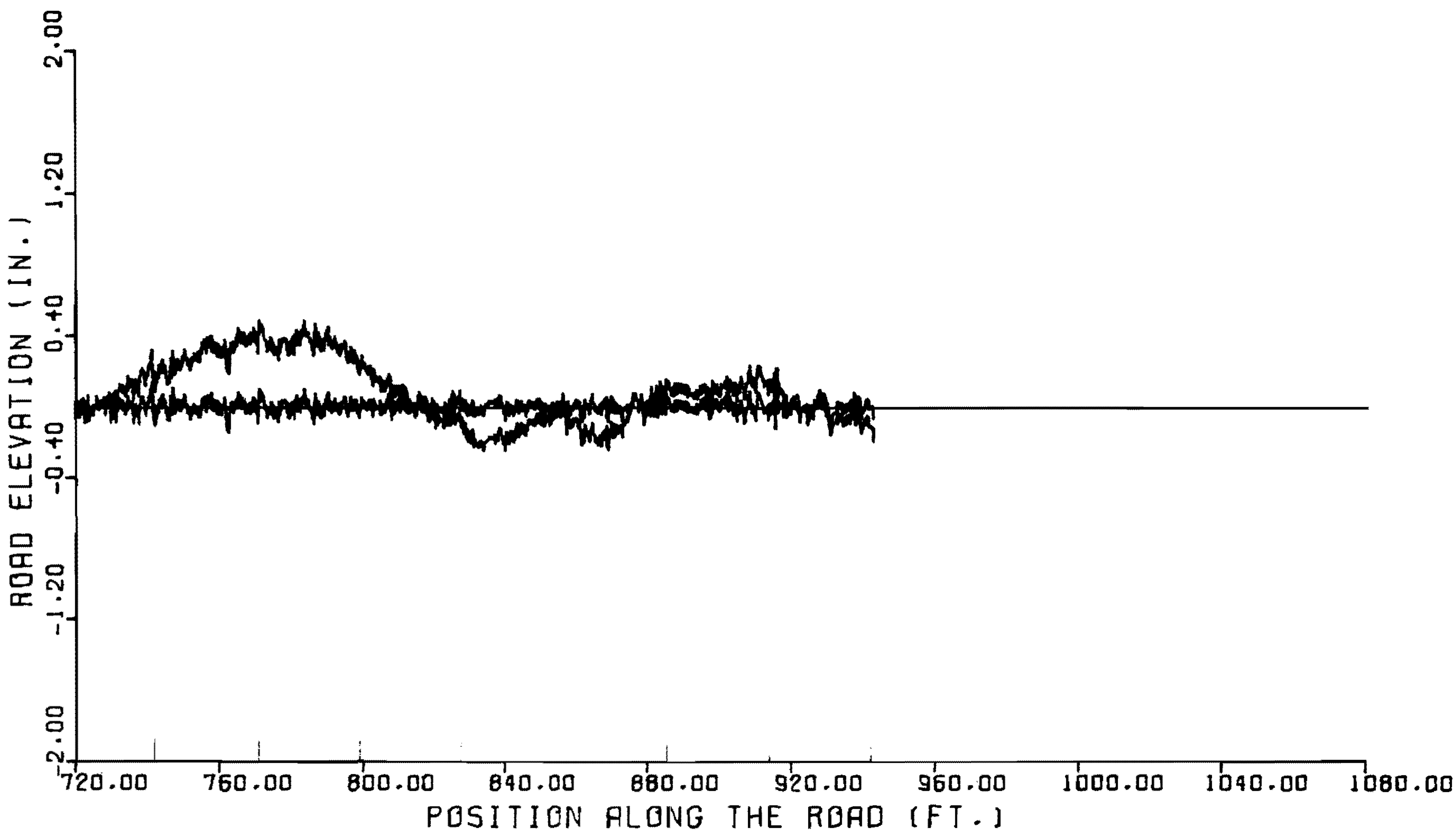

Fig A1.35. Plum Creek Bridge

Filter Passband: 0.0 to 15.0 ft. Wavelengths - Southbound Lane - Right Profile Frame 1

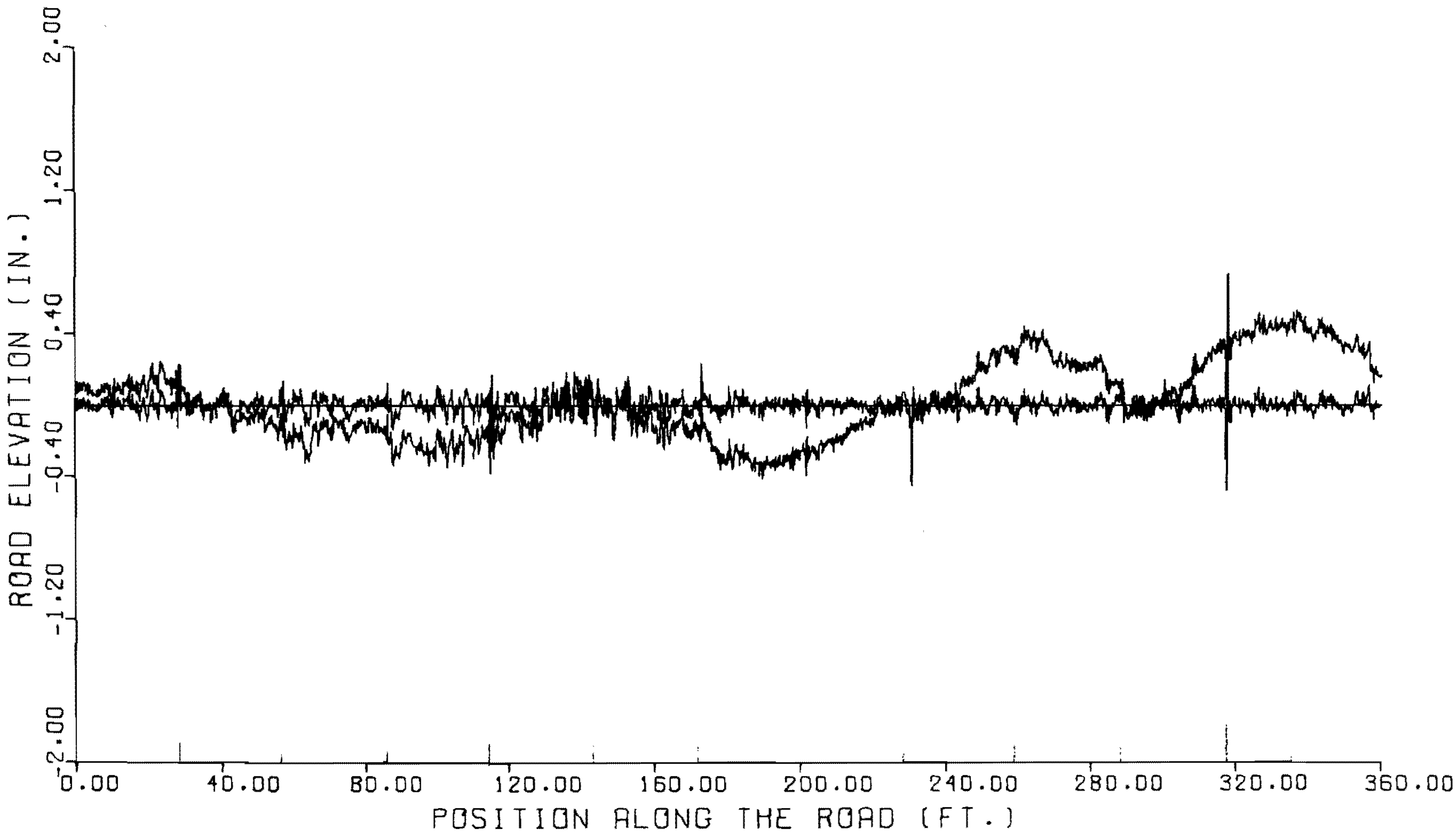

Fig A1.36. Plum Creek Bridge

Filter Passband: 0.0 to 15.0 ft. Wavelengths - Southbound Lane - Right Profile Frame 2

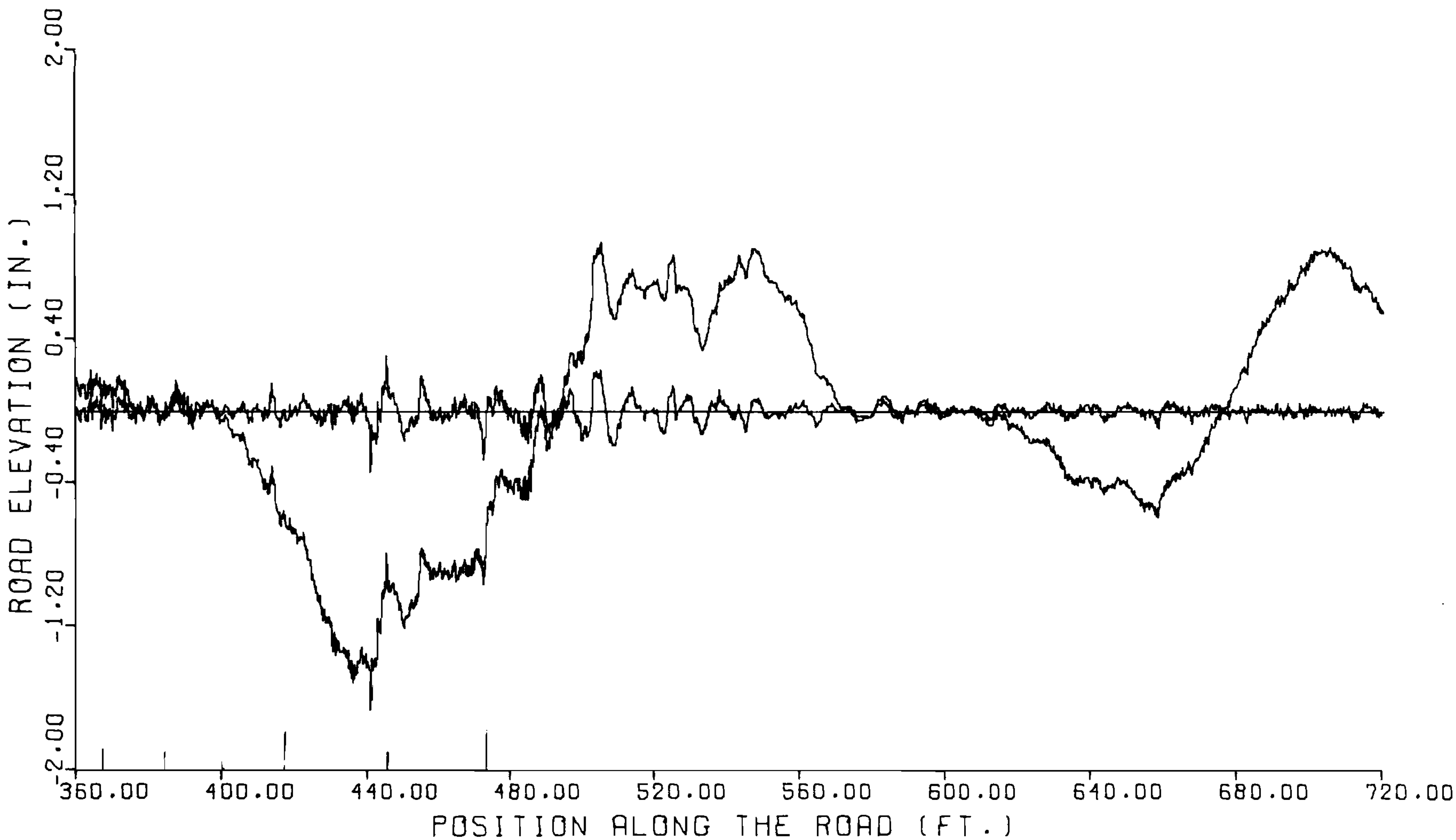

Fig A1.37. Plum Creek Bridge

Filter Passband: 0.0 to 15.0 ft. Wavelengths - Southbound Lane - Right Profile Frame 3

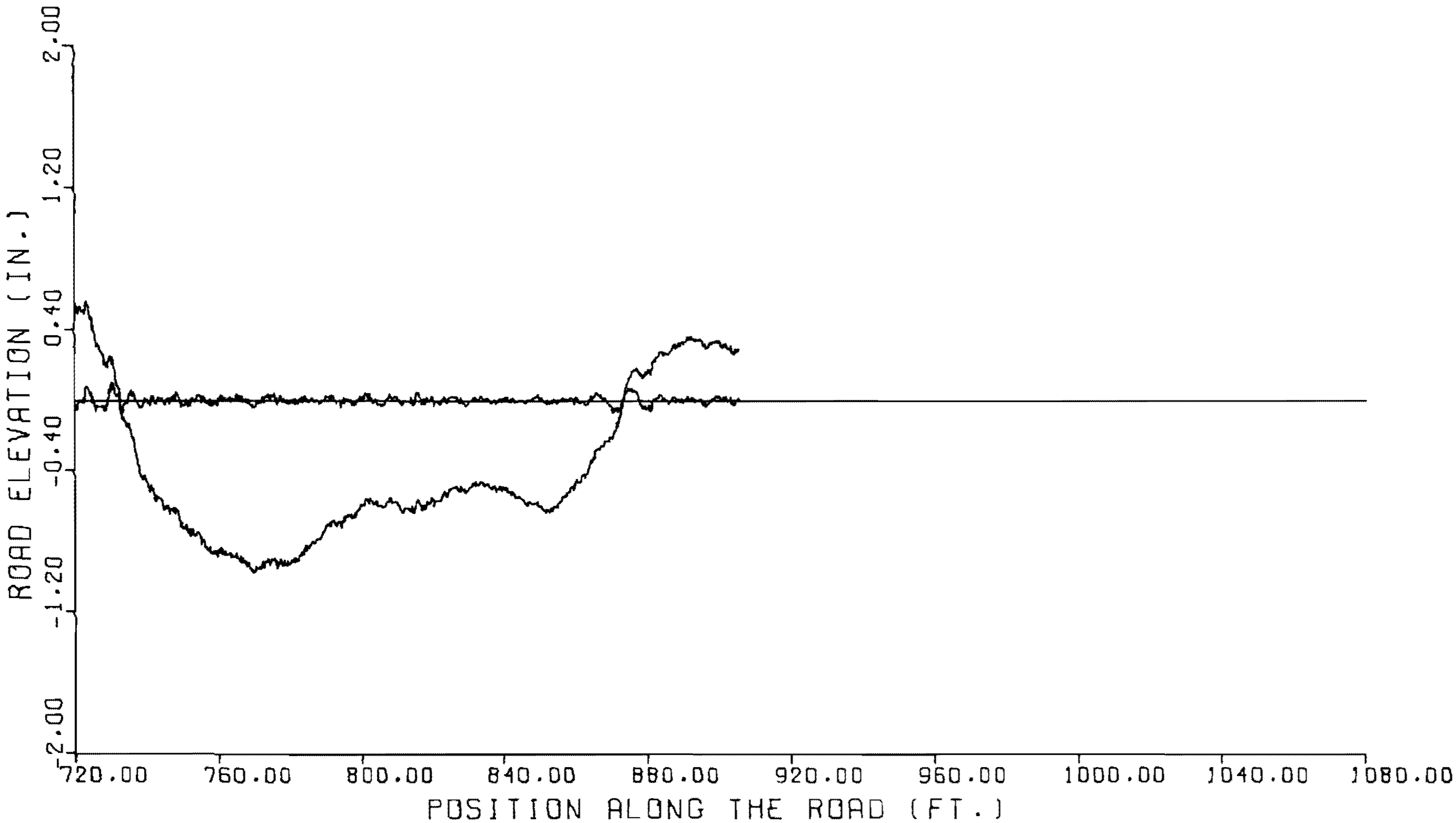

Fig A1.38. Plum Creek Bridge

Filter Passband: 60.0 to 100.0 ft. Wavelengths - Southbound Lane - Right Profile Frame 1

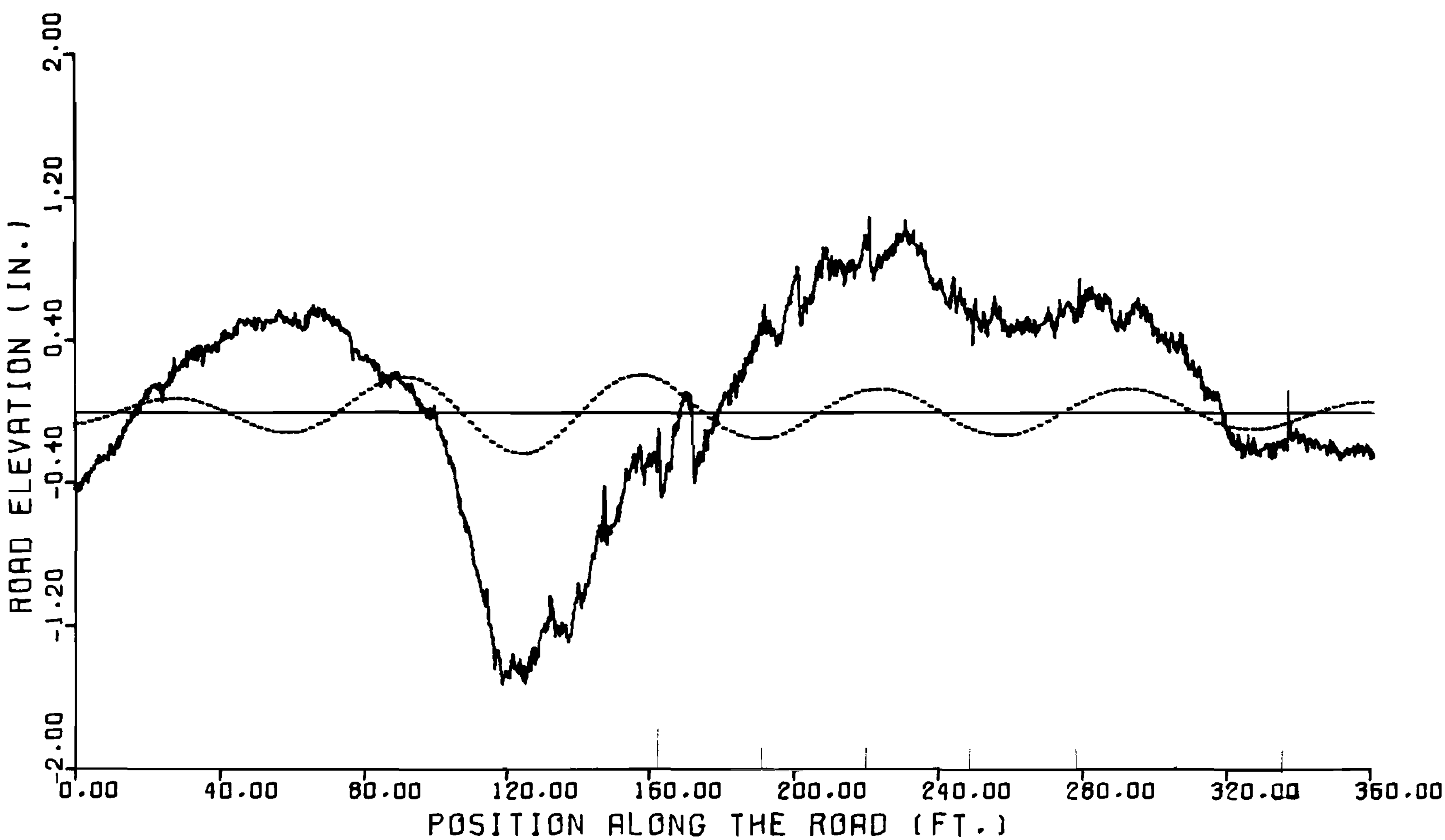

Fig A1.39. Plum Creek Bridge

Filter Passband: 60.0 to 100.0 ft. Wavelengths - Southbound Lane - Right Profile Frame 2

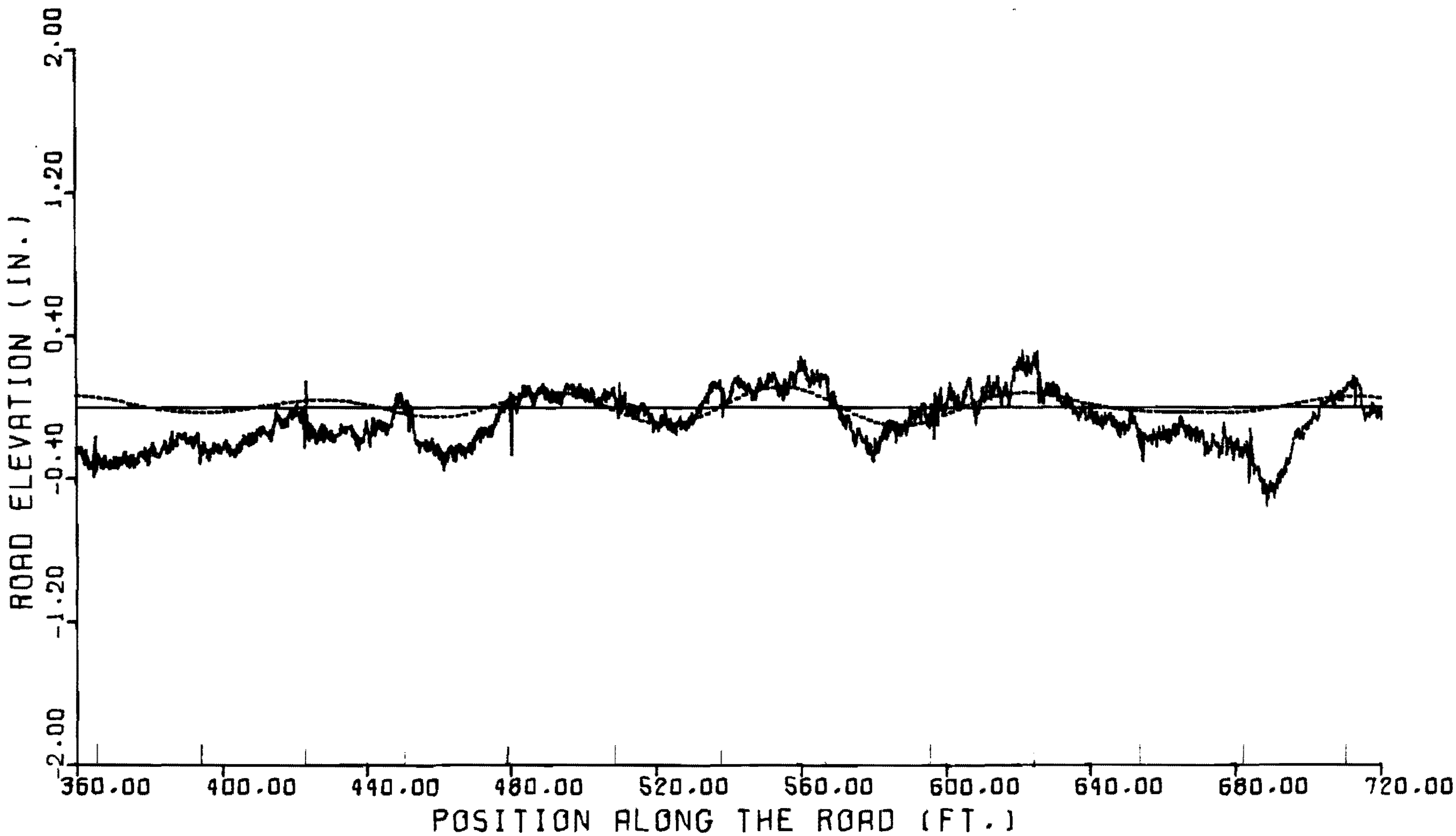

Fig A1.40. Plum Creek Bridge

Filter Passband: 60.0 to 100.0 ft. Wavelengths - Southbound Lane - Right Profile Frame 3

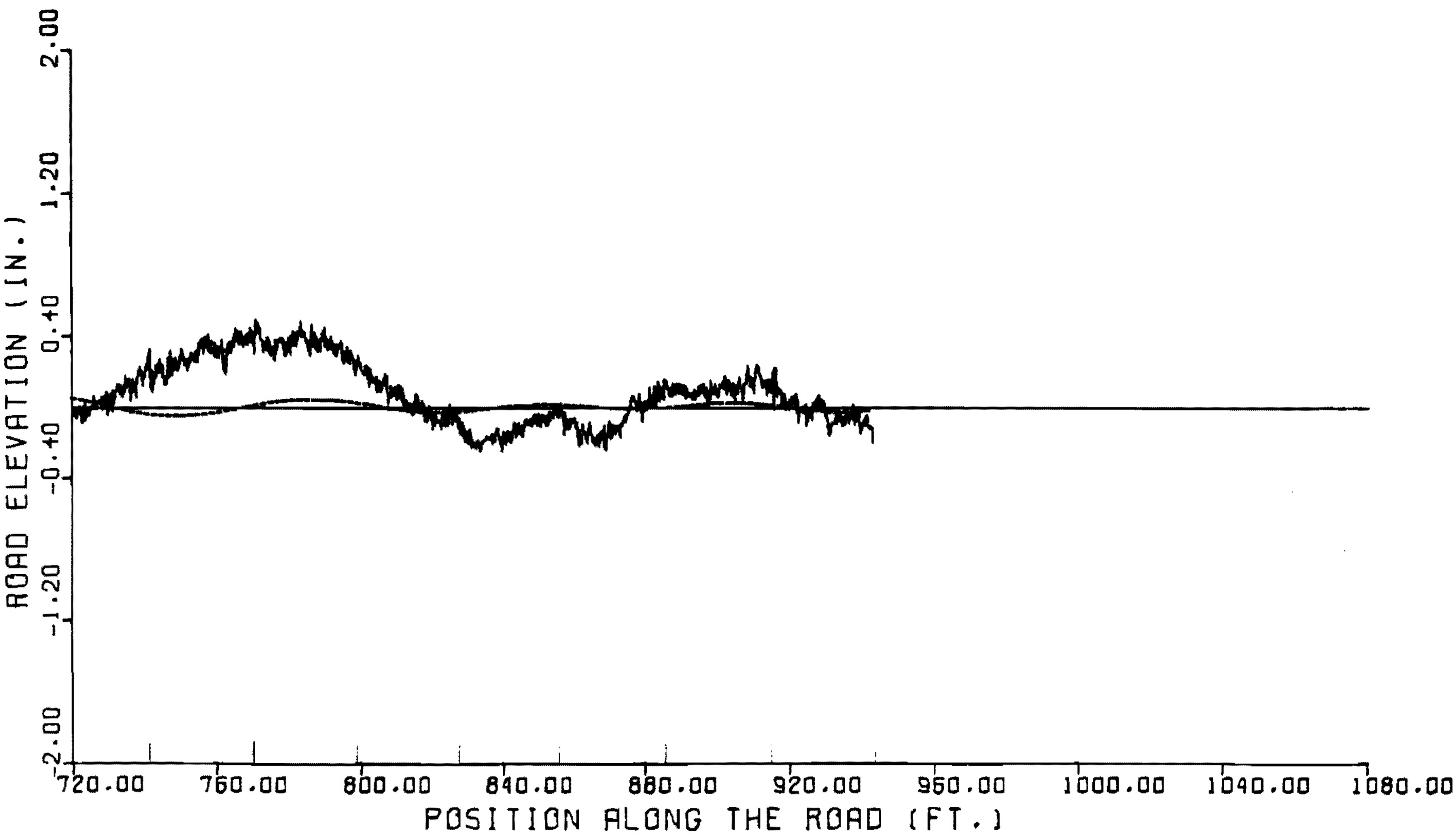

Fig A1.41. Plum Creek Bridge

Filter Passband: 15.0 to 60.0 ft. Wavelengths - Southbound Lane - Right Profile Frame 1

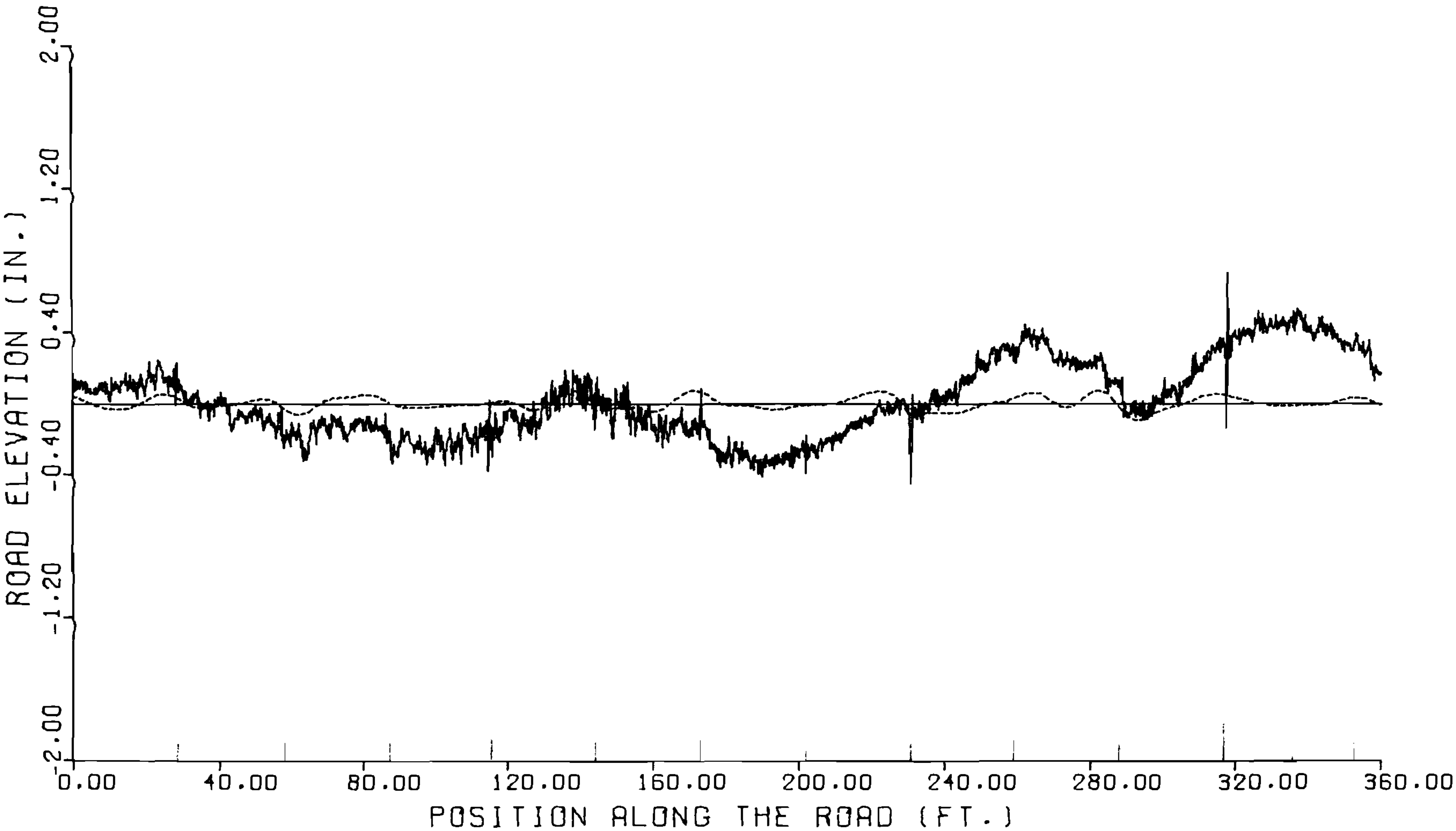

Fig A1.42. Plum Creek Bridge

Filter Passband: 15.0 to 60.0 ft. Wavelengths - Southbound Lane - Right Profile Frame 2

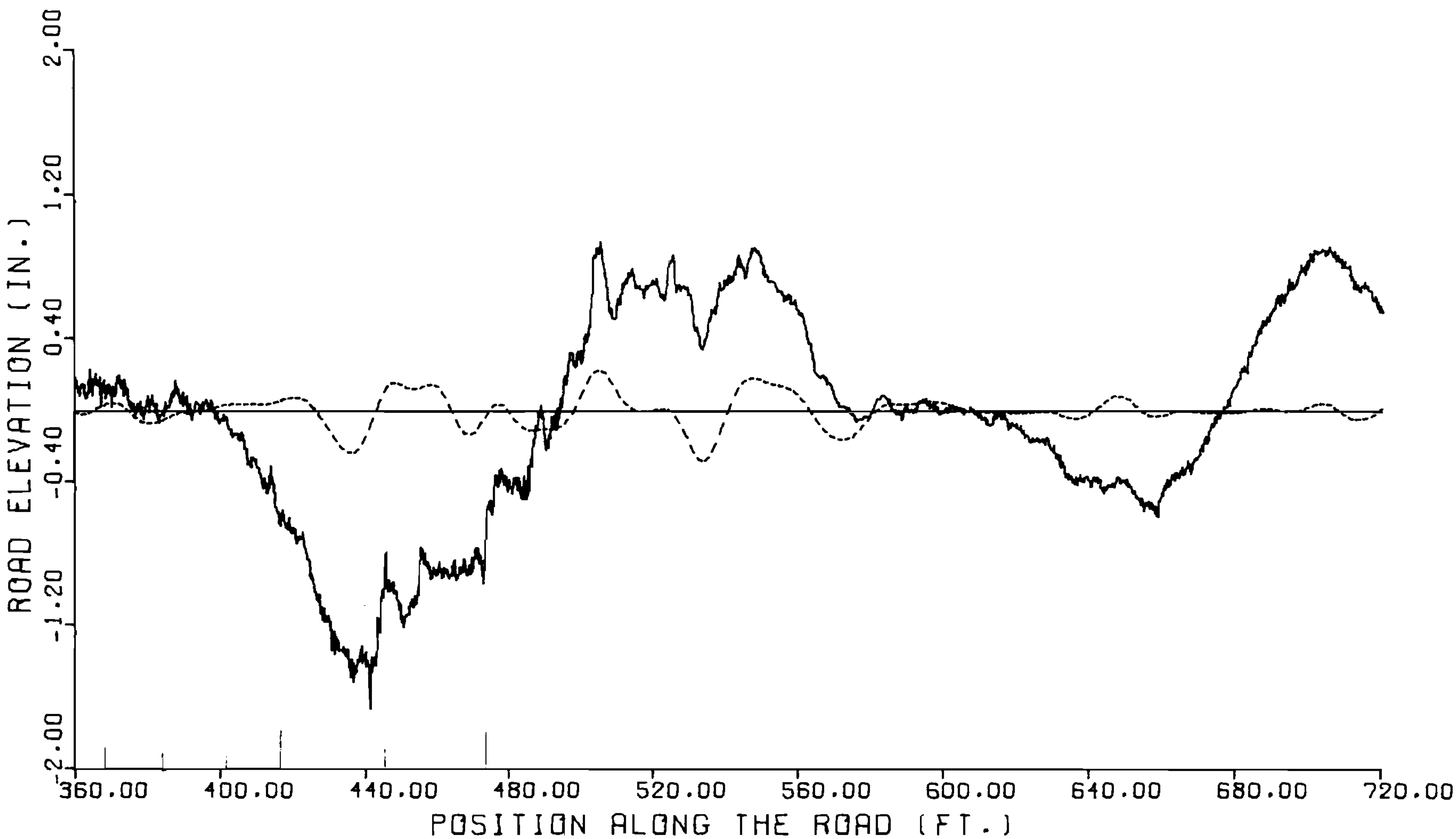

Fig A1.43. Plum Creek Bridge

Filter Passband: 15.0 to 60.0 ft. Wavelengths - Southbound Lane - Right Profile Frame 3

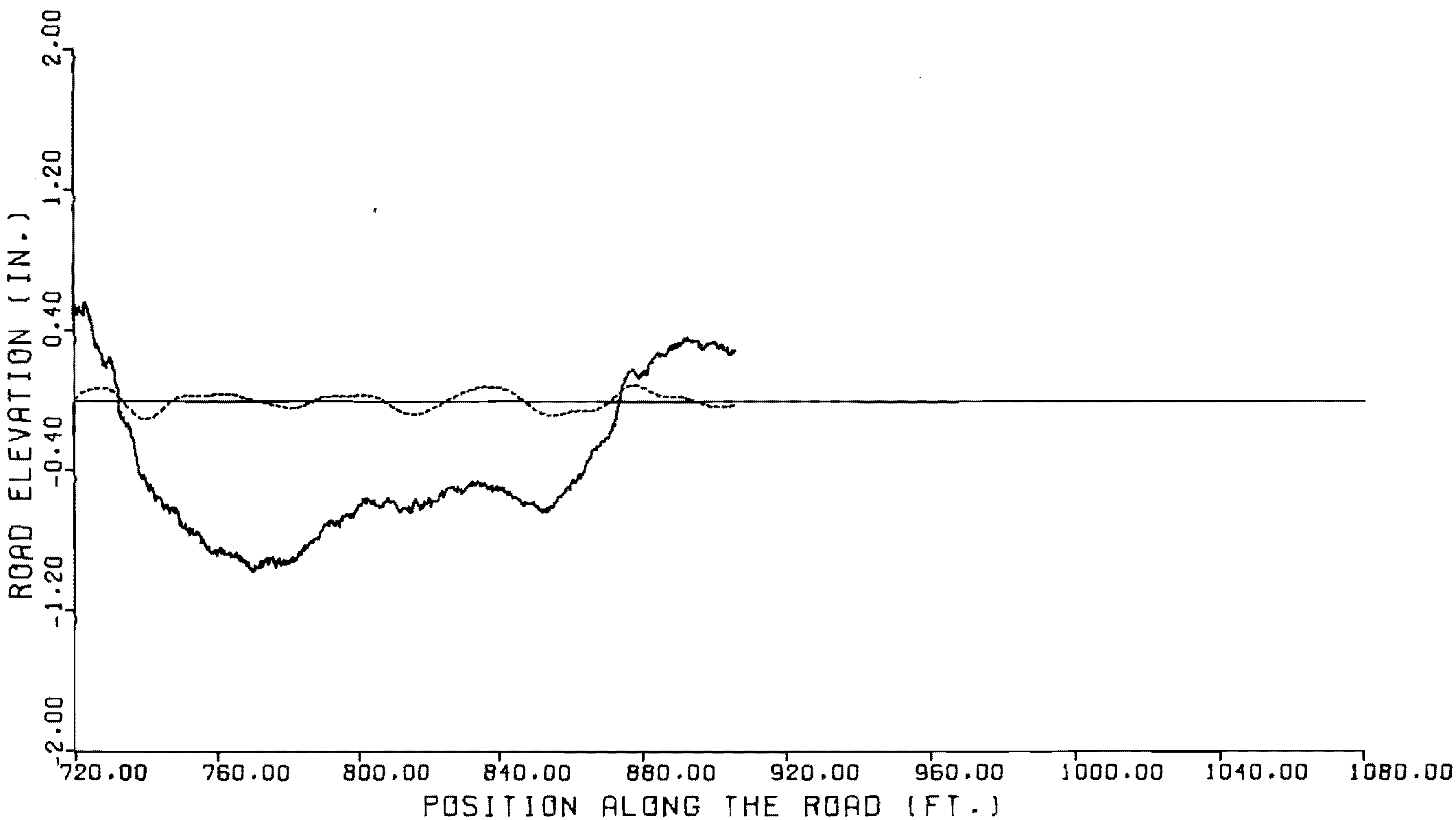

Fig A1.44. Plum Creek Bridge

Filter Passband: 0.0 to 15.0 ft. Wavelengths - Northbound Lane - Right Profile Frame 1

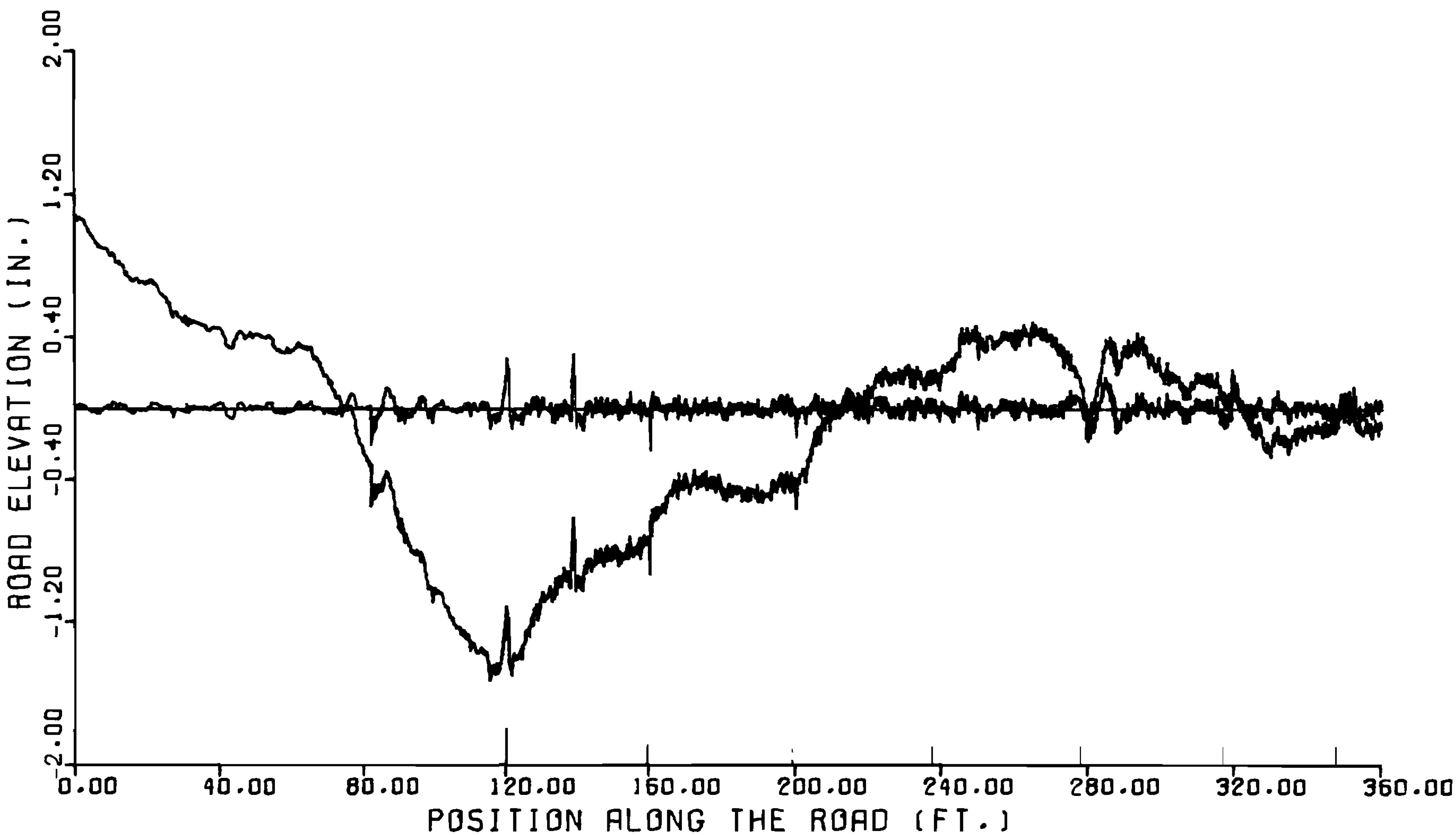

Fig A1.45. Plum Creek Bridge

Filter Passband: 0.0 to 15.0 ft. Wavelengths - Northbound Lane - Right Profile Frame 2

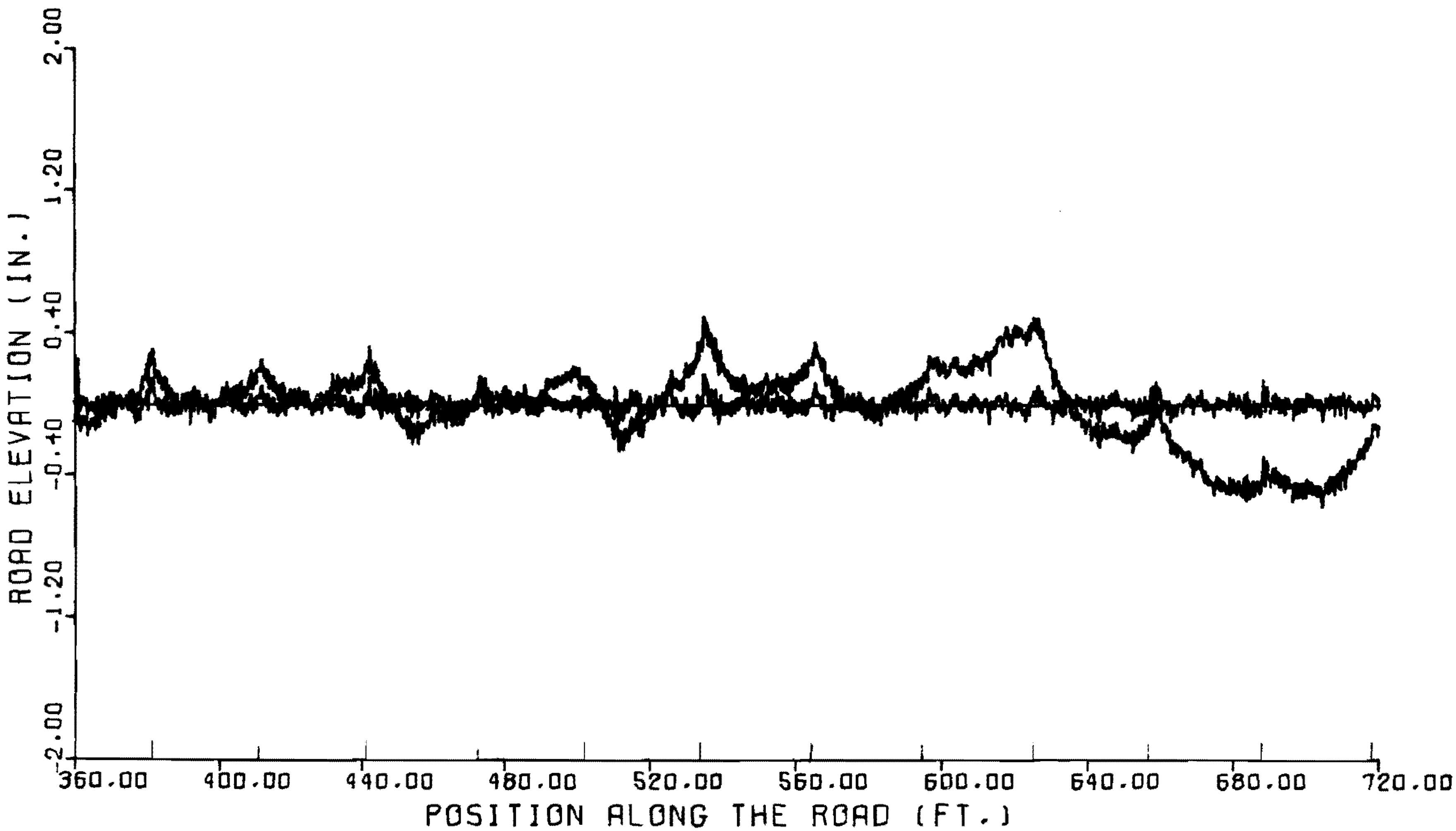

Fig A1.46. Plum Creek Bridge

Filter Passband: 0.0 to 15.0 ft. Wavelengths - Northbound Lane - Right Profile Frame 3

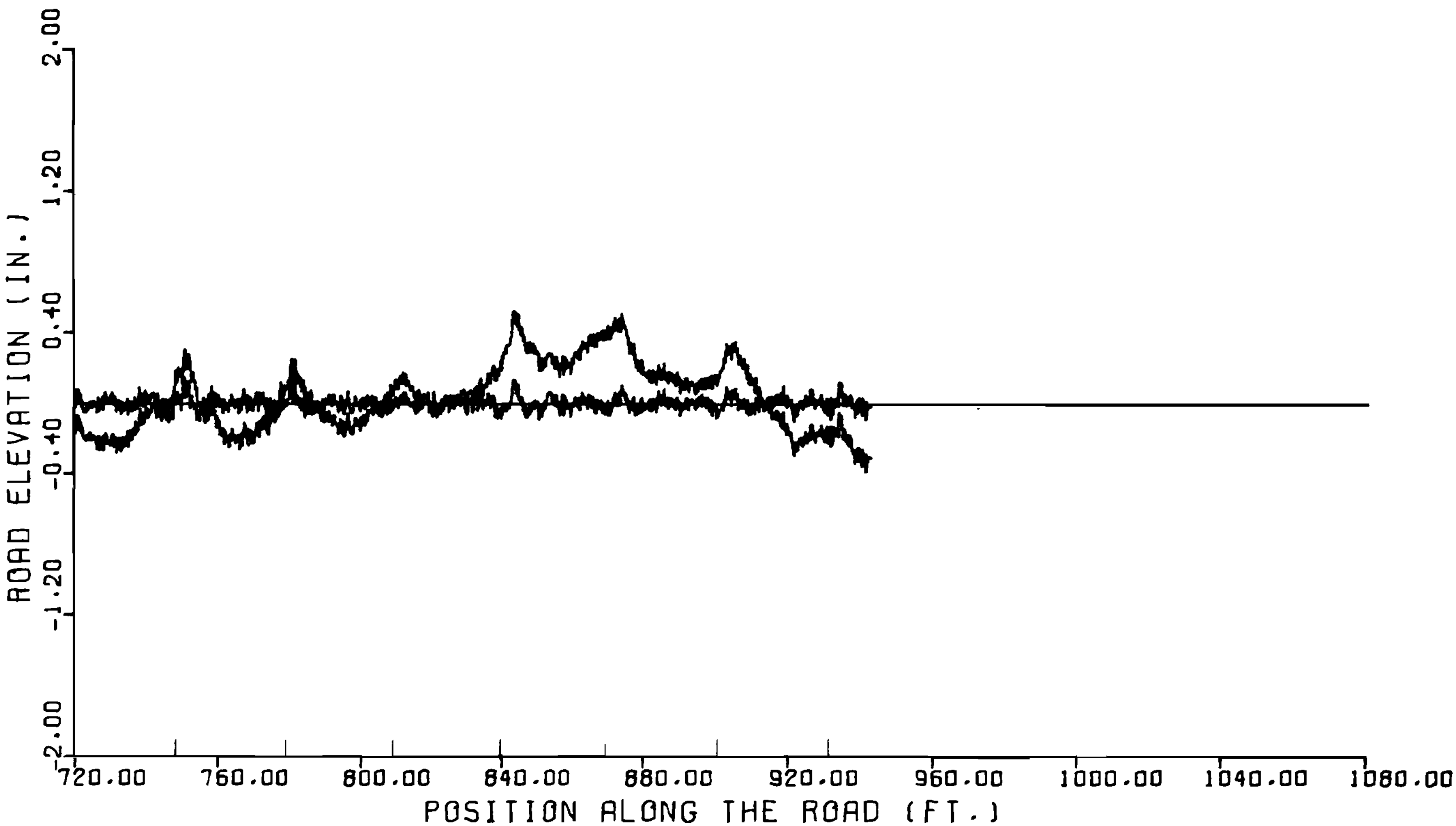

Fig A1.47. Plum Creek Bridge

Filter Passband: 0.0 to 15.0 ft. Wavelengths - Northbound Lane - Right Profile Frame 1

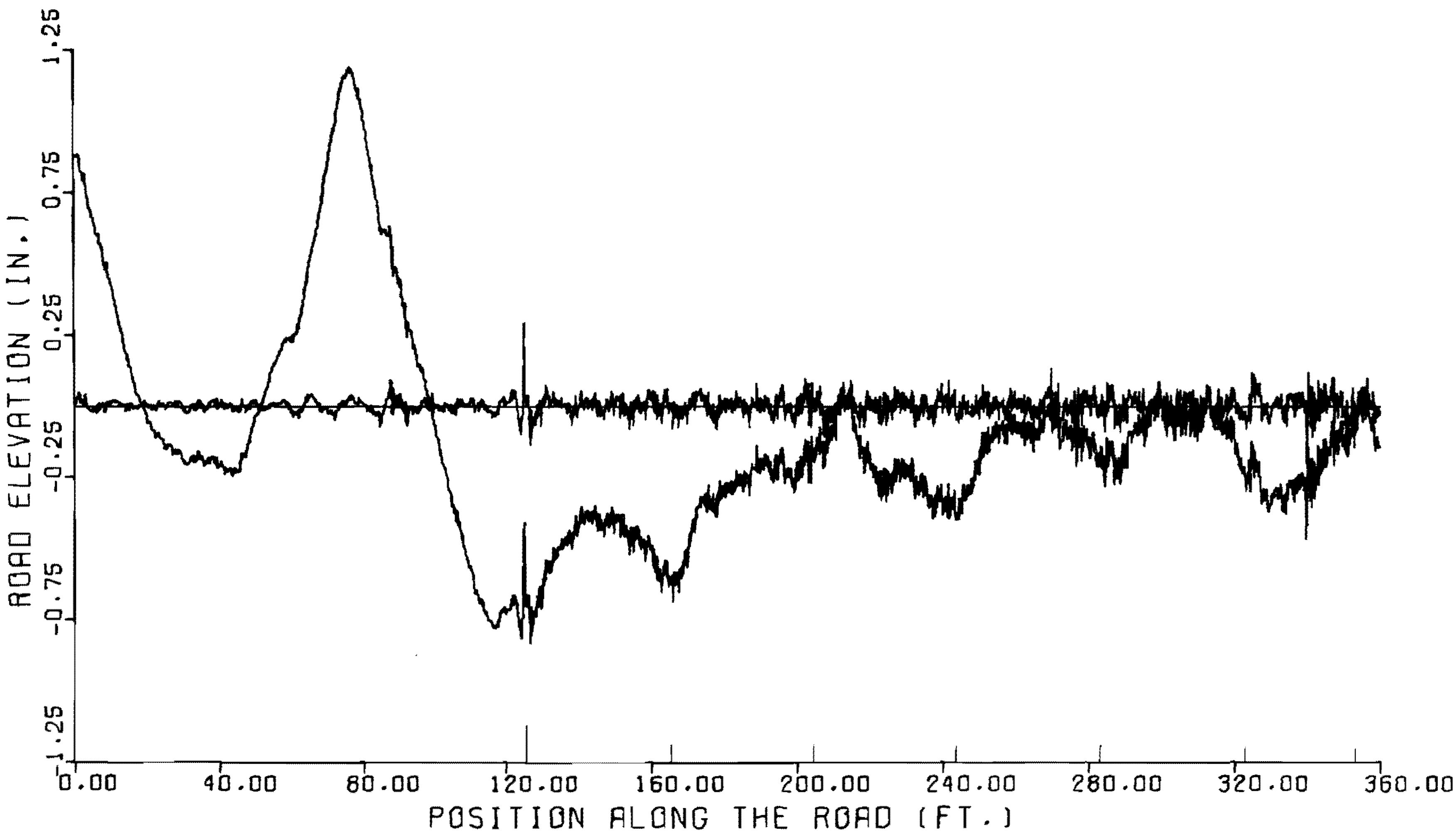

Fig A1.48. Plum Creek Bridge

Filter Passband: 0.0 to 15.0 ft. Wavelengths - Northbound Lane - Right Profile Frame 2

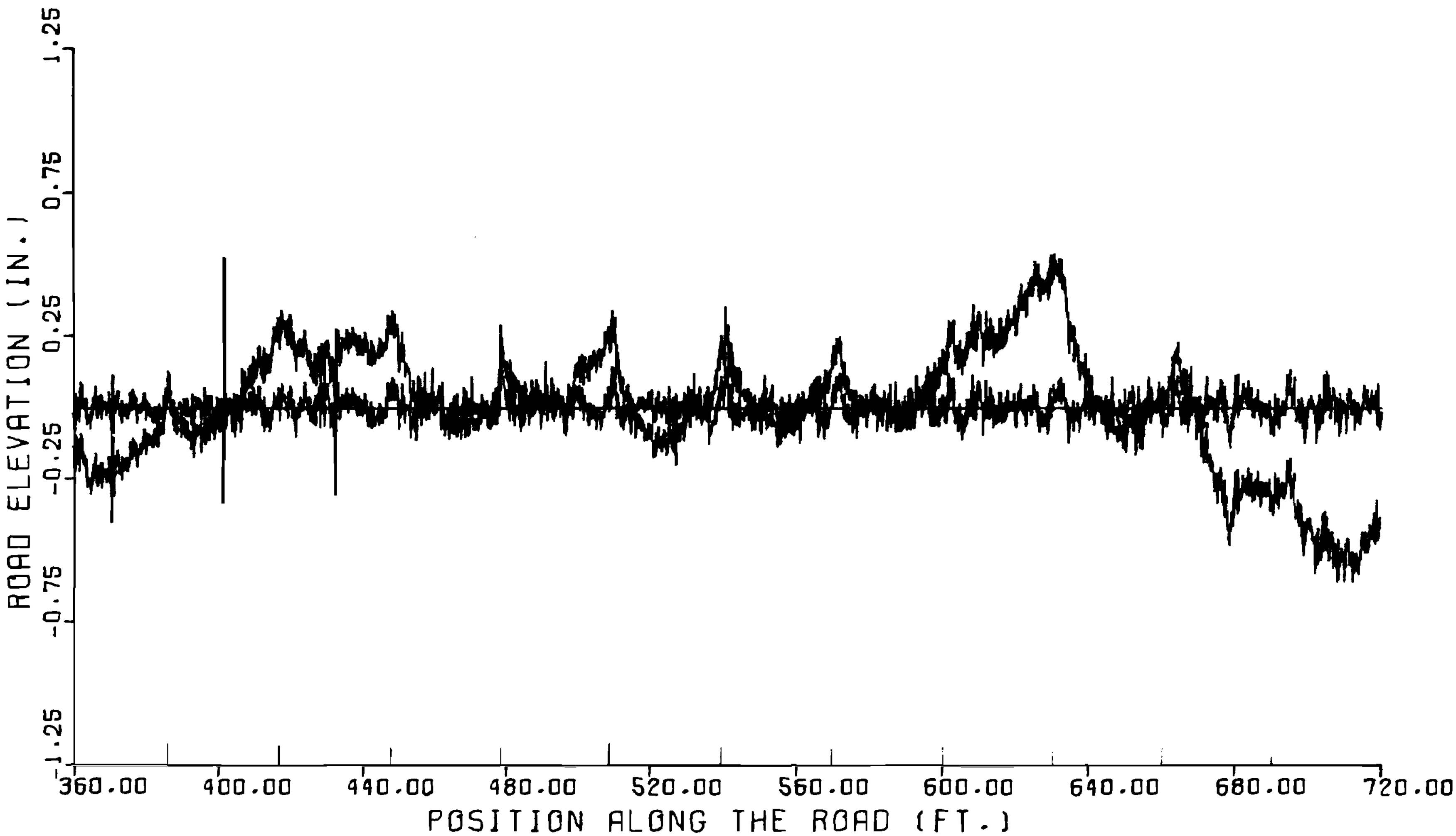

Fig A1.49. Plum Creek Bridge

Filter Passband: 0.0 to 15.0 ft. Wavelengths - Northbound Lane - Right Profile Frame 3

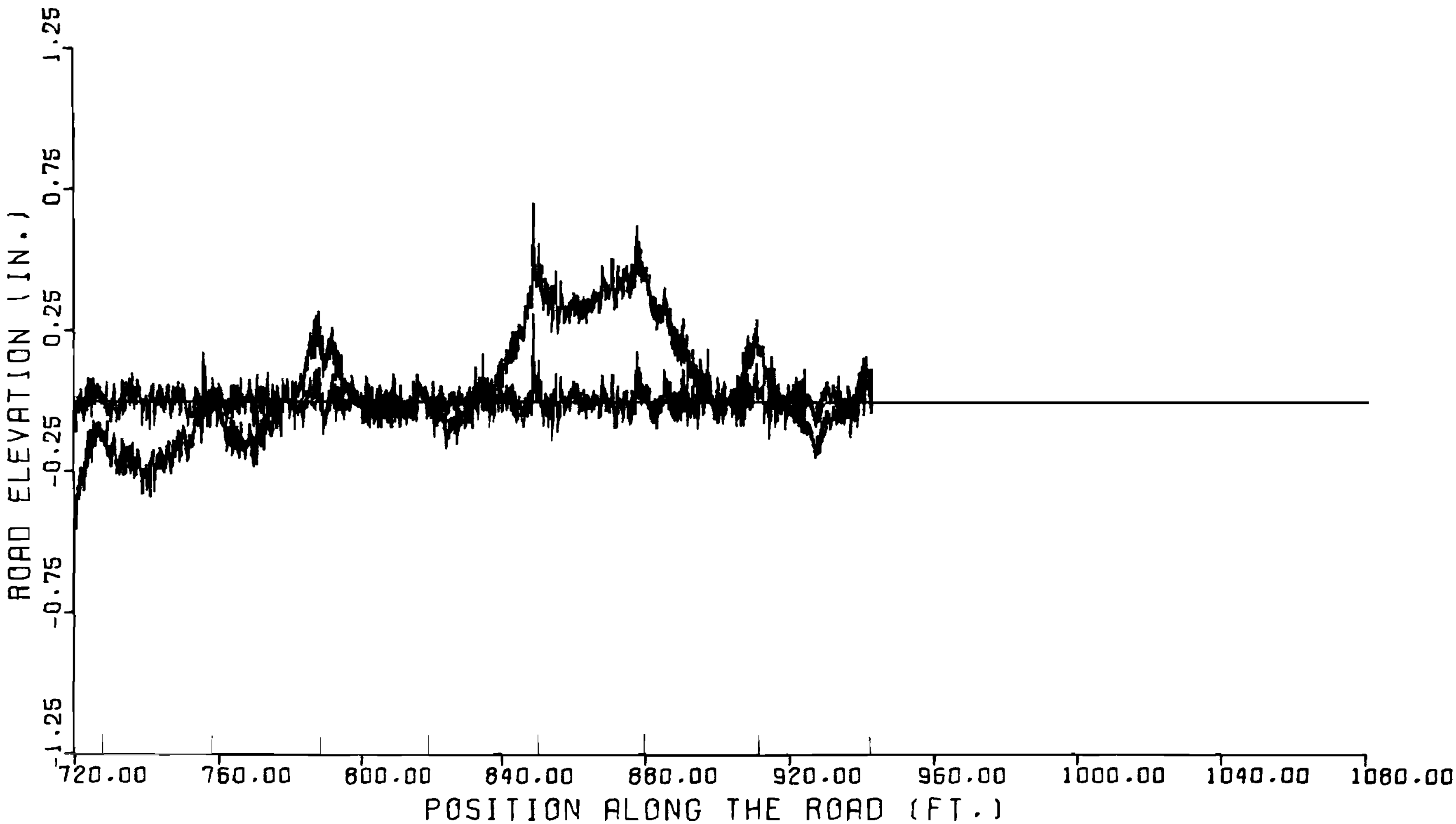

Fig A1.50. Plum Creek Bridge

Filter Passband: 60.0 to 100.0 ft. Wavelengths - Northbound Lane - Right Profile Frame 1

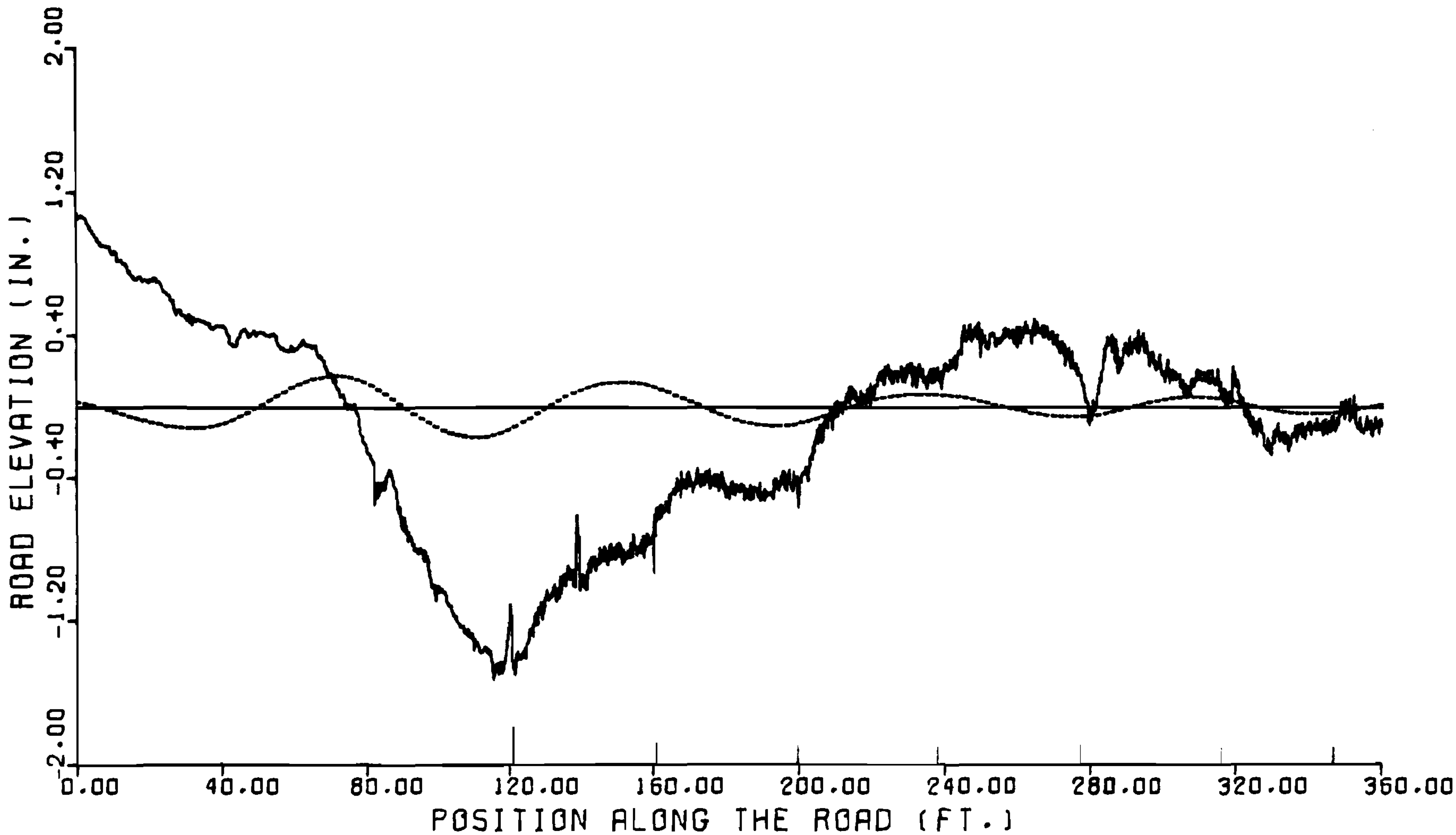

Fig A1.51. Plum Creek Bridge

Filter Passband: 60.0 to 100.0 ft. Wavelengths - Northbound Lane - Right Profile Frame 2

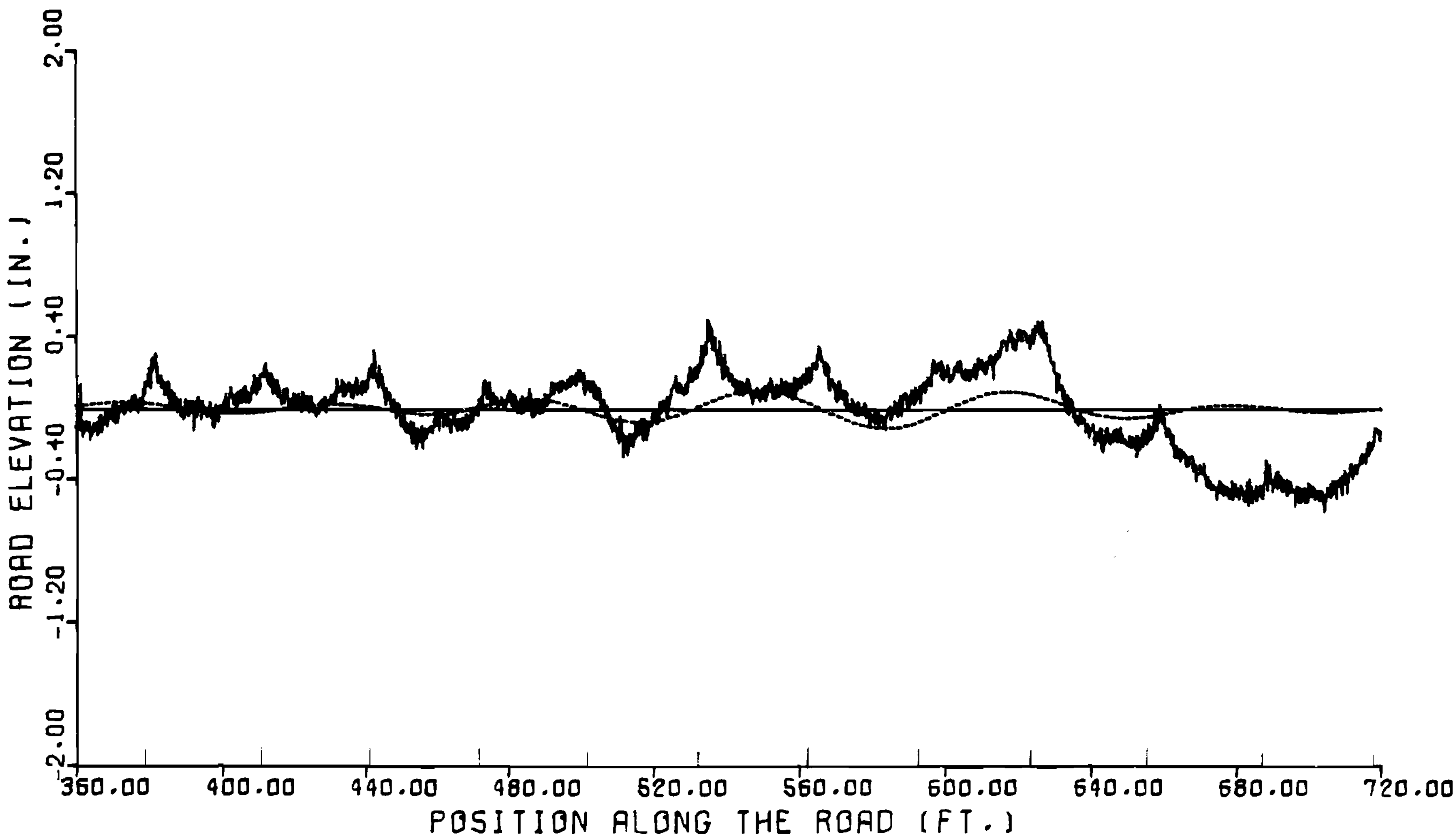

Fig A1.52. Plum Creek Bridge

Filter Passband: 60.0 to 100.0 ft. Wavelengths - Northbound Lane - Right Profile Frame 3

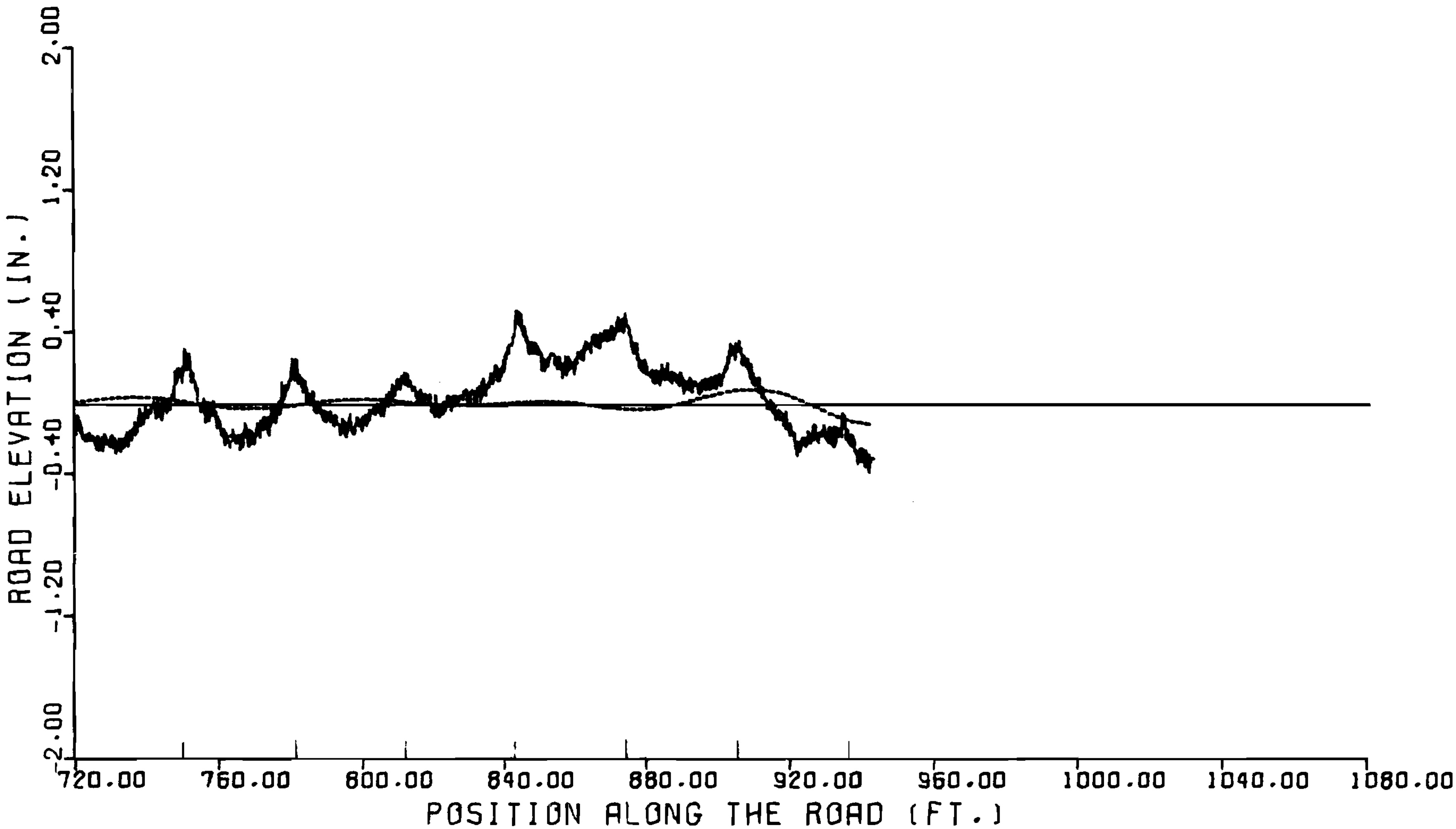

Fig A1.53. Plum Creek Bridge

Filter Passband: 60.0 to 100.0 ft. Wavelengths - Northbound Lane - Right Profile Frame 1

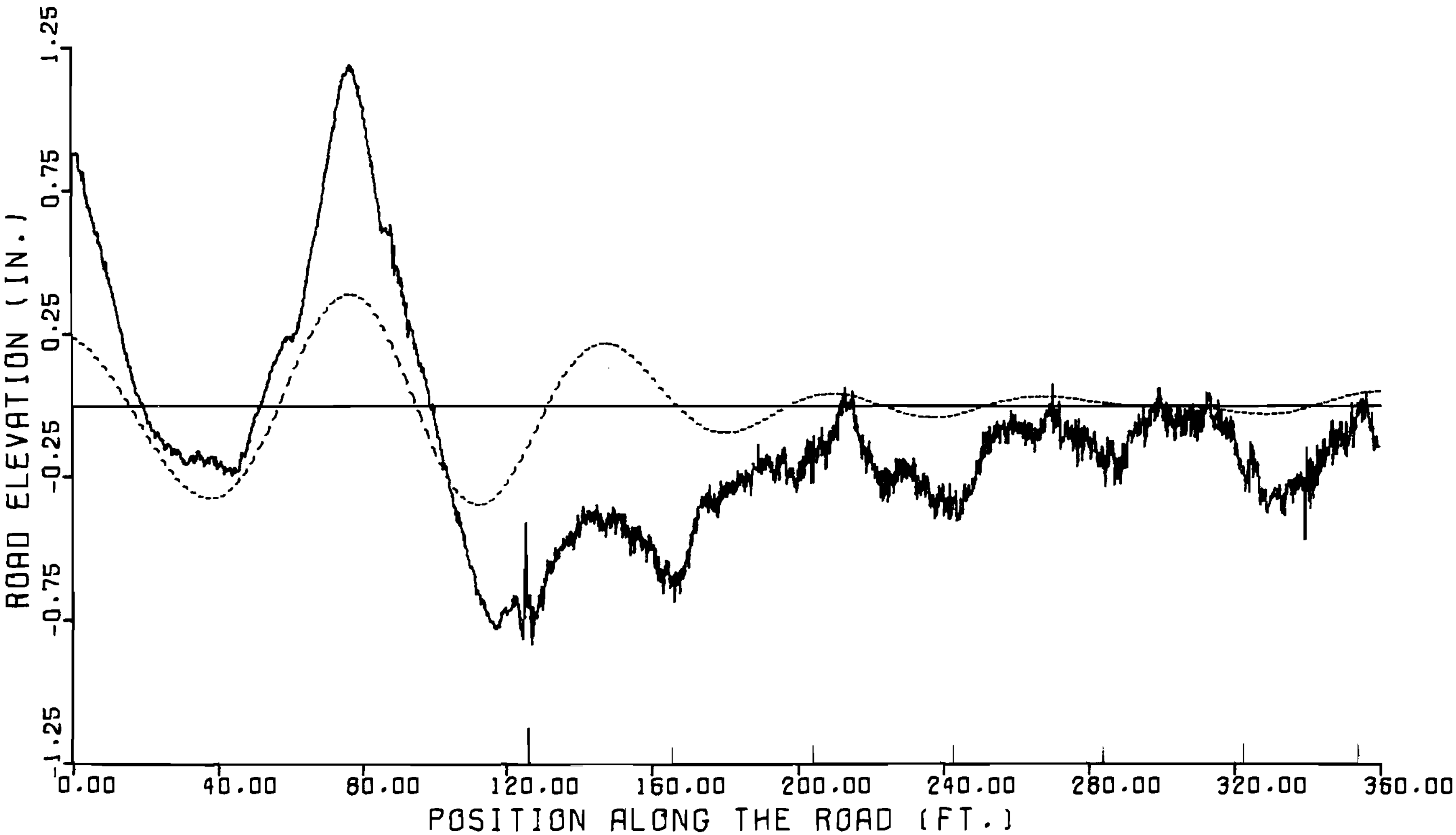

Fig A1.54. Plum Creek Bridge

Filter Passband: 60.0 to 100.0 ft. Wavelengths - Northbound Lane - Right Profile Frame 2

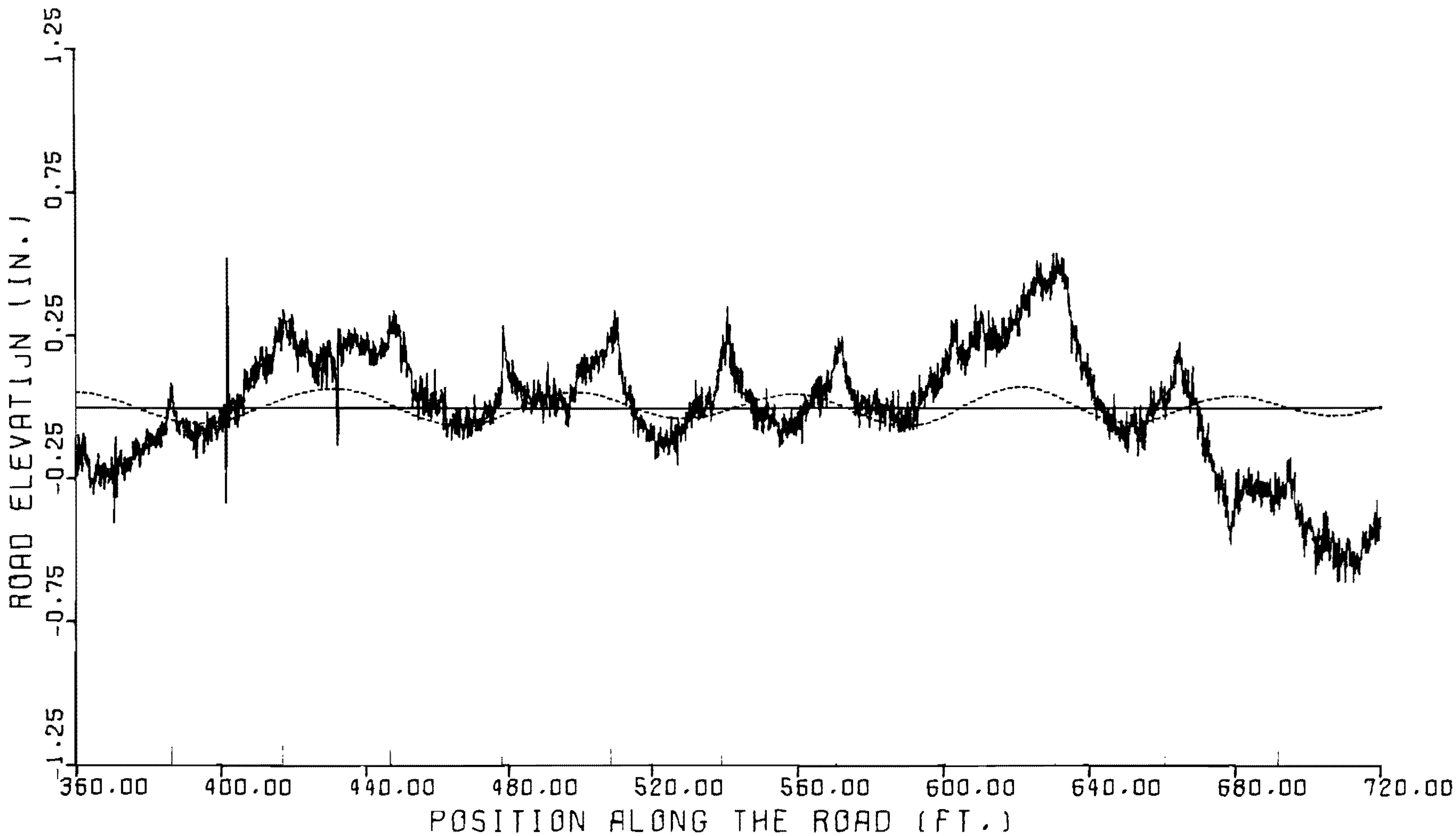

Fig A1.55. Plum Creek Bridge

Filter Passband: 60.0 to 100.0 ft. Wavelengths - Northbound Lane - Right Profile Frame 3

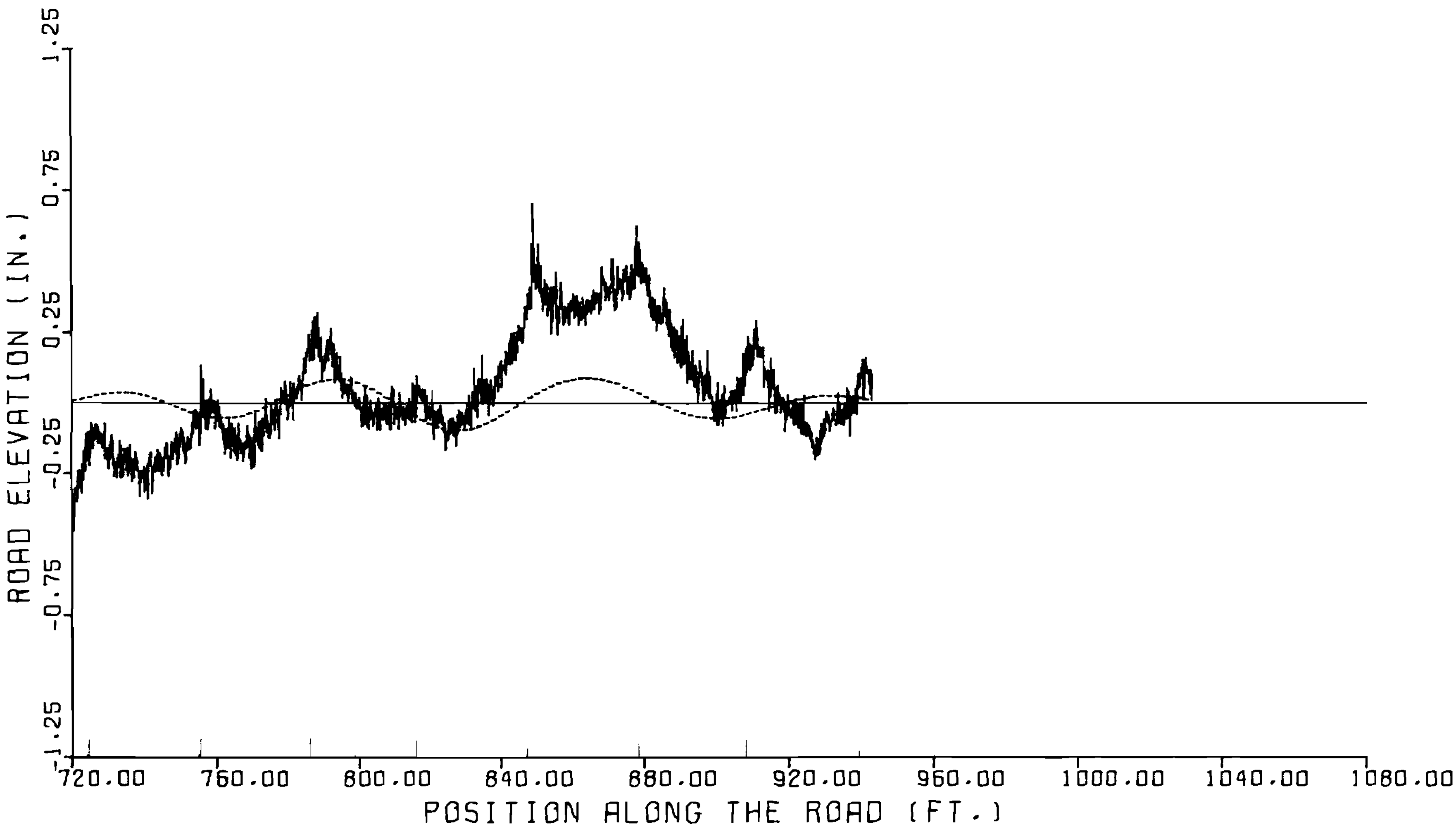

Fig A1.56. Plum Creek Bridge

Filter Passband: 20.0 to 40.0 ft. Wavelengths - Northbound Lane - Right Profile Frame 1

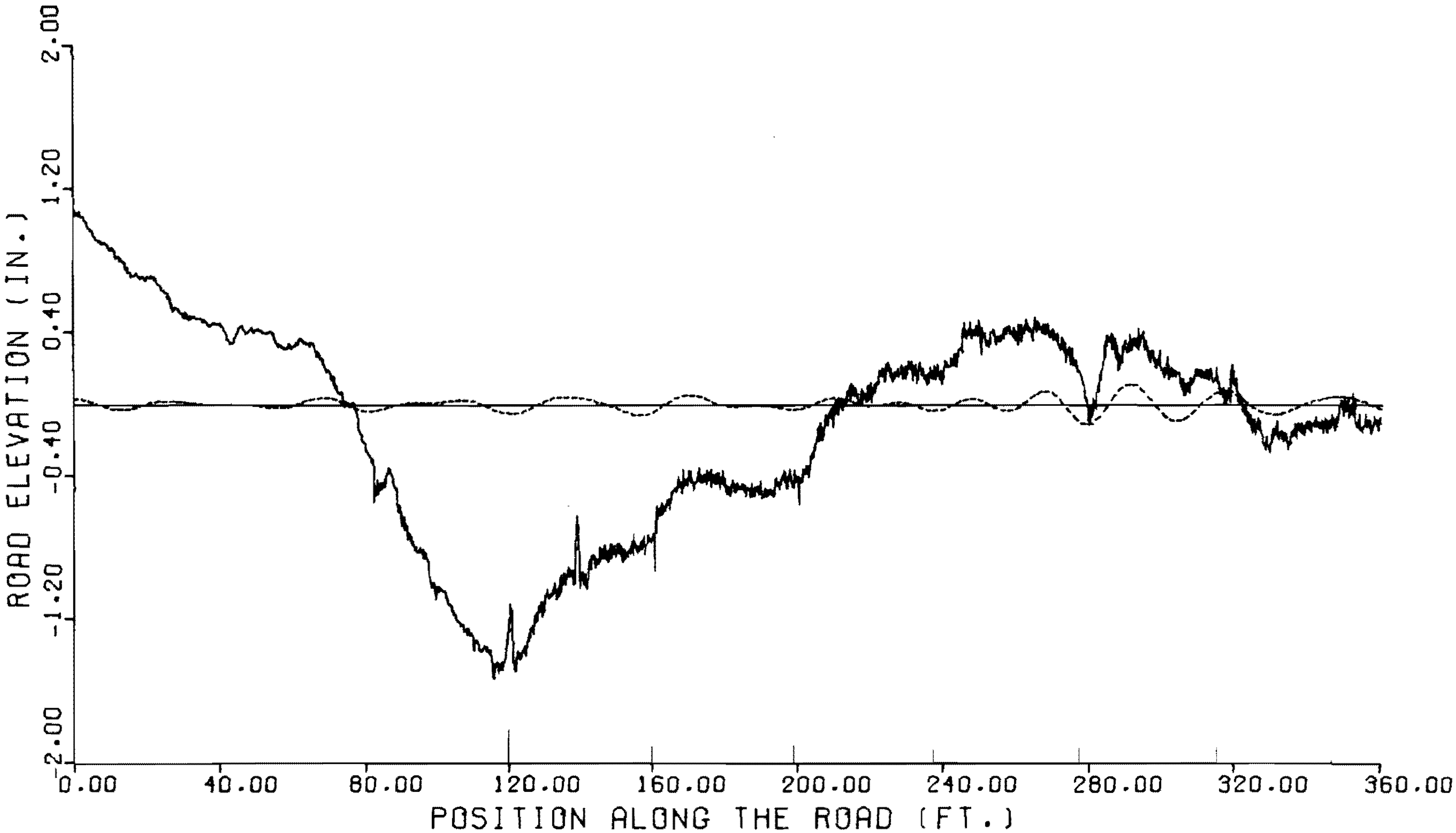

Fig A1.57. Plum Creek Bridge

Filter Passband: 20.0 to 40.0 ft. Wavelengths - Northbound Lane - Right Profile Frame 2

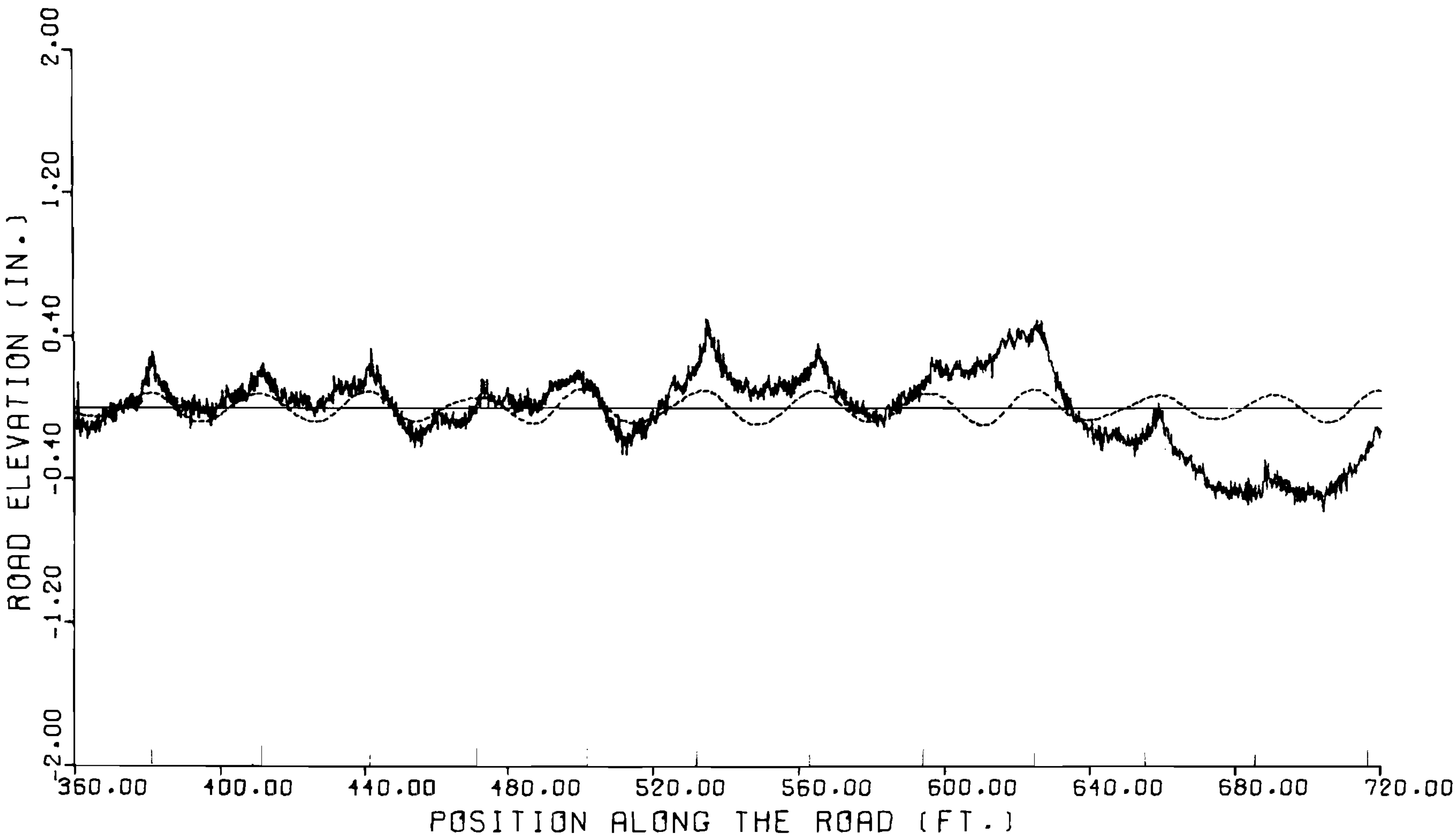

Fig A1.58. Plum Creek Bridge

Filter Passband: 20.0 to 40.0 ft. Wavelengths - Northbound Lane - Right Profile Frame 3

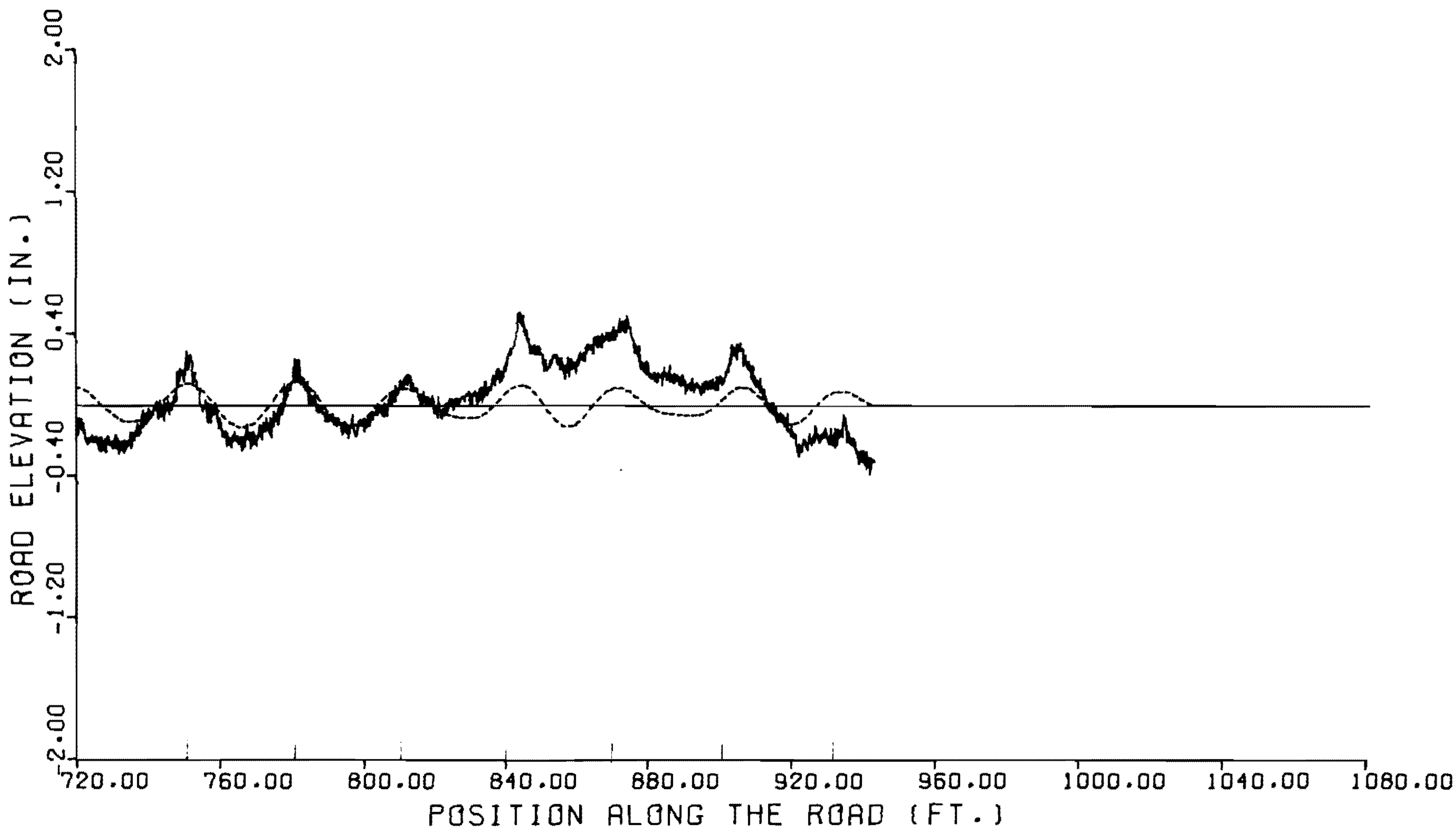

Fig A1.59. Plum Creek Bridge

Filter Passband: 50.0 to 70.0 ft. Wavelengths - Northbound Lane - Right Profile Frame 1

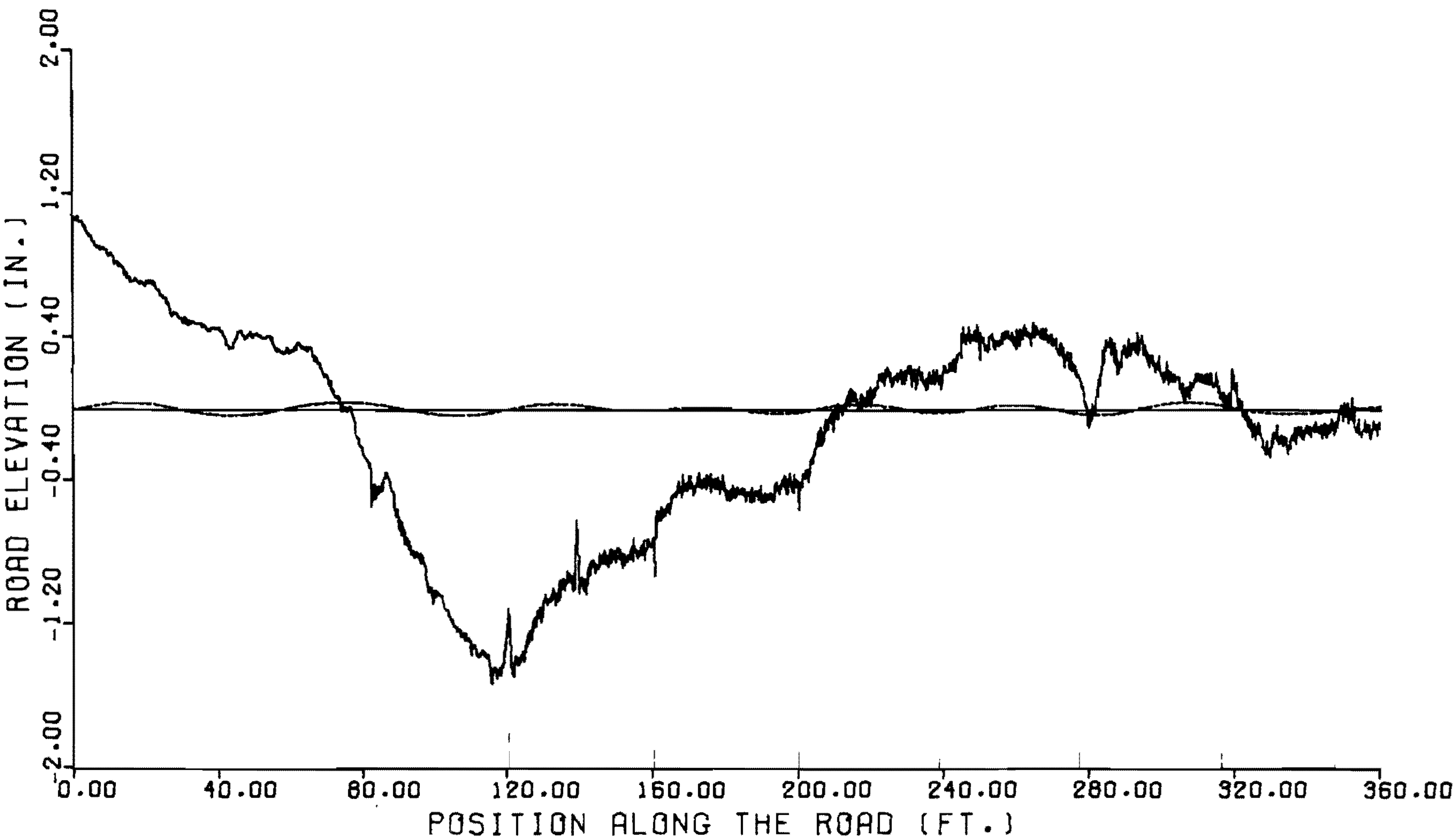

Fig A1.60. Plum Creek Bridge

Filter Passband: 50.0 to 70.0 ft. Wavelengths - Northbound Lane - Right Profile Frame 2

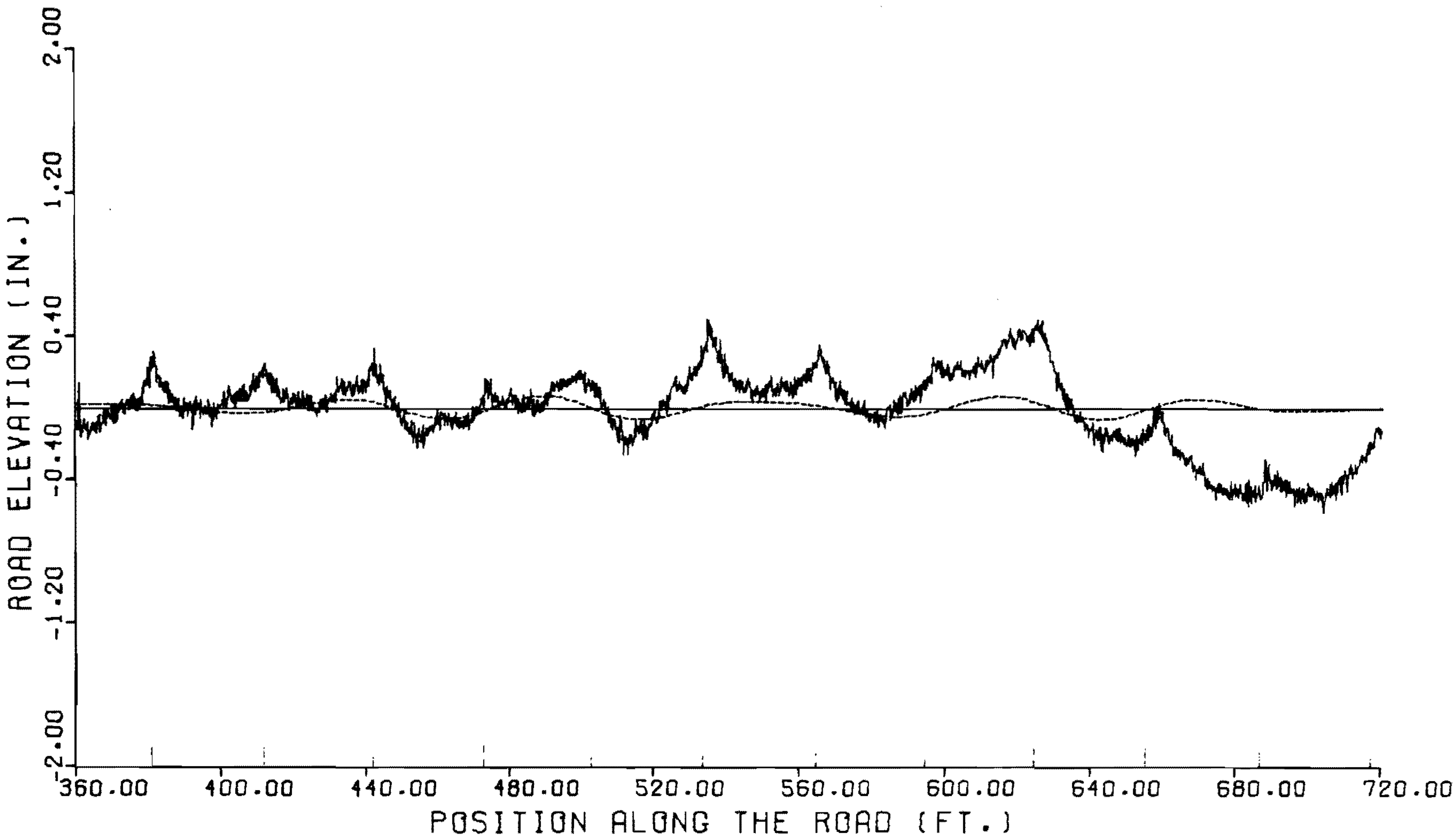

Fig A1.61. Plum Creek Bridge

Filter Passband: 50.0 to 70.0 ft. Wavelengths - Northbound Lane - Right Profile Frame 3

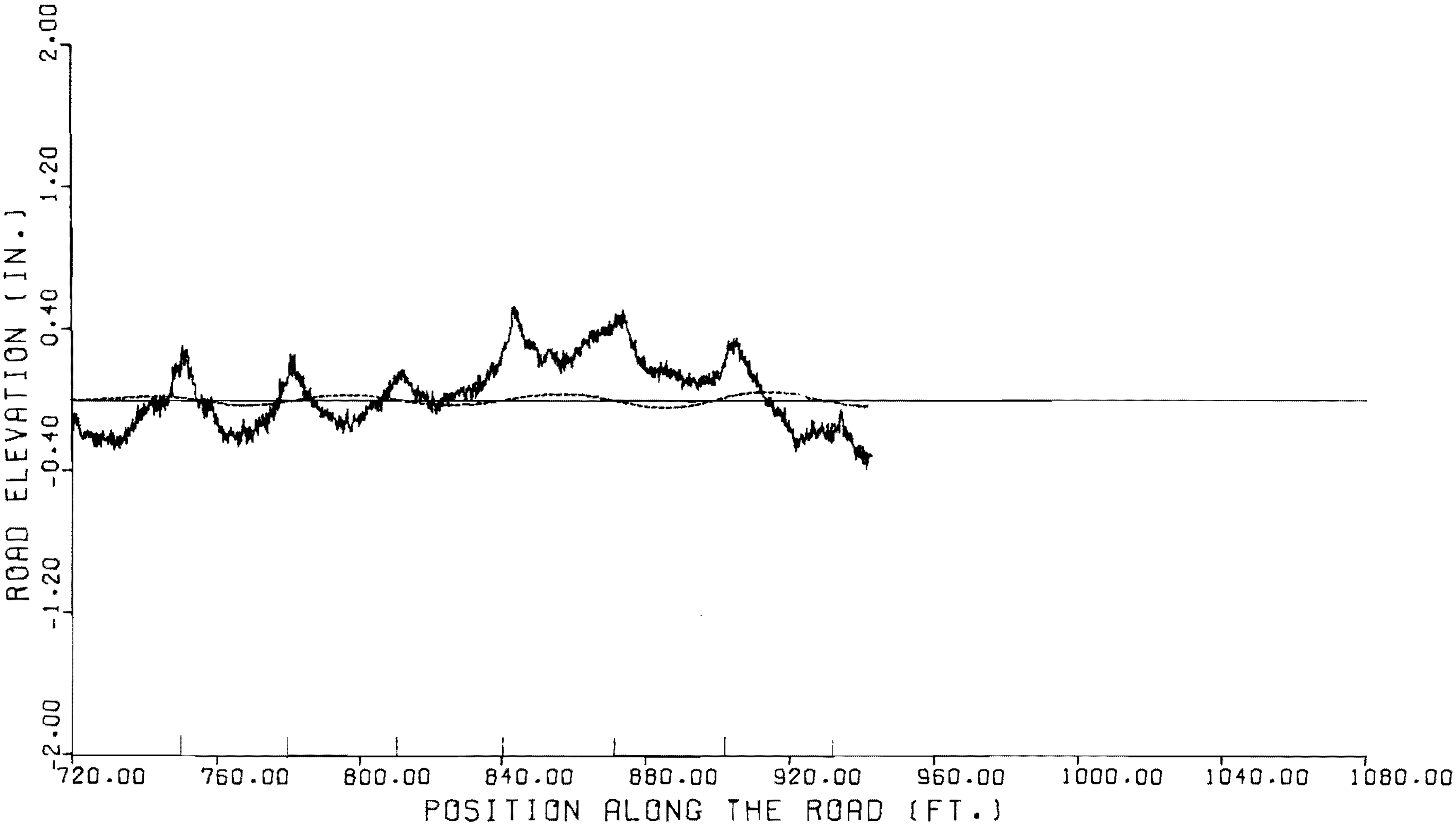

Fig A1.62. Plum Creek Bridge

APPENDIX B

ROUGHNESS AMPLITUDE DISTRIBUTION TABLES

APPENDIX B. ROUGHNESS AMPLITUDE DISTRIBUTION TABLES

This appendix contains the localized, or extreme, measures of roughness computed for both bridge deck and adjoining pavement of each of the three projects studied in detail. The results derived from this method are discussed in Chapter 4, while the methods used to obtain the data are presented in Chapter 5.

Through these measures of localized roughness, both mean amplitude and measures of the worst roughness in a given section can be determined for each pavement type. By means of numerical comparisons of the roughness amplitude distribution measures (the 50th, 75th, 90th, 95th and 99th percentile points were used for this study), the type of roughness present on each pavement type can be better characterized. A percentile point is used as a measure of what amplitude exists such that a given percentage of observations have values less than or equal to this value. The 95th percentile amplitude, for example, is the value greater than or equal to 95 percent of all the local roughness amplitudes for a given road section.

For each roughness measure, two amplitudes are provided for several passbands. The upper value is the amplitude of the right profile, whereas the lower value is the amplitude of the right-left difference profile. The various measures of roughness amplitudes can be obtained from the following tables for both longitudinal and transverse roughness.

TABLE B.1. FLEXIBLE PAVEMENT

Mopac Bridge Project

Wavelength(feet)

	0 - 1	1 - 3	3 - 9	9 - 20	20 - 81	81 - 120
STD DEV.	.00421	.00308	.00256	.00382	.01199	.05251
	.01245	.00763	.00614	.00758	.01995	.02174
MEAN	.00780	.00545	.00534	.00798	.03840	.07571*
	.01560	.00857	.01003	.01193	.03964△	.04452△
50th	.00707	.00480	.00495	.00703	.03980	.06418*
	.01189	.00666	.00847	.01009	.03224△	.03116△
75th	.00927	.00691	.00606	.01021	.04396	.10323*
	.01844	.00975	.01153	.01501	.04968△	.06274△
90th	.01219	.00917	.00732	.01354	.05557	.16175*
	.02975△	.01599	.01637	.02052	.07708△	.08229△
95th	.01472	.01052	.00922	.01564	.05967	.19536*
	.04187△	.02469	.02413	.02282	.08477	.08562
99th	.02351	.01705	.01940	.01851	.06434	.20290*
	.06393△	.03873	.03337	.04358	.08700	.08952△

* denotes that this right profile amplitude was greater than the corresponding amplitude on the bridge deck.

△ denotes that this right-left difference profile amplitude was greater than the corresponding amplitude on the bridge deck.

TABLE B .2. BRIDGE DECK

Mopac Bridge Project

Wavelength(feet)

	0 - 1	1 - 3	3 - 9	9 - 20	20 - 81	81 - 120
STD DEV.	.00624	.00609	.01024	.01081	.01961	.00762
	.00851	.00854	.01180	.00946	.01036	.01246
MEAN	.01119*	.01074*	.01907*	.02385*	.05362*	.04108
	.01649△	.01527△	.02458△	.02074△	.02620	.01629
50th	.01002*	.00973*	.01596*	.02191*	.04895*	.04250
	.01484△	.01395△	.02211△	.01916△	.02386	.00880
75th	.01392*	.01381*	.02440*	.02800*	.07095*	.04796
	.02046△	.01920△	.03144△	.02544△	.03302	.02664
90th	.01860*	.01842*	.03260*	.03948*	.08282*	.05013
	.02767	.02594△	.03901△	.03331△	.04481	.03889
95th	.02284*	.02232*	.03838*	.04858*	.08898*	.05099
	.03305	.03043△	.04436△	.04095△	.04743	.04149
99th	.03462*	.03164*	.05617*	.05830*	.09066*	.05228
	.04397	.04796△	.07516△	.04826△	.04894	.04322

* denotes that this right profile amplitude was greater than the corresponding amplitude on the adjoining pavement.

Δ denotes that this right-left difference profile amplitude was greater than the corresponding amplitude on the adjoining pavement.

TABLE B.3. WESTBOUND FLEXIBLE PAVEMENT

Big Sandy Bridge Project

Wavelength(feet)

	0 - 1	1 - 3	3 - 9	9 - 20	20 - 40	40 - 60	60 - 81
STD DEV.	.00917	.00708	.00525	.00868	.02018	.01027	.01099
	.01486	.00939	.00629	.00838	.01047	.00608	.00693
MEAN	.02266	.01472	.01419	.01807	.03522*	.03379	.04063*
	.03556	.01925	.01943△	.02167△	.02997△	.02049△	.01766△
50th	.02117	.01400	.01336	.01597	.02869*	.03140	.04321*
	.03425	.01747	.01847△	.01937△	.02887△	.02151△	.01892△
75th	.02776	.01860	.01651	.02147	.04757*	.04406	.04994*
	.04522	.02377	.02239△	.02644△	.04006△	.02617△	.02151△
90th	.03508	.02350	.02100	.03116*	.07003*	.04890	.05379*
	.05479	.03224△	.02949△	.03560△	.04428△	.02768△	.02716△
95th	.04012	.02752△	.02441	.03713*	.07825*	.05107	.05563
	.06189	.03665△	.03246△	.03877△	.04565△	.02819△	.02856△
99th	.050403	.03885△	.03459	.04376	.08016*	.05273	.05724*
	.07592	.04939	.03804△	.04097△	.04865△	.02865△	.03605△

* denotes that this right profile amplitude was greater than the corresponding amplitude on the bridge deck.

△ denotes that this right-left difference profile amplitude was greater than the corresponding amplitude on the bridge deck.

TABLE B.4. WESTBOUND BRIDGE DECK

Big Sandy Bridge Project

Wavelength(feet)

	0 - 1	1 - 3	3 - 9	9 - 20	20 - 40	40 - 60	60 - 81
STD DEV.	.01752	.00906	.00749	.00548	.00613	.00775	.00810
	.01653	.00919	.00565	.00401	.00445	.00390	.00575
MEAN	.03253*	.01681*	.01531*	.01937*	.02750	.04351*	.02127
	.04175Δ	.01943Δ	.01555	.01501	.01502	.01056	.01291
50th	.02933*	.01561*	.01370*	.01871*	.02802	.04200*	.02302
	.04010Δ	.01795Δ	.01414	.01438	.01443	.01047	.01271
75th	.03860*	.02113*	.01748*	.02168*	.03109	.05048*	.03007
	.05208Δ	.02439Δ	.01782	.01696	.01839	.01248	.01853
90th	.05051*	.02749*	.02501*	.02724	.03543	.05431*	.03234
	.06412Δ	.03219	.02319	.01947	.02181	.01363	.02101
95th	.06099*	.03242*	.03090*	.03180	.03748	.05585*	.03343
	.06987Δ	.03649	.02823	.02459	.02257	.01851	.02166
99th	.10883*	.05171*	.04343*	.03474	.04028	.05739*	.03451
	.08540Δ	.04424	.03676	.02762	.02366	.02446	.02204

* denotes that this right profile amplitude was greater than the corresponding amplitude on the adjoining pavement.

Δ denotes that this right-left difference profile amplitude was greater than the corresponding amplitude on the adjoining pavement.

TABLE B.5. EASTBOUND FLEXIBLE PAVEMENT

Big Sandy Bridge Project

Wavelength(feet)

	0 - 1	1 - 3	3 - 9	9 - 20	20 - 40	40 - 60	60 - 81
STD DEV.	.00883	.00694	.00466	.01251	.01583	.01878	.02443*
	.01159	.00883	.00686	.01277	.01327	.00909	.00978Δ
MEAN	.02385	.01349*	.01703*	.02243*	.03256	.03913*	.03036*
	.03132	.01813Δ	.02253Δ	.02581Δ	.02346Δ	.01611Δ	.03010Δ
50th	.02280	.01236*	.01674*	.02044*	.03315	.04230*	.01990*
	.03014	.01719Δ	.02178Δ	.02373Δ	.02028Δ	.01569Δ	.03257Δ
75th	.02935	.01680	.02012*	.02715*	.04679*	.05388*	.05613*
	.03881	.02349Δ	.02669Δ	.02878Δ	.02629Δ	.02107Δ	.03949Δ
90th	.03583	.02294*	.02354*	.03739*	.05340*	.06310*	.06729*
	.04743	.02916Δ	.03186Δ	.04043Δ	.04739Δ	.03066Δ	.04233Δ
95th	.04015	.02764*	.02561	.04719*	.05657*	.06576*	.06938*
	.05222	.03329Δ	.03577Δ	.04945Δ	.05800Δ	.03360Δ	.04377Δ
99th	.04950	.03633	.02814	.06889*	.05772*	.06771*	.07321*
	.06126	.04570	.04183Δ	.07561Δ	.06076Δ	.03485Δ	.04470Δ

* denotes that this right profile amplitude was greater than the corresponding amplitude on the bridge deck.

Δ denotes that this right-left difference profile amplitude was greater than the corresponding amplitude on the bridge deck.

TABLE B.6. EASTBOUND BRIDGE DECK

Big Sandy Bridge Project

Wavelength(feet)

	0 - 1	1 - 3	3 - 9	9 - 20	20 - 40	40 - 60	60 - 81
STD DEV.	.01865	.00735	.00666	.00820	.01034	.00771	.00493
	.01897	.00993	.00528	.00514	.00397	.00197	.00242
MEAN	.03021*	.01345	.01548	.01997	.03739*	.03888	.01625
	.03989Δ	.01588	.01740	.01330	.01637	.00900	.00896
50th	.02650	.01215	.01424	.01863	.03858*	.03774	.01455
	.03741Δ	.01361	.01711	.01435	.01780	.00957	.00932
75th	.03635*	.01692*	.01726	.02496	.04546	.04540	.01902
	.04845Δ	.02145	.02141	.01782	.01967	.01061	.01105
90th	.04906*	.02158	.02344	.03248	.05031	.05010	.02315
	.06100Δ	.02883	.02391	.01957	.02128	.01130	.01198
95th	.05942*	.02713	.02716*	.03469	.05272	.05184	.02668
	.07088Δ	.03247	.02620	.02027	.02228	.01160	.01232
99th	.11361*	.03956	.04323*	.03891	.05392	.05292	.02783
	.10199Δ	.05097Δ	.02818	.02117	.02276	.01180	.01316

* denotes that this right profile amplitude was greater than the corresponding amplitude on the adjoining pavement.

Δ denotes that this right-left difference profile amplitude was greater than the corresponding amplitude on the adjoining pavement.

TABLE B.7. NORTHBOUND FLEXIBLE PAVEMENT

Plum Creek Bridge Project

Wavelength (feet)

	0 - 1	1 - 3	3 - 9	9 - 20	20 - 40	40 - 81
STD DEV.	.00787	.01223	.01268	.01736	.01633	.05201
	.01135	.01474	.01202	.01498	.01733	.04475
MEAN	.01544	.01489*	.01956*	.02423	.02670	.07365*
	.02467	.01910Δ	.02352Δ	.02641Δ	.02846Δ	.07714Δ
50th	.01399	.01118	.01616*	.01945	.02223	.06856*
	.02315	.01545	.02088Δ	.02073Δ	.02244Δ	.05811Δ
75th	.01914	.01755	.02529*	.02611	.02937	.09912*
	.03055	.02435Δ	.02954Δ	.03194Δ	.04191Δ	.11104Δ
90th	.02465	.02932*	.03411*	.04185*	.05305	.16844*
	.03864	.03538Δ	.04075Δ	.04831Δ	.05758Δ	.15177Δ
95th	.02967	.04025*	.04713*	.05744*	.07013	.17838*
	.04396	.04307Δ	.05124Δ	.06141Δ	.06195Δ	.16384Δ
99th	.04477	.06101*	.06745*	.10092*	.07768	.18942*
	.05956	.06622Δ	.05802Δ	.07225Δ	.06658Δ	.17047Δ

* denotes that this right profile amplitude was greater than the corresponding amplitude on the bridge deck.

Δ denotes that this right-left difference profile amplitude was greater than the corresponding amplitude on the bridge deck.

TABLE B.8. NORTHBOUND BRIDGE DECK
Plum Creek Bridge Project

Wavelength(feet)

	0 - 1	1 - 3	3 - 9	9 - 20	20 - 40	40 - 81
STD DEV.	.00937 .01141	.00709 .00837	.00593 .00468	.00856 .00496	.01032 .00427	.01823 .00664
MEAN	.02055* .02939Δ	.01448 .01818	.01419 .01423	.02713* .01264	.06517* .01132	.05636 .02514
50th	.01944* .02806Δ	.01311* .01729Δ	.01327 .01372	.02677* .01114	.06401* .01069	.05636 .02455
75th	.02524* .03607Δ	.01867* .02288	.01724 .01711	.03399* .01586	.06889* .01442	.06845 .03008
90th	.03109* .04401Δ	.02444 .02942	.02187 .01984	.03754 .02061	.08004* .01809	.07860 .03491
95th	.03513* .04900Δ	.02765 .03342	.02516 .02220	.04120 .02210	.08745* .01887	.08126 .03612
99th	.04689* .05982Δ	.03696 .04207	.03399 .02862	.04771 .02369	.09490* .01978	.08332 .03860

* denotes that this right profile amplitude was greater than the corresponding amplitude on the adjoining pavement.

Δ denotes that this right-left difference profile amplitued was greater than the corresponding amplitude on the adjoining pavement.

TABLE B.9. SOUTHBOUND FLEXIBLE PAVEMENT

Plum Creek Bridge Project

Wavelength (feet)

	0 - 1	1 - 3	3 - 9	9 - 20	20 - 40	40 - 81
STD DEV.	.00212	.00274	.00390	.00395	.01122	.03558
	.00303	.00286	.00377	.00379	.00515	.01265
MEAN	.00523	.00495	.00845	.01238	.01806	.07727*
	.00743	.00578	.00901	.01114	.01492	.02678
50th	.00489	.00442	.00768	.01130	.01347	.07401*
	.00708	.00531	.00763	.01117	.01612	.02129
75th	.00633	.00647	.01003	.01497	.02211	.11418*
	.00922	.00727	.01078	.01406	.01921	.03202
90th	.00776	.00821	.01301	.01867	.03792	.12719*
	.01142	.00938	.01582	.01606	.02081	.04720
95th	.00877	.00992	.01702	.02026	.04762	.12905*
	.01301	.01121	.01741	.01737	.02164	.05592
99th	.1361	.01373	.02294	.02119	.05164	.13055*
	.01665	.01604	.01806	.01835	.02391	.06338Δ

* denotes that this right profile amplitude was greater than the corresponding amplitude on the bridge deck.

Δ denotes that this right-left difference profile amplitude was greater than the corresponding amplitude on the bridge deck.

TABLE B.10. SOUTHBOUND BRIDGE DECK

Plum Creek Bridge Project

Wavelength(feet)

	0 - 1	1 - 3	3 - 9	9 - 20	20 - 40	40 - 81
STD DEV.	.01274	.00741	.01080	.01233	.01870	.02483
	.01532	.00889	.01218	.01757	.01622	.01675
MEAN	.02698*	.01560*	.02035*	.03036	.04751*	.05346
	.03596△	.01923△	.02385△	.02647△	.02757△	.03576△
50th	.02474*	.01461*	.01737*	.02801*	.04306*	.04671
	.03375△	.01802△	.02011△	.02254△	.02321△	.03489△
75th	.03318*	.01999*	.02495*	.03488*	.06466*	.06392
	.04382△	.02433△	.02905△	.03263△	.04262△	.04880△
90th	.04354*	.02565*	.03570*	.05090*	.07393*	.09848
	.05668△	.03097△	.04321△	.05235△	.05213△	.05989△
95th	.05168*	.02892*	.04360*	.05966*	.07650*	.10521
	.06588△	.03580△	.04896△	.06170△	.05441△	.06157△
99th	.06974*	.03638*	.05588*	.06584*	.08035*	.10815
	.08287△	.04495△	.06040△	.08547△	.05834△	.06264

* denotes that this right profile amplitude was greater than the corresponding amplitude on the adjoining pavement.

△ denotes that this right-left difference profile amplitude was greater than the corresponding amplitude on the adjoining pavement.

THE AUTHORS

David B. Law is currently employed by the Federal Highway Administration. While employed with the Center for Highway Research as a Research Engineer Assistant, his main interests were pavement design and performance.

Hugh J. Williamson is a Research Engineer with the Center for Highway Research at The University of Texas at Austin. He is the author of several publications, and his primary areas of specialization are statistics and operations research.

W. Ronald Hudson is a Professor of Civil Engineering and Director of Research, Council for Advanced Transportation Studies at The University of Texas at Austin. He has had a wide variety of experience as a research engineer with the Texas Highway Department and the Center for Highway Research at The University of Texas at Austin and was Assistant Chief of the Rigid Pavement Branch of the AASHO Road Test. He is the author of numerous publications and was the recipient of the 1967 ASCE J. James R. Croes Medal. He is presently concerned with research in the areas of (1) analysis and design of pavement management systems, (2) measurement of pavement roughness performance, (3) slab analysis and design, and (4) tensile strength of stabilized subbase materials.